CHAPTER 4† THERMAL EVALUATION

4.0 OVERVIEW

The HI-STORM System is designed for long-term storage of spent nuclear fuel (SNF) in a vertical orientation. An array of HI-STORM Systems laid out in a rectilinear pattern will be stored on a concrete ISFSI pad in an open environment. In this section, compliance of the HI-STORM thermal performance to 10CFR72 requirements for outdoor storage at an ISFSI is established. The analysis considers passive rejection of decay heat from the stored SNF assemblies to the environment under the most severe design basis ambient conditions. Effects of incident solar radiation (insolation) and partial radiation blockage due to the presence of neighboring casks at an ISFSI site are included in the analyses. Finally, the thermal margins of safety for long-term storage of both moderate burnup (up to 45,000 MWD/MTU) and high burnup spent nuclear fuel (greater than 45,000 MWD/MTU) in the HI-STORM 100 System are quantified. Safe thermal performance during on-site loading, unloading and transfer operations utilizing the HI-TRAC transfer cask is also demonstrated.

The HI-STORM thermal evaluation adopts NUREG-1536 [4.4.10] and ISG-11 [4.1.4] guidelines to demonstrate safe storage of Commercial Spent Fuel (CSF)*. These guidelines are stated below:

1. The fuel cladding temperature for long-term storage and short-term operations shall be limited to 400°C (752°F).

2. The fuel cladding temperature should be maintained below 570°C (1058°F) for accident and off-normal event conditions.

3. The maximum internal pressure of the cask should remain within its design pressures for normal (1% rod rupture), off-normal (10% rod rupture), and accident (100% rod rupture) conditions.

4. The cask and fuel materials should be maintained within their minimum and maximum temperature criteria for normal, off-normal, and accident conditions.

5. For fuel assemblies proposed for storage, the cask system should ensure a very low probability of cladding breach during long-term storage.

---

† This chapter has been prepared in the format and section organization set forth in Regulatory Guide 3.61. However, the material content of this chapter also fulfills the requirements of NUREG-1536. Pagination and numbering of sections, figures, and tables are consistent with the convention set down in Chapter 1, Section 1.0, herein. Finally, all terms-of-art used in this chapter are consistent with the terminology of the glossary (Table 1.0.1) and component nomenclature of the Bill-of-Materials (Section 1.5).

* Defined as nuclear fuel that is used to produce energy in a commercial nuclear reactor (See Table 1.0.1).

6. The HI-STORM System should be passively cooled.

7. The thermal performance of the cask should be within the allowable design criteria specified in FSAR Chapters 2 and 3 for normal, off-normal, and accident conditions.

As demonstrated in this chapter (see Subsections 4.4.6 and 4.5.6), the HI-STORM System is designed to comply with all of the criteria listed above. All thermal analyses to evaluate normal conditions of storage in a HI-STORM storage module are described in Section 4.4. All thermal analyses to evaluate normal handling and on-site transfer in a HI-TRAC transfer cask are described in Section 4.5. All analyses for off-normal conditions are described in Section 11.1. All analyses for accident conditions are described in Section 11.2. Sections 4.1 through 4.3 describe thermal analyses and input data that are common to all conditions. This FSAR chapter is in full compliance with NUREG-1536 requirements, subject to the exceptions and clarifications discussed in Chapter 1, Table 1.0.3 and to ISG-11 requirements (no exceptions).

This revision to the HI-STORM Safety Analysis Report incorporates several features into the thermal analysis to respond to the changing needs of the U.S. nuclear power generation industry and revisions to NRC regulations. The most significant change is:

- The thermal analysis is revised to comply with recently issued NRC Staff Guidance ("Cladding Considerations for the Transportation and Storage of Spent Fuel," ISG-11, Rev. 3).

- The Aluminum Heat Conduction Elements (ACHEs), optional under Amendment 1 of CoC 1014, are removed from the design. Removing the ACHEs from the MPC eliminates the constriction of the downcomer flow and thus further enhances the thermal performance of the MPC.

HOLTEC INTERNATIONAL COPYRIGHTED MATERIAL

4.1 DISCUSSION

As discussed in Chapter 2, this revision of the HI-STORM FSAR seeks to establish complete compliance with the provisions of ISG-11 [4.1.4]. To ensure explicit compliance, the new condition "short term operations," corresponding to fuel loading activities, is defined in Chapter 2.

In Revision 1 of this FSAR, fuel loading, which includes MPC cavity drying, MPC lid welding, helium pressurization, and MPC transfer operations, was treated as part of the "off-normal" condition. It is not treated as a distinct fuel thermal state. Specifically, the maximum fuel cladding temperature for the fuel loading condition now formally referred to as "short term operations" is set equal to the PCT limit for normal storage conditions for all high-burnup CSF (see Section 4.3). Potential thermally challenging states for the spent fuel arise if the fuel drying process utilizes pressure reduction (i.e., vacuum drying) or when the loaded MPC is inside the HI-TRAC transfer cask. In the latter state, the rate of heat rejection from the MPC is somewhat less compared to the normal storage condition when the MPC is inside the ventilated overpack. Because the HI-TRAC transfer cask handling subsequent to helium pressurization of the MPC typically involves keeping the equipment vertical, the thermosiphon action inside the MPC is fully operational during these activities. As a result, the increase in the fuel cladding temperature in the HI-TRAC compared to the HI-STORM storage condition is fairly modest. The increase is more significant in the case where the HI-TRAC transfer cask, for reasons such as vertical height restrictions or seismic constraints as a plant, must be handled in the horizontal orientation. When the HI-TRAC is horizontal, the cessation of the thermosiphon action result in an additional rise in the fuel cladding temperature. Therefore, the short term evolutions that may be thermally limiting are analyzes as listed below:

i. Vacuum Drying
ii. Loaded MPC in HI-TRAC in the vertical orientation
iii. Loaded MPC in HI-TRAC in the horizontal orientation

The threshold MPC heat generation rate at which the HI-STORM peak cladding temperature reaches a steady state equilibrium value approaching the normal storage peak clad temperature limit is computed in this chapter. Likewise, the MPC heat generation rates that produce the steady state equilibrium temperature approaching the normal storage peak clad temperature limit for the MPC-in-HI-TRAC condition in both vertical and horizontal configurations are computed in this chapter. These computed heat generation rates directly bear upon the compliance of the system with ISG-11 [4.1.4] and are, accordingly, adopted in the system Technical Specifications for high burnup fuel (HBF).

A cutaway view of the HI-STORM dry storage system has been presented earlier (see Figure 1.2.1). The system consists of a sealed MPC situated inside a vertical ventilated storage overpack. Air inlet and outlet ducts that allow for air cooling of the stored MPC are located at the bottom and top, respectively, of the cylindrical overpack. The SNF assemblies reside inside the MPC, which is sealed with a welded lid to form the confinement boundary. The MPC contains an all-alloy

HOLTEC INTERNATIONAL COPYRIGHTED MATERIAL

honeycomb basket structure with square-shaped compartments of appropriate dimensions to allow insertion of the fuel assemblies prior to welding of the MPC lid and closure ring. Each box panel, with the exception of exterior panels on the MPC-68 and MPC-32, is equipped with a thermal neutron absorber panel sandwiched between an Alloy X steel sheathing plate and the box panel, along the entire length of the active fuel region. The MPC is backfilled with helium up to the design-basis initial fill level (Table 1.2.2). This provides a stable, inert environment for long-term storage of the SNF. Heat is rejected from the SNF in the HI-STORM System to the environment by passive heat transport mechanisms only.

The helium backfill gas is an integral part of the MPC thermal design. The helium fills all the spaces between solid components and provides an improved conduction medium (compared to air) for dissipating decay heat in the MPC. To ensure that the helium gas is retained and is not diluted by lower conductivity air, the MPC confinement boundary is designed and fabricated to comply with the provisions of the ASME B&PV Code Section III, Subsection NB (to the maximum extent practical), as an all-seal-welded pressure vessel with redundant closures. It is demonstrated in Section 11.1.3 that the failure of one field-welded pressure boundary seal will not result in a breach of the pressure boundary. The helium gas is therefore retained and undiluted, and may be credited in the thermal analyses.

An important thermal design criterion imposed on the HI-STORM System is to limit the maximum fuel cladding temperature to within design basis limits (Table 4.3.1) for long-term storage of design basis SNF assemblies. An equally important design criterion is to minimize temperature gradients in the MPC so as to minimize thermal stresses. In order to meet these design objectives, the MPC baskets are designed to possess certain distinctive characteristics, which are summarized in the following.

The MPC design minimizes resistance to heat transfer within the basket and basket periphery regions. This is ensured by an uninterrupted panel-to-panel connectivity realized in the all-welded honeycomb basket structure. The MPC design incorporates top and bottom plenums with interconnected downcomer paths. The top plenum is formed by the gap between the bottom of the MPC lid and the top of the honeycomb fuel basket, and by elongated semicircular holes in each basket cell wall. The bottom plenum is formed by large elongated semicircular holes at the base of all cell walls. The MPC basket is designed to eliminate structural discontinuities (i.e., gaps) which introduce large thermal resistances to heat flow. Consequently, temperature gradients are minimized in the design, which results in lower thermal stresses within the basket. Low thermal stresses are also ensured by an MPC design that permits unrestrained axial and radial growth of the basket. The possibility of stresses due to restraint on basket periphery thermal growth is eliminated by providing adequate basket-to-canister shell gaps to allow for basket thermal growth during heat-up to design basis temperatures.

It is heuristically apparent from the geometry of the MPC that the basket metal, the fuel assemblies, and the contained helium mass will be at their peak temperatures at or near the longitudinal axis of

HOLTEC INTERNATIONAL COPYRIGHTED MATERIAL

the MPC. The temperatures will attenuate with increasing radial distance from this axis, reaching their lowest values at the outer surface of the MPC shell. Conduction along the metal walls and radiant heat exchange from the fuel assemblies to the MPC metal mass would therefore result in substantial differences in the bulk temperatures of helium columns in different fuel storage cells. Since two fluid columns at different temperatures in communicative contact cannot remain in static equilibrium, the non-isotropic temperature field in the MPC internal space due to conduction and radiation heat transfer mechanisms guarantee the incipience of the third mode of heat transfer: natural convection.

The preceding paragraph introduced the internal helium thermosiphon feature engineered into the MPC design. It is recognized that the backfill helium pressure, in combination with low pressure drop circulation passages in the MPC design, induces a thermosiphon upflow through the multi-cellular basket structure to aid in removing the decay heat from the stored fuel assemblies. The decay heat absorbed by the helium during upflow through the basket is rejected to the MPC shell during the subsequent downflow of helium in the peripheral downcomers. This helium thermosiphon heat extraction process significantly reduces the burden on the MPC metal basket structure for heat transport by conduction, thereby minimizing internal basket temperature gradients and resulting thermal stresses.

The helium columns traverse the vertical storage cavity spaces, redistributing heat within the MPC. Elongated holes in the bottom of the cell walls, liberal flow space and elongated holes at the top, and wide-open downcomers along the outer periphery of the basket ensure a smooth helium flow regime. The most conspicuous beneficial effect of the helium thermosiphon circulation, as discussed above, is the mitigation of internal thermal stresses in the MPC. Another beneficial effect is reduction of the peak fuel cladding temperatures of the fuel assemblies located in the interior of the basket.

Four distinct MPC basket geometries are evaluated for thermal performance in the HI-STORM System. For intact PWR fuel storage, the MPC-24, MPC-24E, and MPC-32 designs are available. Four locations are designated for storing damaged PWR fuel in the MPC-24E design. A 68-cell MPC design (MPC-68, MPC-68F, and MPC-68FF) is available for storing BWR fuel (intact or damaged (including fuel debris)). All of the four basic MPC geometries (MPC-32, MPC-24, MPC-24E and MPC-68) are described in Chapter 1 wherein their licensing drawings can also be found.

The design maximum decay heat loads for storage of intact zircaloy clad fuel in the four MPCs are listed in Tables 4.4.20, 4.4.21, 4.4.28, and 4.4.29. Storage of intact stainless steel clad fuel is permitted for a low decay heat limit set forth in Chapter 2 (Tables 2.1.17 through 2.1.21). Storage of zircaloy clad fuel with stainless steel clad fuel in an MPC is permitted. In this scenario, the zircaloy clad fuel must meet the lower decay heat limits for stainless steel clad fuel. Storage of damaged, zircaloy clad fuel is evaluated in Subsection 4.4.1.1.4. The axial heat distribution in each fuel assembly is assumed to follow the burnup profiles set forth by Table 2.1.11.

HOLTEC INTERNATIONAL COPYRIGHTED MATERIAL

Thermal analysis of the HI-STORM System is based on including all three fundamental modes of heat transfer, namely conduction, natural convection and radiation. Different combinations of these modes are active in different parts of the system. These modes are properly identified and conservatively analyzed within each part of the MPC, the HI-STORM storage overpack and the HI-TRAC transfer cask, to enable bounding calculations of the temperature distribution within the HI-STORM System to be performed. In addition to storage within the HI-STORM overpack, loaded MPCs will also be located for short durations inside the transfer cask (HI-TRAC) designed for moving MPCs into and out of HI-STORM storage modules.

Heat is dissipated from the outer surface of the HI-STORM storage overpack and HI-TRAC transfer cask to the environment by buoyancy induced airflow (natural convection) and thermal radiation. Heat transport through the cylindrical wall of the storage overpack and HI-TRAC is solely by conduction. While stored in a HI-STORM overpack, heat is rejected from the surface of the MPC via the parallel action of thermal radiation to the inner shell of the overpack and convection to a buoyancy driven airflow in the annular space between the outer surface of the MPC and the inner shell of the overpack. This situation is similar to the familiar case of natural draft flow in furnace stacks. When placed into a HI-TRAC cask for transfer operations, heat is rejected from the surface of the MPC to the inner shell of the HI-TRAC by conduction and thermal radiation.

Within the MPC, heat is transferred between metal surfaces (e.g., between neighboring fuel rod surfaces) via a combination of conduction through a gaseous medium (helium) and thermal radiation. Heat is transferred between the fuel basket and the MPC shell by thermal radiation and conduction.

As discussed later in this chapter, an array of conservative assumptions bias the results of the thermal analysis towards much reduced computed margins than would be obtained by a rigorous analysis of the problem.

The complete thermal analysis is performed using the industry standard ANSYS finite element modeling package [4.1.1] and the finite volume Computational Fluid Dynamics (CFD) code FLUENT [4.1.2]. ANSYS has been previously used and accepted by the NRC on numerous dockets [4.4.10,4.V.5.a]. The FLUENT CFD program is independently benchmarked and validated with a wide class of theoretical and experimental studies reported in the technical journals. Additionally, Holtec has confirmed the code's capability to reliably predict temperature fields in dry storage applications in a benchmark report [4.1.5] using independent full-scale test data from a loaded cask [4.1.3]. In this benchmarking report, the Holtec thermal model is shown to overpredict the measured fuel cladding temperature by a modest amount for every test set. In early 2000, PNL evaluated the thermal performance of HI-STORM 100 at discrete ambient temperatures using the COBRA-SFS Code. (Summary report communicated by T.E. Michener to J. Guttman (NRC staff) dated May 31, 2000 titled "TEMPEST Analysis of the Utah ISFSI Private Fuel Storage Facility and COBRA-SFS Analysis of the Holtec HI-STORM 100 Storage System"). The above-mentioned benchmarking report includes a comparison of the Holtec thermal model results with the PNL solution. The

comparison shows that Holtec thermal model continues to be uniformly conservative. The benchmarking of the Holtec thermal model [4.1.5] against the EPRI test data [4.1.3] and PNL COBRA-SFS study validate the suitability of the thermal model employed to evaluate the thermal performance of the HI-STORM 100 System in this document.

4.2 SUMMARY OF THERMAL PROPERTIES OF MATERIALS

Materials present in the MPCs include stainless steels (Alloy X), neutron absorber (Boral or METAMIC) and helium. Materials present in the HI-STORM storage overpack include carbon steels and concrete. Materials present in the HI-TRAC transfer cask include carbon steels, lead, Holtite-A neutron shield, and demineralized water†. In Table 4.2.1, a summary of references used to obtain cask material properties for performing all thermal analyses is presented.

Individual thermal conductivities of the alloys that comprise the Alloy X materials and the bounding Alloy X thermal conductivity are reported in Appendix 1.A of this report. Tables 4.2.2 and 4.2.3 provide numerical thermal conductivity data of materials at several representative temperatures. Thermal conductivity data for constituents of Boral (i.e., B_4C core and aluminum cladding) is provided in Table 4.2.8. Boral is a compressed neutron absorbing core with a thin layer of aluminum on both sides. Because of its sandwich construction, its conduction properties are directionally dependent (i.e., non-isotropic). In contract to Boral, METAMIC is a homogeneous neutron absorbing material with a thermal conductivity that is higher than the Boral neutron absorbing B_4C core (Figure 4.2.3) but lower than Boral's aluminum cladding. The equivalent conductivity of a Boral panel, defined as the Square Root of the Mean Sum of Squares (SRMSS) conductivity in two principal directions (through thickness and width) is closely matched by METAMIC‡. Therefore, the two materials are considered equivalent in their heat transfer performance.

For the HI-STORM overpack, the thermal conductivity of concrete and the emissivity/absorptivity of painted surfaces are particularly important. Recognizing the considerable variations in reported values for these properties, we have selected values that are conservative with respect to both authoritative references and values used in analyses on previously licensed cask dockets. Specific discussions of the conservatism of the selected values are included in the following paragraphs.

As specified in Table 4.2.1, the concrete thermal conductivity is taken from Marks' Standard Handbook for Mechanical Engineers, which is conservative compared to a variety of recognized concrete codes and references. Neville, in his book "Properties of Concrete" (4^{th} Edition, 1996), gives concrete conductivity values as high as 2.1 Btu/(hr×ft×°F). For concrete with siliceous aggregates, the type to be used in HI-STORM overpacks, Neville reports conductivities of at least 1.2 Btu/(hr×ft×°F). Data from Loudon and Stacey, extracted from Neville, reports conductivities of 0.980 to 1.310 Btu/(hr×ft×°F) for normal weight concrete protected from the weather. ACI-207.1R provides thermal conductivity values for seventeen structures (mostly dams) at temperatures from 50-150°F. Every thermal conductivity value reported in ACI-207.1R is greater than the 1.05 Btu/(hr×ft×°F) value used in the HI-STORM thermal analyses.

---

† Water from a primary source (e.g., lake or river) from which ionic impurities and precipitates have been removed.

‡ For example, at 482°F, the through-thickness and width direction conductivities of Boral (B_4C thickness fraction = 0.82) are computed as 52.9 and 58.2 Btu/hr-ft-°F respectively. The SRMSS conductivity = $[(52.9^2 + 58.2^2)/2]^{0.5}$ is 55.61 Btu/ hr-ft-°F compared to a lowerbound METAMIC conductivity (Figure 4.2.3) of 55.68 Btu/ hr-ft-°F (at 482°F).

Additionally, the NRC has previously approved analyses that use higher conductivity values than those applied in the HI-STORM thermal analysis. For example, thermal calculations for the NRC approved Vectra NUHOMS cask system (June 1996, Rev. 4A) used thermal conductivities as high as 1.17 Btu/(hr×ft×°F) at 100°F. Based on these considerations, the concrete thermal conductivity value stipulated for HI-STORM thermal analyses is considered to be conservative.

Holtite-A is a composite material consisting of approximately 37 wt% epoxy polymer, 1 wt% B_4C and 62 wt% Aluminum trihydrate. Thermal conductivity of the polymeric component is low because polymers are generally characterized by a low conductivity (0.05 to 0.2 Btu/ft-hr-°F). Addition of fillers in substantial amounts raises the mixture conductivity up to a factor of ten. Thermal conductivity of epoxy filled resins with Alumina is reported in the technical literature† as approximately 0.5 Btu/ft-hr-°F and higher. In the HI-STORM FSAR, a conservatively postulated conductivity of 0.3 Btu/ft-hr-°F is used in the thermal models for the neutron shield region (in the HI-TRAC transfer cask). As the thermal inertia of the neutron shield is not credited in the analyses, the density and heat capacity properties are not reported herein.

Surface emissivity data for key materials of construction are provided in Table 4.2.4. The emissivity properties of painted external surfaces are generally excellent. Kern [4.2.5] reports an emissivity range of 0.8 to 0.98 for a wide variety of paints. In the HI-STORM thermal analysis, an emissivity of 0.85†† is applied to painted surfaces. A conservative solar absorptivity coefficient of 1.0 is applied to all exposed overpack surfaces.

In Table 4.2.5, the heat capacity and density of the MPC, overpack and CSF materials are presented. These properties are used in performing transient (i.e., hypothetical fire accident condition) analyses. The temperature dependence of the viscosities of helium and air are provided in Table 4.2.6.

The heat transfer coefficient for exposed surfaces is calculated by accounting for both natural convection and thermal radiation heat transfer. The natural convection coefficient depends upon the product of Grashof (Gr) and Prandtl (Pr) numbers. Following the approach developed by Jakob and Hawkins [4.2.9], the product Gr×Pr is expressed as $L^3\Delta TZ$, where L is height of the overpack, ΔT is overpack surface temperature differential and Z is a parameter based on air properties, which are known functions of temperature, evaluated at the average film temperature. The temperature dependence of Z is provided in Table 4.2.7.

---

† "Principles of Polymer Systems", F. Rodriguez, Hemisphere Publishing Company (Chapter 10).

†† This is conservative with respect to prior cask industry practice, which has historically utilized higher emissivities. For example, a higher emissivity for painted surfaces ($\varepsilon = 0.95$) is used in the previously licensed TN-32 cask TSAR (Docket 72-1021).

HOLTEC INTERNATIONAL COPYRIGHTED MATERIAL

Table 4.2.1

SUMMARY OF HI-STORM SYSTEM MATERIALS
THERMAL PROPERTY REFERENCES

Material	Emissivity	Conductivity	Density	Heat Capacity
Helium	N/A	Handbook [4.2.2]	Ideal Gas Law	Handbook [4.2.2]
Air	N/A	Handbook [4.2.2]	Ideal Gas Law	Handbook [4.2.2]
Zircaloy	EPRI [4.2.3]	NUREG [4.2.6], [4.2.7]	Rust [4.2.4]	Rust [4.2.4]
UO_2	Not Used	NUREG [4.2.6], [4.2.7]	Rust [4.2.4]	Rust [4.2.4]
Stainless Steel	Kern [4.2.5]	ASME [4.2.8]	Marks' [4.2.1]	Marks' [4.2.1]
Carbon Steel	Kern [4.2.5]	ASME [4.2.8]	Marks' [4.2.1]	Marks' [4.2.1]
Boral†	Not Used	Test Data	Test Data	Test Data
Holtite-A	Not Used	Lower Bound Value Used	Not Used	Not Used
Concrete	Not Used	Marks' [4.2.1]	Marks' [4.2.1]	Handbook [4.2.2]
Lead	Not Used	Handbook [4.2.2]	Handbook [4.2.2]	Handbook [4.2.2]
Water	Not Used	ASME [4.2.10]	ASME [4.2.10]	ASME [4.2.10]
METAMIC§	Not Used	Test Data	Test Data	Test Data

† AAR Structures Boral thermophysical test data.

§ Test data provided by METAMIC Inc.

Table 4.2.2

SUMMARY OF HI-STORM SYSTEM MATERIALS
THERMAL CONDUCTIVITY DATA

Material	**@ 200°F (Btu/ft-hr-°F)**	**@ 450°F (Btu/ft-hr-°F)**	**@ 700°F (Btu/ft-hr-°F)**
Helium	0.0976	0.1289	0.1575
Air**	0.0173	0.0225	0.0272
Alloy X	8.4	9.8	11.0
Carbon Steel	24.4	23.9	22.4
Concrete††	1.05	1.05	1.05
Lead	19.4	17.9	16.9
Water	0.392	0.368	N/A

** At lower temperatures, Air conductivity is between 0.0139 Btu/ft-hr-°F (at 32°F) and 0.0176 Btu/ft-hr-°F.at 212°F.

†† Assumed constant for the entire range of temperatures.

HOLTEC INTERNATIONAL COPYRIGHTED MATERIAL

Table 4.2.3

SUMMARY OF FUEL ELEMENT COMPONENTS
THERMAL CONDUCTIVITY DATA

Zircaloy Cladding		**Fuel (UO_2)**	
Temperature (°F)	Conductivity (Btu/ft-hr-°F)	Temperature (°F)	Conductivity (Btu/ft-hr-°F)
392	8.28†	100	3.48
572	8.76	448	3.48
752	9.60	570	3.24
932	10.44	793	2.28†

† Lowest values of conductivity used in the thermal analyses for conservatism.

Table 4.2.4

SUMMARY OF MATERIALS SURFACE EMISSIVITY DATA

Material	**Emissivity**
Zircaloy	0.80
Painted surfaces	0.85
Stainless steel	0.36
Carbon Steel	0.66

Note: The emissivity of a metal surface is a function of the surface finish. In general, oxidation of a metal surface increases the emissivity. As stated in Marks' Standard Handbook for Mechanical Engineers: "Unless extraordinary pains are taken to prevent oxidation, however, a metallic surface may exhibit several times the emittance or absorptance of a polished specimen." This general statement is substantiated with a review of tabulated emissivity data from several standard references. These comparisons show that oxidized metal surfaces do indeed have higher emissivities than clean surfaces.

HOLTEC INTERNATIONAL COPYRIGHTED MATERIAL

Table 4.2.5

DENSITY AND HEAT CAPACITY PROPERTIES SUMMARY

Material	**Density (lbm/ft^3)**	**Heat Capacity (Btu/lbm-°F)**
Helium	(Ideal Gas Law)	1.24
Zircaloy	409	0.0728
Fuel (UO_2)	684	0.056
Carbon steel	489	0.1
Stainless steel	501	0.12
Boral	154.7	0.13
Concrete	142[†]	0.156
Lead	710	0.031
Water	62.4	0.999
METAMIC	163.4 – 166.6	0.22 – 0.29

[†] For conservatism in transient heatup calculations, the density is understated.

Table 4.2.6

GASES VISCOSITY† VARIATION WITH TEMPERATURE

Temperature (°F)	Helium Viscosity (Micropoise)	Temperature (°F)	Air Viscosity (Micropoise)
167.4	220.5	32.0	172.0
200.3	228.2	70.5	182.4
297.4	250.6	260.3	229.4
346.9	261.8	-	-
463.0	288.7	-	-
537.8	299.8	-	-
737.6	338.8	-	-

† Obtained from Rohsenow and Hartnett [4.2.2].

Table 4.2.7

VARIATION OF NATURAL CONVECTION PROPERTIES
PARAMETER "Z" FOR AIR WITH TEMPERATURE†

Temperature (°F)	Z ($ft^{-3}°F^{-1}$)
40	2.1×10^{6}
140	9.0×10^{5}
240	4.6×10^{5}
340	2.6×10^{5}
440	1.5×10^{5}

† Obtained from Jakob and Hawkins [4.2.9].

Table 4.2.8

BORAL COMPONENT MATERIALS[†]
THERMAL CONDUCTIVITY DATA

Temperature (°F)	B_4C Core Conductivity (Btu/ft-hr-°F)	Aluminum Cladding Conductivity (Btu/ft-hr-°F)
212	48.09	100.00
392	48.03	104.51
572	47.28	108.04
752	46.35	109.43

[†] Both B_4C and aluminum cladding thermal conductivity values are obtained from AAR Structures Boral thermophysical test data.

FIGURES 4.2.1 and 4.2.2

[INTENTIONALLY DELETED]

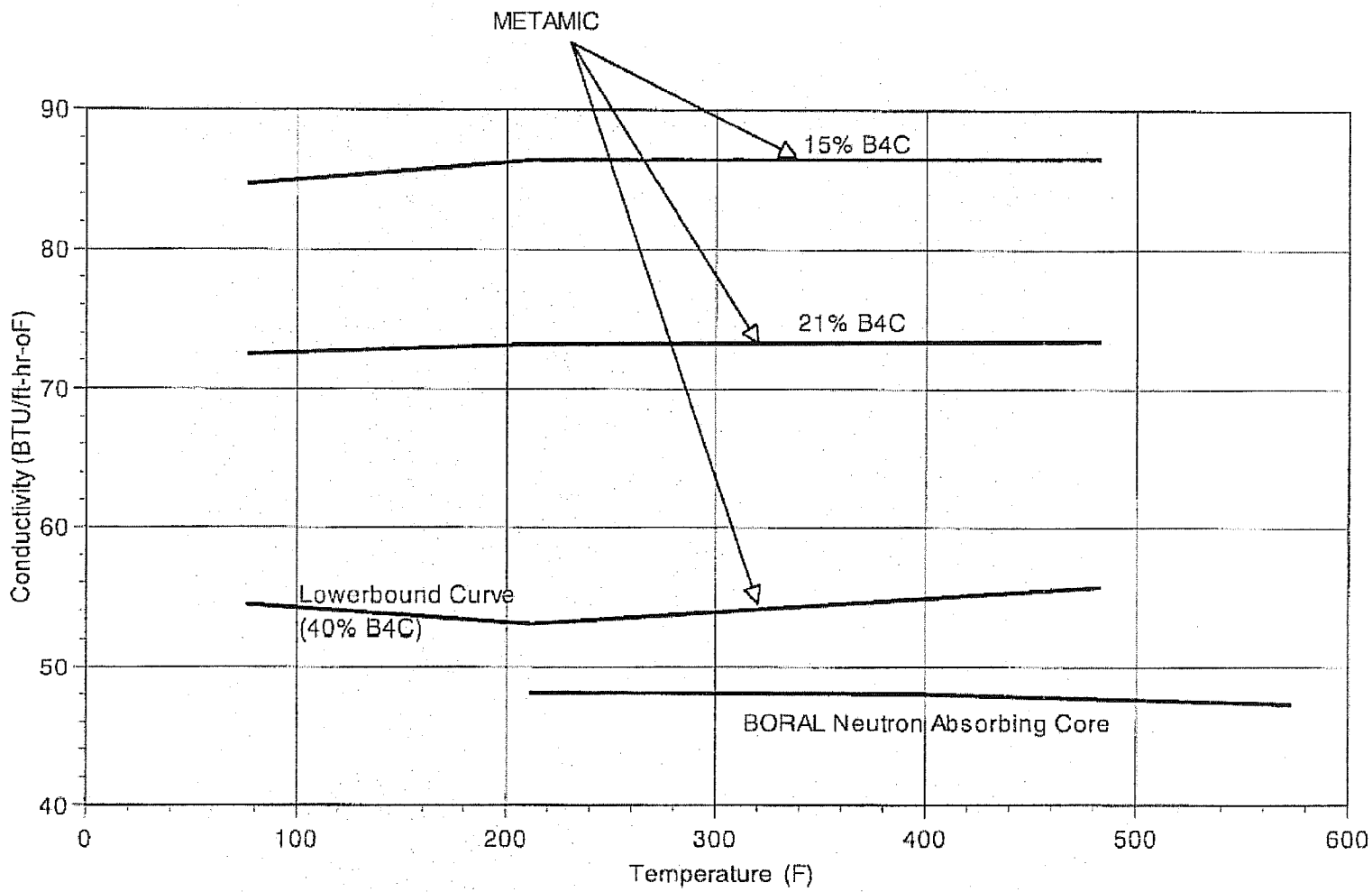

FIGURE 4.2.3: COMPARISON OF THERMAL CONDUCTIVITY OF METAMIC AND THE CERMET CORE OF A BORAL NEUTRON ABSORBER

4.3 SPECIFICATIONS FOR COMPONENTS

HI-STORM System materials and components designated as "Important to Safety" (i.e., required to be maintained within their safe operating temperature ranges to ensure their intended function) which warrant special attention are summarized in Table 4.3.1. The neutron shielding ability of Holtite-A neutron shield material used in the HI-TRAC transfer cask is ensured by demonstrating that the material exposure temperatures are maintained below the maximum allowable limit. Long-term integrity of SNF is ensured by the HI-STORM System thermal evaluation which demonstrates that fuel cladding temperatures are maintained below design basis limits. Neutron absorber materials used in MPC baskets for criticality control (made from B_4C and aluminum) are stable up to 1000°F[†]. However, for conservatism, a significantly lower temperature limit is specified for thermal evaluation. The overpack concrete, the primary function of which is shielding, will maintain its structural, thermal and shielding properties provided that American Concrete Institute (ACI) guidance on temperature limits (see Appendix 1.D) is followed.

Compliance to 10CFR72 requires, in part, identification and evaluation of short-term off-normal and severe hypothetical accident conditions. The inherent mechanical characteristics of cask materials and components ensure that no significant functional degradation is possible due to exposure to short-term temperature excursions outside the normal long-term temperature limits. For evaluation of HI-STORM System thermal performance, material temperature limits for long-term normal, short-term operations, and off-normal and accident conditions are provided in Table 4.3.1. In Table 4.3.1, ISG-11 [4.1.4] temperature limits are adopted for Commercial Spent Fuel (CSF). These limits are applicable to all fuel types, burnup levels and cladding materials approved by the NRC for power generation.

4.3.1 Evaluation of Moderate Burnup Fuel

It is recognized that hydrides present in irradiated fuel rods (predominantly circumferentially oriented) dissolve at cladding temperatures above 400°C [4.3.8]. Upon cooling below a threshold temperature (T_p), the hydrides precipitate and reorient to an undesirable (radial) direction if cladding stresses at the hydride precipitation temperature T_p are excessive. For moderate burnup fuel, T_p is conservatively estimated as 350°C [4.3.8]. In a recent study, PNNL has evaluated a number of bounding fuel rods for reorientation under hydride precipitation temperatures for MBF [4.3.8]. The study concludes that hydride reorientation is not credible during short-term operations involving low to moderate burnup fuel (up to 45 GWD/MTU). Accordingly, the higher ISG-11 temperature limit is justified for moderate burnup fuel and is adopted in the HI-STORM FSAR for short-term operations with MBF fueled MPCs (see Table 4.3.1).

[†] B4C is a refractory material that is unaffected by high temperature (on the order of 1000°F) and aluminum is solid at temperatures in excess of 1000°F.

Table 4.3.1

HI-STORM SYSTEM MATERIAL TEMPERATURE LIMITS

Material	**Normal Long-Term Temperature Limits [°F]**	**Short-Term Temperature Limits [°F]**
CSF cladding (zirconium alloys and stainless steel)	752	Short-Term Operations 752 (HBF) 1058 (MBF) Off-Normal and Accident 1058
Neutron Absorber	800	950
Holtite-A†††	N/A	350 (Short Term Operations)
Concrete†	300	350
Water	N/A	307‡ (Short Term Operations) N/A (Off-Normal and Accident)

††† See Section 1.2.1.3.2.

† These values are applicable for concrete in the overpack body, the overpack lid and, where applicable, the overpack pedestal. As stated in Chapter 1 (Appendix 1.D, Table 1.D.1), these limits are compared to the through-thickness section average temperature.

‡ Saturation temperature at HI-TRAC water jacket design pressure.

HOLTEC INTERNATIONAL COPYRIGHTED MATERIAL

4.4 THERMAL EVALUATION FOR NORMAL CONDITIONS OF STORAGE

Under long-term storage conditions, the HI-STORM System (i.e., HI-STORM overpack and MPC) thermal evaluation is performed with the MPC cavity backfilled with helium. Thermal analysis results for the long-term storage scenarios are obtained and reported in this section.

4.4.1 Thermal Model

The MPC basket design consists of four distinct geometries to hold 24 or 32 PWR, or 68 BWR fuel assemblies. The basket is a matrix of square compartments designed to hold the fuel assemblies in a vertical position. The basket is a honeycomb structure of alloy steel (Alloy X) plates with full-length edge-welded intersections to form an integral basket configuration. All individual cell walls, except outer periphery cell walls in the MPC-68 and MPC-32, are provided with Boral neutron absorber sandwiched between the box wall and a stainless steel sheathing plate over the full length of the active fuel region.

The design basis decay heat generation (per PWR or BWR assembly) for long-term normal storage is specified in Table 2.1.26. The decay heat is conservatively considered to be non-uniformly distributed over the active fuel length based on the design basis axial burnup distributions provided in Chapter 2 (Table 2.1.11).

Transport of heat from the interior of the MPC to its outer surface is accomplished by a combination of conduction through the MPC basket metal grid structure, and conduction and radiation heat transfer in the relatively small helium gaps between the fuel assemblies and basket cell walls. Heat dissipation across the gap between the MPC basket periphery and the MPC shell is by a combination of helium conduction and radiation across the gap. MPC internal helium circulation is recognized in the thermal modeling analyses reported herein. Heat rejection from the outer surface of the MPC to the environment is primarily accomplished by convective heat transfer to a buoyancy driven airflow through the MPC-to-overpack annular gap. Inlet and outlet ducts in the overpack cylinder at its bottom and top, respectively, allow circulation of air through the annulus. A secondary heat rejection path from the outer surface of the MPC to the environment involves thermal radiation heat transfer across the annular gap, radial conduction through the overpack cylinder, and natural convection and thermal radiation from the outer surface of the overpack to the atmosphere.

4.4.1.1 Analytical Model - General Remarks

Transport of heat from the heat generation region (fuel assemblies) to the outside environment (ambient air or ground) is analyzed broadly in terms of three interdependent thermal models.

1. The first model considers transport of heat from the fuel assembly to the basket cell walls. This model recognizes the combined effects of conduction (through helium) and radiation, and is essentially a finite element technology based update of the classical Wooton & Epstein [4.4.1] (which considered radiative heat exchange between fuel rod surfaces) formulation.

HOLTEC INTERNATIONAL COPYRIGHTED MATERIAL

2. The second model considers heat transport within an MPC cross section by conduction and radiation. The effective cross sectional thermal conductivity of the basket region, obtained from a combined fuel assembly/basket heat conduction-radiation model developed on ANSYS, is applied to an axisymmetric thermal model of the HI-STORM System on the FLUENT [4.1.2] code.

3. The third model deals with the transmission of heat from the MPC exterior surface to the external environment (heat sink). The upflowing air stream in the MPC/cask annulus extracts most of the heat from the external surface of the MPC, and a small amount of heat is radially deposited on the HI-STORM inner surface by conduction and radiation. Heat rejection from the outside cask surfaces to ambient air is considered by accounting for natural convection and radiative heat transfer mechanisms from the vertical (cylindrical shell) and top cover (flat) surfaces. The reduction in radiative heat exchange between cask outside vertical surfaces and ambient air, because of blockage from the neighboring casks arranged for normal storage at an ISFSI pad as described in Section 1.4, is recognized in the analysis. The overpack top plate is modeled as a heated surface in convective and radiative heat exchange with air and as a recipient of heat input through insolation. Insolation on the cask surfaces is based on 12-hour levels prescribed in 10CFR71, averaged over a 24-hour period, after accounting for partial blockage conditions on the sides of the overpack.

Subsections 4.4.1.1.1 through 4.4.1.1.9 contain a systematic description of the mathematical models devised to articulate the temperature field in the HI-STORM System. The description begins with the method to characterize the heat transfer behavior of the prismatic (square) opening referred to as the "fuel space" with a heat emitting fuel assembly situated in it. The methodology utilizes a finite element procedure to replace the heterogeneous SNF/fuel space region with an equivalent solid body having a well-defined temperature-dependent conductivity. In the following subsection, the method to replace the "composite" walls of the fuel basket cells with an equivalent "solid" wall is presented. Having created the mathematical equivalents for the SNF/fuel spaces and the fuel basket walls, the method to represent the MPC cylinder containing the fuel basket by an equivalent cylinder whose thermal conductivity is a function of the spatial location and coincident temperature is presented.

Following the approach of presenting descriptions starting from the inside and moving to the outer region of a cask, the next subsections present the mathematical model to simulate the overpack. Subsection 4.4.1.1.9 concludes the presentation with a description of how the different models for the specific regions within the HI-STORM System are assembled into the final FLUENT model.

4.4.1.1.1 Overview of the Thermal Model

Thermal analysis of the HI-STORM System is performed by assuming that the system is subject to its maximum heat duty with each storage location occupied and with the heat generation rate in each stored fuel assembly equal to the design-basis maximum value. While the assumption of equal heat generation imputes a certain symmetry to the cask thermal problem, the thermal model must incorporate three attributes of the physical problem to perform a rigorous analysis of a fully loaded cask:

HOLTEC INTERNATIONAL COPYRIGHTED MATERIAL

i. While the rate of heat conduction through metals is a relatively weak function of temperature, radiation heat exchange is a nonlinear function of surface temperatures.

ii. Heat generation in the MPC is axially non-uniform due to non-uniform axial burnup profiles in the fuel assemblies.

iii. Inasmuch as the transfer of heat occurs from inside the basket region to the outside, the temperature field in the MPC is spatially distributed with the maximum values reached in the central core region.

It is clearly impractical to model every fuel rod in every stored fuel assembly explicitly. Instead, the cross section bounded by the inside of the storage cell, which surrounds the assemblage of fuel rods and the interstitial helium gas, is replaced with an "equivalent" square (solid) section characterized by an effective thermal conductivity. Figure 4.4.1 pictorially illustrates the homogenization concept. Further details of this procedure for determining the effective conductivity are presented in Subsection 4.4.1.1.2; it suffices to state here that the effective conductivity of the cell space will be a function of temperature because the radiation heat transfer (a major component of the heat transport between the fuel rods and the surrounding basket cell metal) is a strong function of the temperatures of the participating bodies. Therefore, in effect, every storage cell location will have a different value of effective conductivity (depending on the coincident temperature) in the homogenized model. The temperature-dependent fuel assembly region effective conductivity is determined by a finite volume procedure, as described in Subsection 4.4.1.1.2.

In the next step of homogenization, a planar section of MPC is considered. With each storage cell inside space replaced with an equivalent solid square, the MPC cross section consists of a metallic gridwork (basket cell walls with each square cell space containing a solid fuel cell square of effective thermal conductivity, which is a function of temperature) circumscribed by a circular ring (MPC shell). There are four distinct materials in this section, namely the homogenized fuel cell squares, the Alloy X structural materials in the MPC (including neutron absorber sheathing), neutron absorber and helium gas. Each of the four constituent materials in this section has a different conductivity. It is emphasized that the conductivity of the homogenized fuel cells is a strong function of temperature.

In order to replace this thermally heterogeneous MPC section with an equivalent conduction-only region, resort to the finite element procedure is necessary. Because the rate of transport of heat within the MPC is influenced by radiation, which is a temperature-dependent effect, the equivalent conductivity of the MPC region must also be computed as a function of temperature. Finally, it is recognized that the MPC section consists of two discrete regions, namely, the basket region and the peripheral region. The peripheral region is the space between the peripheral storage cells and the MPC shell. This space is essentially full of helium surrounded by Alloy X plates. Accordingly, as illustrated in Figure 4.4.2 for MPC-68, the MPC cross section is replaced with two homogenized regions with temperature-dependent conductivities. In particular, the effective conductivity of the fuel cells is subsumed into the equivalent conductivity of the basket cross section. The finite element procedure used to accomplish this is described in Subsection 4.4.1.1.4. The ANSYS finite element code is the vehicle for all modeling efforts described in the foregoing.

HOLTEC INTERNATIONAL COPYRIGHTED MATERIAL

In summary, appropriate finite-element models are used to replace the MPC cross section with an equivalent two-region homogeneous conduction lamina whose local conductivity is a known function of coincident absolute temperature. Thus, the MPC cylinder containing discrete fuel assemblies, helium, neutron absorber and Alloy X, is replaced with a right circular cylinder whose material conductivity will vary with radial and axial position as a function of the coincident temperature. Finally, HI-STORM is simulated as a radially symmetric structure with a buoyancy-induced flow in the annular space surrounding the heat generating MPC cylinder.

The thermal analysis procedure described above makes frequent use of equivalent thermal properties to ease the geometric modeling of the cask components. These equivalent properties are rigorously calculated values based on detailed evaluations of actual cask system geometries. All these calculations are performed conservatively to ensure a bounding representation of the cask system. This process, commonly referred to as submodeling, yields accurate (not approximate) results. Given the detailed nature of the submodeling process, experimental validation of the individual submodels is not necessary.

Internal circulation of helium in the sealed MPC is modeled as flow in a porous media in the fueled region containing the SNF (including top and bottom plenums). The basket-to-MPC shell clearance space is modeled as a helium filled radial gap to include the downcomer flow in the thermal model. The downcomer region, as illustrated in Figure 4.4.2, consists of an azimuthally varying gap formed by the square-celled basket outline and the cylindrical MPC shell. At the locations of closest approach a differential expansion gap (a small clearance on the order of 1/10 of an inch) is engineered to allow free thermal expansion of the basket. At the widest locations, the gaps are on the order of the fuel cell opening (~6" (BWR) and ~9" (PWR) MPCs). It is heuristically evident that heat dissipation by conduction is maximum at the closest approach locations (low thermal resistance path) and that convective heat transfer is highest at the widest gap locations (large downcomer flow). In the FLUENT thermal model, a radial gap that is large compared to the basket-to-shell clearance and small compared to the cell opening is used. As a relatively large gap penalizes heat dissipation by conduction and a small gap throttles convective flow, the use of a single gap in the FLUENT model understates both conduction and convection heat transfer in the downcomer region.

The FLUENT thermal modeling methodology has been benchmarked with full-scale cask test data (EPRI TN-24P cask testing), as well as with PNNL's COBRA-SFS modeling of the HI-STORM System. The benchmarking work has been documented in a Holtec topical report HI-992252 ("Topical Report on the HI-STAR/HI-STORM Thermal Model and Its Benchmarking with Full-Size Cask Test Data").

In this manner, a loaded MPC standing upright on the ISFSI pad in a HI-STORM overpack is replaced with a right circular cylinder with spatially varying temperature-dependent conductivity. Heat is generated within the basket space in this cylinder in the manner of the prescribed axial burnup distribution. In addition, heat is deposited from insolation on the external surface of the overpack. Under steady state conditions the total heat due to internal generation and insolation is dissipated from the outer cask surfaces by natural convection and thermal radiation to the ambient

environment and from heating of upward flowing air in the annulus. Details of the elements of mathematical modeling are provided in the following.

4.4.1.1.2 Fuel Region Effective Thermal Conductivity Calculation

Thermal properties of a large number of PWR and BWR fuel assembly configurations manufactured by the major fuel suppliers (i.e., Westinghouse, CE, B&W, and GE) have been evaluated for inclusion in the HI-STORM System thermal analysis. Bounding PWR and BWR fuel assembly configurations are determined using the simplified procedure described below. This is followed by the determination of temperature-dependent properties of the bounding PWR and BWR fuel assembly configurations to be used for cask thermal analysis using a finite volume (FLUENT) approach.

To determine which of the numerous PWR assembly types listed in Table 4.4.1 should be used in the thermal model for the PWR fuel baskets (MPC-24, MPC-24E, MPC-32), we must establish which assembly type has the maximum thermal resistance. The same determination must be made for the MPC-68, out of the menu of SNF types listed in Table 4.4.2. For this purpose, we utilize a simplified procedure that we describe below.

Each fuel assembly consists of a large array of fuel rods typically arranged on a square layout. Every fuel rod in this array is generating heat due to radioactive decay in the enclosed fuel pellets. There is a finite temperature difference required to transport heat from the innermost fuel rods to the storage cell walls. Heat transport within the fuel assembly is based on principles of conduction heat transfer combined with the highly conservative analytical model proposed by Wooton and Epstein [4.4.1]. The Wooton-Epstein model considers radiative heat exchange between individual fuel rod surfaces as a means to bound the hottest fuel rod cladding temperature.

Transport of heat energy within any cross section of a fuel assembly is due to a combination of radiative energy exchange and conduction through the helium gas that fills the interstices between the fuel rods in the array. With the assumption of uniform heat generation within any given horizontal cross section of a fuel assembly, the combined radiation and conduction heat transport effects result in the following heat flow equation:

$$Q = \sigma C_o F_\varepsilon A [T_C^4 - T_B^4] + 13.5740 L K_{cs} [T_C - T_B]$$

where:

F_ε = Emissivity Factor

$$= \frac{1}{\left(\frac{1}{\varepsilon_C} + \frac{1}{\varepsilon_B} - 1\right)}$$

ε_C, ε_B = emissivities of fuel cladding, fuel basket (see Table 4.2.4)

C_o = Assembly Geometry Factor

$$= \frac{4N}{(N+1)^2} \text{ (when N is odd)}$$

$$= \frac{4}{N+2} \text{ (when N is even)}$$

N = Number of rows or columns of rods arranged in a square array
A = fuel assembly "box" heat transfer area = 4 × width × length
L = fuel assembly length
K_{cs} = fuel assembly constituent materials volume fraction weighted mixture conductivity
T_C = hottest fuel cladding temperature (°R)
T_B = box temperature (°R)
Q = net radial heat transport from the assembly interior
σ = Stefan-Boltzmann Constant (0.1714×10^{-8} Btu/ft^2-hr-°R^4)

In the above heat flow equation, the first term is the Wooten-Epstein radiative heat flow contribution while the second term is the conduction heat transport contribution based on the classical solution to the temperature distribution problem inside a square shaped block with uniform heat generation [4.4.5]. The 13.574 factor in the conduction term of the equation is the shape factor for two-dimensional heat transfer in a square section. Planar fuel assembly heat transport by conduction occurs through a series of resistances formed by the interstitial helium fill gas, fuel cladding and enclosed fuel. An effective planar mixture conductivity is determined by a volume fraction weighted sum of the individual constituent material resistances. For BWR assemblies, this formulation is applied to the region inside the fuel channel. A second conduction and radiation model is applied between the channel and the fuel basket gap. These two models are combined, in series, to yield a total effective conductivity.

The effective conductivity of the fuel for several representative PWR and BWR assemblies is presented in Tables 4.4.1 and 4.4.2. At higher temperatures (approximately 450°F and above), the zircaloy clad fuel assemblies with the lowest effective thermal conductivities are the W-17×17 OFA (PWR) and the GE11-9×9 (BWR). A discussion of fuel assembly conductivities for some of the recent vintage 10×10 array and certain plant specific BWR fuel designs is presented near the end of this subsection. As noted in Table 4.4.2, the Dresden 1 (intact and damaged) fuel assemblies are excluded from consideration. The design basis decay heat load for Dresden-1 intact and damaged fuel (Table 2.1.7) is approximately 58% lower than the MPC-68 design-basis maximum heat load (Table 2.1.6). Examining Table 4.4.2, the effective conductivity of the damaged Dresden-1 fuel assembly in a damaged fuel container is approximately 40% lower than the bounding (GE-11 9×9) fuel assembly. Consequently, the fuel cladding temperatures in the HI-STORM System with Dresden-1 intact or damaged fuel assemblies will be bounded by design basis fuel cladding temperatures. Based on this simplified analysis, the W-17×17 OFA PWR and GE11-9×9 BWR fuel assemblies are determined to be the bounding configurations for analysis of zircaloy clad fuel at design basis maximum heat loads.

HOLTEC INTERNATIONAL COPYRIGHTED MATERIAL

For the purpose of determining axial flow resistance for inclusion of MPC thermosiphon effect in the HI-STORM system modeling, equivalent porous media parameters for the W-17x17OFA and GE11-9x9 fuels are computed. Theoretically bounding expansion and contraction loss factors are applied at the grid spacer locations to conservatively maximize flow resistance. As an additional measure of conservatism, the grids are modeled by postulating that they are formed using thick metal sheets which have the effect of artificially throttling flow. Heat transfer enhancement by grid spacers turbulation is conservatively ignored in the analysis.

Having established the governing (most resistive) PWR and BWR SNF types, we use a finite-volume code to determine the effective conductivities in a conservative manner. Detailed conduction-radiation finite-volume models of the bounding PWR and BWR fuel assemblies developed on the FLUENT code are shown in Figures 4.4.3 and 4.4.4, respectively. The PWR model was originally developed on the ANSYS code, which enables individual rod-to-rod and rod-to-basket wall view factor calculations to be performed using the AUX12 processor. Limitations of radiation modeling techniques implemented in ANSYS do not permit taking advantage of quarter symmetry of the fuel assembly geometry. Unacceptably long CPU time and large workspace requirements necessary for performing gray body radiation calculations for a complete fuel assembly geometry on ANSYS prompted the development of an alternate simplified model on the FLUENT code. The FLUENT model is benchmarked with the ANSYS model results for a Westinghouse 17×17 fuel assembly geometry for the case of black body radiation (emissivities = 1). The FLUENT model is found to yield conservative results in comparison to the ANSYS model for the "black" surface case. The FLUENT model benchmarked in this manner is used to solve the gray body radiation problem to provide the necessary results for determining the effective thermal conductivity of the governing PWR fuel assembly. The same modeling approach using FLUENT is then applied to the governing BWR fuel assembly, and the effective conductivity of GE-11 9×9 fuel determined.

The combined fuel rods-helium matrix is replaced by an equivalent homogeneous material that fills the basket opening by the following two-step procedure. In the first step, the FLUENT-based fuel assembly model is solved by applying equal heat generation per unit length to the individual fuel rods and a uniform boundary temperature along the basket cell opening inside periphery. The temperature difference between the peak cladding and boundary temperatures is used to determine an effective conductivity as described in the next step. For this purpose, we consider a two-dimensional cross section of a square shaped block with an edge length of 2L and a uniform volumetric heat source (q_g), cooled at the periphery with a uniform boundary temperature. Under the assumption of constant material thermal conductivity (K), the temperature difference (ΔT) from the center of the cross section to the periphery is analytically given by [4.4.5]:

$$\Delta T = 0.29468 \frac{q_g L^2}{K}$$

This analytical formula is applied to determine the effective material conductivity from a known quantity of heat generation applied in the FLUENT model (smeared as a uniform heat source, q_g) basket opening size and ΔT calculated in the first step.

HOLTEC INTERNATIONAL COPYRIGHTED MATERIAL

As discussed earlier, the effective fuel space conductivity must be a function of the temperature coordinate. The above two-step analysis is carried out for a number of reference temperatures. In this manner, the effective conductivity as a function of temperature is established.

In Table 4.4.5, 10×10 array type BWR fuel assembly conductivity results from a simplified analysis are presented to determine the most resistive fuel assembly in this class. The Atrium-10 fuel type is determined to be the most resistive in this class of fuel assemblies. A detailed finite-element model of this assembly type was developed to rigorously quantify the heat dissipation characteristics. The results of this study are presented in Table 4.4.6 and compared to the BWR bounding fuel assembly conductivity depicted in Figure 4.4.5. The results of this study demonstrate that the bounding fuel assembly conductivity is conservative with respect to the 10×10 class of BWR fuel assemblies.

Table 4.4.23 summarizes plant specific fuel types' effective conductivities. From these analytical results, SPC-5 is determined to be the most resistive fuel assembly in this group of fuel. A finite element model of the SPC-5 fuel assembly was developed to confirm that its in-plane heat dissipation characteristics are bounded from below by the Design Basis BWR fuel conductivities used in the HI-STORM thermal analysis.

Temperature-dependent effective conductivities of PWR and BWR design basis fuel assemblies (most resistive SNF types) are shown in Figure 4.4.5. The finite volume results are also compared to results reported from independent technical sources. From this comparison, it is readily apparent that FLUENT-based fuel assembly conductivities are conservative. The FLUENT computed values (not the published literature data) are used in the MPC thermal analysis presented in this document.

4.4.1.1.3 Effective Thermal Conductivity of Neutron Absorber/Sheathing/Box Wall Sandwich

Each MPC basket cell wall (except the MPC-68 and MPC-32 outer periphery cell walls) is manufactured with a neutron absorbing plate for criticality control. Each neutron absorber plate is sandwiched in a sheathing-to-basket wall pocket. A schematic of the "Box Wall - Neutron Absorber - Sheathing" sandwich geometry of an MPC basket is illustrated in Figure 4.4.6. During fabrication, a uniform normal pressure is applied to each "Box Wall - Neutron Absorber - Sheathing" sandwich in the assembly fixture during welding of the sheathing periphery on the box wall. This ensures adequate surface-to-surface contact for elimination of any macroscopic air gaps. The mean coefficient of linear expansion of the neutron absorber is higher than the thermal expansion coefficients of the basket and sheathing materials. Consequently, basket heat-up from the stored SNF will further ensure a tight fit of the neutron absorber plate in the sheathing-to-box pocket. The presence of small microscopic gaps due to less than perfect surface finish characteristics requires consideration of an interfacial contact resistance between the neutron absorber and box-sheathing surfaces. A conservative contact resistance resulting from a 2 mil neutron absorber to pocket gap is applied in the analysis. In other words, no credit is taken for the interfacial pressure between neutron absorber and stainless plate/sheet stock produced by the fixturing and welding process. Furthermore, no credit is taken for radiative heat exchange across the neutron absorber to sheathing or neutron absorber to box wall gaps.

HOLTEC INTERNATIONAL COPYRIGHTED MATERIAL

Heat conduction properties of a composite "Box Wall - Neutron Absorber - Sheathing" sandwich in the two principal basket cross sectional directions as illustrated in Figure 4.4.6 (i.e., lateral "out-of-plane" and longitudinal "in-plane") are unequal. In the lateral direction, heat is transported across layers of sheathing, air-gap, neutron absorber and box wall resistances that are essentially in series (except for the small helium filled end regions shown in Figure 4.4.7). Heat conduction in the longitudinal direction, in contrast, is through an array of essentially parallel resistances comprised of these several layers listed above. Resistance network models applicable to the two directions are illustrated in Figure 4.4.7. It is noted that, in addition to the essentials series and parallel resistances of the composite wall layers for the "out-of-plane" and "in-plane" directions, respectively, the effect of small helium end regions is also included in the network resistance analogy. For the ANSYS based MPC basket thermal model, corresponding non-isotropic effective thermal conductivities in the two orthogonal sandwich directions are determined and applied in the analysis.

4.4.1.1.4 Modeling of Basket Conductive Heat Transport

The total conduction heat rejection capability of a fuel basket is a combination of planar and axial contributions. These component contributions are calculated independently for each MPC basket design and then combined to obtain an equivalent isotropic thermal conductivity value.

The planar heat rejection capability of each MPC basket design (i.e., MPC-24, MPC-68, MPC-32 and MPC-24E) is evaluated by developing a thermal model of the combined fuel assemblies and composite basket walls geometry on the ANSYS finite element code. The ANSYS model includes a geometric layout of the basket structure in which the basket "Box Wall - Neutron Absorber - Sheathing" sandwich is replaced by a "homogeneous wall" with an equivalent thermal conductivity. Since the thermal conductivity of the Alloy X material is a weakly varying function of temperature, the equivalent "homogeneous wall" must have a temperature-dependent effective conductivity. Similarly, as illustrated in Figure 4.4.7, the conductivities in the "in-plane" and "out-of-plane" directions of the equivalent "homogeneous wall" are different. Finally, as discussed earlier, the fuel assemblies and the surrounding basket cell openings are modeled as homogeneous heat generating regions with an effective temperature dependent in-plane conductivity. The methodology used to reduce the heterogeneous MPC basket - fuel assemblage to an equivalent homogeneous region with effective thermal properties is discussed in the following.

Consider a cylinder of height, L, and radius, r_o, with a uniform volumetric heat source term, q_g, insulated top and bottom faces, and its cylindrical boundary maintained at a uniform temperature, T_c. The maximum centerline temperature (T_h) to boundary temperature difference is readily obtained from classical one-dimensional conduction relationships (for the case of a conducting region with uniform heat generation and a constant thermal conductivity K_s):

$$(T_h - T_c) = q_g r_o^2/(4 K_s)$$

Noting that the total heat generated in the cylinder (Q_t) is $\pi r_o^2 L q_g$, the above temperature rise formula can be reduced to the following simplified form in terms of total heat generation per unit length (Q_t/L):

HOLTEC INTERNATIONAL COPYRIGHTED MATERIAL

$$(T_h - T_c) = (Q_t / L)/ (4 \pi K_s)$$

This simple analytical approach is employed to determine an effective basket cross-sectional conductivity by applying an equivalence between the ANSYS finite element model of the basket and the analytical case. The equivalence principle employed in the thermal analysis is depicted in Figure 4.4.2. The 2-dimensional ANSYS finite element model of the MPC basket is solved by applying a uniform heat generation per unit length in each basket cell region (depicted as Zone 1 in Figure 4.4.2) and a constant basket periphery boundary temperature, T_c'. Noting that the basket region with uniformly distributed heat sources and a constant boundary temperature is equivalent to the analytical case of a cylinder with uniform volumetric heat source discussed earlier, an effective MPC basket conductivity (K_{eff}) is readily derived from the analytical formula and ANSYS solution leading to the following relationship:

$$K_{eff} = N (Q_f'/L) / (4 \pi [T_h' - T_c'])$$

where:

N = number of fuel assemblies
(Q_f'/L) = per fuel assembly heat generation per unit length applied in ANSYS model
T_h' = peak basket cross-section temperature from ANSYS model

Cross sectional views of MPC basket ANSYS models are depicted in Figures 4.4.9 and 4.4.10. Temperature-dependent equivalent thermal conductivities of the fuel regions and composite basket walls, as determined from analysis procedures described earlier, are applied to the ANSYS model. The planar ANSYS conduction model is solved by applying a constant basket periphery temperature with uniform heat generation in the fuel region. The equivalent planar thermal conductivity values are lower bound values because, among other elements of conservatism, the effective conductivity of the most resistive SNF types (Tables 4.4.1 and 4.4.2) is used in the MPC finite element simulations.

The basket in-plane conductivities are computed for intact fuel storage and containerized fuel stored in Damaged Fuel Containers (DFCs). The MPC-24E is provided with four enlarged cells designated for storing damaged fuel. The MPC-68 has sixteen peripheral locations for damaged fuel storage in generic DFC designs. The MPC-32 has eight peripheral locations for damaged fuel storage in generic DFC designs. As a substantial fraction of the basket cells are occupied by intact fuel, the overall effect of DFC fuel storage on the basket heat dissipation rate is quite small. Including the effect of reduced conductivity of the DFC cells in MPC-24E, the basket conductivity is computed to drop slightly (~0.6%). In a bounding calculation in which all cells of MPC-68 are assumed occupied by fuel in DFC, the basket conductivity drops by about 5%. In a bounding calculation in which all cells of an MPC-32 are assumed occupied by fuel in DFCs, the basket conductivity drops by about 17%. Conservatively, assuming 95% of intact fuel basket heat load adequately covers damaged fuel storage in the MPC-24E and MPC-68 and assuming 80% of intact fuel basket heat load adequately covers damaged fuel storage in the MPC-32.

The axial heat rejection capability of each MPC basket design is determined by calculating the area occupied by each material in a fuel basket cross-section, multiplying by the corresponding material thermal conductivity, summing the products and dividing by the total fuel basket cross-sectional

area. In accordance with NUREG-1536 guidelines, the only portion of the fuel assemblies credited in these calculations is the fuel rod cladding (i.e., the contribution of fuel pellets to axial heat conduction is ignored).

Having obtained planar and axial effective thermal conductivity contributions as described above, an equivalent isotropic thermal conductivity that yields the same overall heat transfer can be obtained. Two-dimensional conduction heat transfer in relatively short cylinders cannot be readily evaluated analytically, so an alternate approach is used herein.

Instead of computing precise isotropic conductivities, an RMS function of the planar and axial effective thermal conductivity values is used as follows:

$$k_{iso} = \sqrt{\frac{k_{rad}^{\ 2} + k_{ax}^{\ 2}}{2}}$$

where:

k_{iso} = equivalent isotropic thermal conductivity
k_{rad} = equivalent planar thermal conductivity
k_{ax} = equivalent axial thermal conductivity

This formulation has been benchmarked for specific application to the MPC basket designs and found to yield conservative equivalent isotropic thermal conductivities and, subsequently, conservative temperature results from subsequent thermal analyses.

Table 4.4.3 summarizes the isotropic MPC basket thermal conductivity values used in the subsequent cask thermal modeling. It should be noted that the isotropic conductivities calculated as described above are actually higher than those reported in Table 4.4.3, imparting additional conservatism to the subsequent calculations.

4.4.1.1.5 Subsection Intentionally Deleted

4.4.1.1.6 Subsection Intentionally Deleted

4.4.1.1.7 Annulus Air Flow and Heat Exchange

The HI-STORM storage overpack is provided with four inlet ducts at the bottom and four outlet ducts at the top. The ducts are provided to enable relatively cooler ambient air to flow through the annular gap between the MPC and storage overpack in the manner of a classical "chimney". Hot air is vented from the top outlet ducts to the ambient environment. Buoyancy forces induced by density differences between the ambient air and the heated air column in the MPC-to-overpack annulus sustain airflow through the annulus.

In contrast to a classical chimney, however, the heat input to the HI-STORM annulus air does not occur at the bottom of the stack. Rather, the annulus air picks up heat from the lateral surface of the MPC shell as it flows upwards. The height dependent heat absorption by the annulus air must be

properly accounted for to ensure that the buoyant term in the Bernoulli equation is not overstated making the solution unconservative. To fix ideas, consider two cases of stack heat input; Case A where the heat input to the rising air is all at the bottom (the "fireplace" scenario), and Case B, where the heat input is uniform along the entire height (more representative of the ventilated cask conditions). In both cases, we will assume that the air obeys the perfect gas law; i.e., at constant pressure, $\rho = C/T$ where ρ and T are the density and the absolute temperature of the air and C is a constant.

Case A: Entire Heat Input at the Bottom

In a stack of height H, where the temperature of the air is raised from T_i to T_o at the bottom (Figure 4.4.12; Case A), the net fluid "head" p_l is given by:

$$p_l = \rho_i H - \rho_o H$$

ρ_I and ρ_o are the densities of air corresponding to absolute temperatures T_i and T_o, respectively.

Since $\rho_i = \frac{C}{T_i}$ and $\rho_o = \frac{C}{T_o}$, we have:

$$p_l = CH\left(\frac{1}{T_i} - \frac{1}{T_o}\right)$$

or

$$p_l = \frac{CH\,\Delta T}{T_i\,T_o}$$

where: $\Delta T = T_o - T_i$

Let $\Delta T << Ti$, then we can write:

$$\frac{1}{T_o} = \frac{1}{T_i\left(1+\frac{\Delta T}{T_i}\right)}$$

$$= \frac{1}{T_i}\left[1 - \frac{\Delta T}{T_i} + ...\right]$$

Substituting in the above we have:

$$p_l = \frac{CH}{T_i}\delta\,(1 - \delta + ...)$$

where $\delta = \frac{\Delta T}{T_i}$ (dimensionless temperature rise)

or $p_1 = \rho_i H \delta - O(\delta^2)$.

Case B: Uniform Heat Input

In this case, the temperature of air rises linearly from T_i at the bottom to T_o at the top (Figure 4.4.12; Case B):

$$T_o = T_i + \zeta h \; ; 0 \le h \le H$$

where:

$$\zeta = \frac{T_o - T_i}{H} = \frac{\delta T_i}{H}$$

The total buoyant head, in this case, is given by:

$$p_2 = \rho_i H - \int_0^H \rho \, dh$$

$$= \rho_i H - C \int_0^H \frac{1}{T} dh$$

$$= \rho_i H - C \int_0^H \frac{dh}{(T_i + \zeta h)}$$

$$= \rho_i H - \frac{C}{\zeta} \ell n (1 + \delta)$$

Using the logarithmic expansion relationship and simplifying we have:

$$p_2 = \frac{\rho_i H \delta}{2} - O(\Delta^2)$$

Neglecting terms of higher order, we conclude that p_2 is only 50% of p_1, i.e., the buoyancy driver in the case of uniformly distributed heat input to the air is half of the value if the heat were all added at the bottom.

In the case of HI-STORM, the axial heat input profile into the annulus air will depend on the temperature difference between the MPC cylindrical surface and the rising air along the height (Case C in Figure 4.4.12). The MPC surface temperature profile, of course, is a strong function of the axial decay heat generation profile in the SNF. Previous analyses show that the HI-STORM "chimney" is less than 50% as effective as a classical chimney. As we explain in Subsection 4.4.1.1.9, this fact is fully recognized in the global HI-STORM thermal model implementation of FLUENT.

4.4.1.1.8 Determination of Solar Heat Input

The intensity of solar radiation incident on an exposed surface depends on a number of time varying terms. The solar heat flux strongly depends upon the time of the day as well as on latitude and day of

the year. Also, the presence of clouds and other atmospheric conditions (dust, haze, etc.) can significantly attenuate solar intensity levels. Rapp [4.4.2] has discussed the influence of such factors in considerable detail.

Consistent with the guidelines in NUREG-1536 [4.4.10], solar input to the exposed surfaces of the HI-STORM overpack is determined based on 12-hour insolation levels recommended in 10CFR71 (averaged over a 24-hour period) and applied to the most adversely located cask after accounting for partial blockage of incident solar radiation on the lateral surface of the cask by surrounding casks. In reality, the lateral surfaces of the cask receive solar heat depending on the azimuthal orientation of the sun during the course of the day. In order to bound this heat input, the lateral surface of the cask is assumed to receive insolation input with the solar insolation applied horizontally into the cask array. The only reduction in the heat input to the lateral surface of the cask is due to partial blockage offered by the surrounding casks. In contrast to its lateral surface, the top surface of HI-STORM is fully exposed to insolation without any mitigation effects of blockage from other bodies. In order to calculate the view factor between the most adversely located HI-STORM system in the array and the environment, a conservative geometric simplification is used. The system is reduced to a concentric cylinder model, with the inner cylinder representing the HI-STORM unit being analyzed and the outer shell representing a reflecting boundary (no energy absorption).

Thus, the radius of the inner cylinder (R_i) is the same as the outer radius of a HI-STORM overpack. The radius of the outer cylinder (R_o) is set such that the rectangular space ascribed to a cask is preserved. This is further explained in the next subsection. It can be shown that the view factor from the outer cylinder to the inner cylinder (F_{o-i}) is given by [4.4.3]:

$$F_{o-i} = \frac{1}{R} - \frac{1}{\pi R} \times \left[\cos^{-1}\left(\frac{B}{A}\right) - \frac{1}{2L}\left\{\sqrt{(A+2)^2 - (2R)^2} \times \cos^{-1}\left(\frac{B}{RA}\right) + B\sin^{-1}\left(\frac{1}{R}\right) - \frac{\pi A}{2}\right\}\right]$$

where:

F_{o-i} = View Factor from the outer cylinder to the inner cylinder
R = Outer Cylinder Radius to Inner Cylinder Radius Ratio (R_o/R_i)
L = Overpack Height to Radius Ratio
$A = L^2 + R^2 - 1$
$B = L^2 - R^2 + 1$

Applying the theorem of reciprocity, the view factor (F_{i-a}) from outer overpack surface, represented by the inner cylinder, to the ambient can be determined as:

$$F_{i-a} = 1 - F_{o-i}\frac{R_o}{R_i}$$

Finally, to bound the quantity of heat deposited onto the HI-STORM surface by insolation, the absorptivity of the cask surfaces is assumed to be unity.

HOLTEC INTERNATIONAL COPYRIGHTED MATERIAL

4.4.1.1.9 FLUENT Model for HI-STORM

In the preceding subsections, a series of analytical and numerical models to define the thermal characteristics of the various elements of the HI-STORM System are presented. The thermal modeling begins with the replacement of the Spent Nuclear Fuel (SNF) cross section and surrounding fuel cell space with a solid region with an equivalent conductivity. Since radiation is an important constituent of the heat transfer process in the SNF/storage cell space, and the rate of radiation heat transfer is a strong function of the surface temperatures, it is necessary to treat the equivalent region conductivity as a function of temperature. Because of the relatively large range of temperatures in a loaded HI-STORM System under the design basis heat loads, the effects of variation in the thermal conductivity of the Alloy X basket wall with temperature are included in the numerical analysis model. The presence of significant radiation effects in the storage cell spaces adds to the imperative to treat the equivalent storage cell lamina conductivity as temperature-dependent.

Numerical calculations and FLUENT finite-volume simulations have been performed to establish the equivalent thermal conductivity as a function of temperature for the limiting (thermally most resistive) BWR and PWR spent fuel types. Utilizing the most limiting SNF (established through a simplified analytical process for comparing conductivities) ensures that the numerical idealization for the fuel space effective conductivity is conservative for all non-limiting fuel types.

Having replaced the fuel spaces by solid square blocks with a temperature-dependent conductivity essentially renders the basket into a non-homogeneous three-dimensional solid where the non-homogeneity is introduced by the honeycomb basket structure composed of interlocking basket panels. The basket panels themselves are a composite of Alloy X cell wall, neutron absorber, and Alloy X sheathing metal. A conservative approach to replace this composite section with an equivalent "solid wall" was described earlier.

In the next step, a planar section of the MPC is considered. The MPC contains a non-symmetric basket lamina wherein the equivalent fuel spaces are separated by the "equivalent" solid metal walls. The space between the basket and the MPC, called the peripheral gap, is filled with helium gas. At this stage in the thermal analysis, the SNF/basket/MPC assemblage has been replaced with a two-zone (Figure 4.4.2) cylindrical solid whose thermal conductivity is a strong function of temperature.

The fuel assembly and MPC basket effective conductivity evaluations are performed for two distinct scenarios described earlier in this section. In the first scenario, the MPC cavity is backfilled with helium only. In the second scenario, gaseous fission products from a hypothetical rupture of 10% of the stored fuel rods dilute the backfill helium gas. As previously stated, thermal analysis results for both scenarios are obtained and reported in this section.

The thermal model for the HI-STORM overpack is prepared as a two-dimensional axisymmetric body. For this purpose, the hydraulic resistances of the inlet ducts and outlet ducts, respectively, are represented by equivalent axisymmetric porous media. Three overpack configurations are evaluated – HI-STORM 100 and two shorter variations (HI-STORM 100S and 100S Version B). HI-STORM

HOLTEC INTERNATIONAL COPYRIGHTED MATERIAL

100S features a smaller inlet duct-to-outlet duct separation and an optional enhanced gamma shield cross plate. Since the optional gamma shield cross plate flow resistance is bounding, the optional design was conservatively evaluated in the thermal analysis.The fuel cladding temperatures for MPC emplaced in a HI-STORM 100S overpack are confirmed to be bounded by the HI-STORM 100 System thermal model solution. Thus, separate table summaries for HI-STORM 100S overpack are not provided. HI-STORM 100S Version B features smaller inlet and outlet ducts with larger width to height aspect ratios and an even smaller inlet duct-to-outlet duct separation. Both the gamma shield cross plates and the duct "screens" in the 100S Version B are also modified. As the fuel clad temperatures for MPCs emplaced in a HI-STORM 100S Version B are confirmed to be bounded by the HI-STORM 100 System, only uniform loading conditions are evaluated for the Version B. The axial resistance to airflow in the MPC/overpack annulus (which includes longitudinal channels to "cushion" the stresses in the MPC structure during a postulated non-mechanistic tip-over event) is replaced by a hydraulically equivalent annulus. Finally, it is necessary to describe the external boundary conditions to the overpack situated on an ISFSI pad. An isolated HI-STORM will take suction of cool air from and reject heated air to, a semi-infinite half-space. In a rectilinear HI-STORM array, however, the unit situated in the center of the grid is evidently hydraulically most disadvantaged, because of potential interference to air intake from surrounding casks. To simulate this condition in a conservative manner, we erect a hypothetical cylindrical barrier around the centrally local HI-STORM. The radius of this hypothetical cylinder, R_o, is computed from the equivalent cask array downflow hydraulic diameter (D_h) which is obtained as follows:

$$D_h = \frac{4 \times \text{Flow Area}}{\text{Wetted Perimeter}}$$

$$= \frac{4\left(A_o - \frac{\pi}{4} d_o^{\,2}\right)}{\pi d_o}$$

where:

A_o = Minimum tributary area ascribable to one HI-STORM (see Figure 4.4.24).
d_o = HI-STORM overpack outside diameter

The hypothetical cylinder radius, R_o, is obtained by adding half D_h to the radius of the HI-STORM overpack. In this manner, the hydraulic equivalence between the cask array and the HI-STORM overpack to hypothetical cylindrical annulus is established.

For purposes of the design basis analyses reported in this chapter, the tributary area A_o is assumed to be equal to 346 sq. ft. Sensitivity studies on the effect of the value of A_o on the thermal performance of the HI-STORM System shows that the system response is essentially insensitive to the assumed value of the tributary area. For example, a thermal calculation using A_o=225 sq. ft. (corresponding to 15 ft. square pitch) and design basis heat load showed that the peak cladding temperature is less than 1°C greater than that computed using A_o= 346 sq. ft. Therefore, the distance between the vertically

HOLTEC INTERNATIONAL COPYRIGHTED MATERIAL

arrayed HI-STORMs in an ISFSI should be guided by the practical (rather than thermal) considerations, such as personnel access to maintain air ducts or painting the cask external surfaces.

The internal surface of the hypothetical cylinder of radius R_o surrounding the HI-STORM module is conservatively assumed to be insulated. Any thermal radiation heat transfer from the HI-STORM overpack to this insulated surface will be perfectly reflected, thereby bounding radiative blocking from neighboring casks. Then, in essence, the HI-STORM module is assumed to be confined in a large cylindrical "tank" whose wall surface boundaries are modeled as zero heat flux boundaries. The air in the "tank" is the source of "feed air" to the overpack. The air in the tank is replenished by ambient air from above the top of the HI-STORM overpacks. There are two sources of heat input to the exposed surface of the HI-STORM overpack. The most important source of heat input is the internal heat generation within the MPC. The second source of heat input is insolation, which is conservatively quantified in the manner of the preceding subsection.

The FLUENT model consisting of the axisymmetric 2-D MPC space, the overpack, and the enveloping tank is schematically illustrated in Figure 4.4.13. The HI-STORM thermosiphon-enabled solution is computed in a two-step process. In the first step, a HI-STORM overpack thermal model computes the ventilation effect from annulus heating by MPC decay heat. In this model, heat dissipation is conservatively restricted to the MPC shell (i.e., heat dissipation from MPC lid and baseplate completely neglected. This modeling assumption has the effect of overstating the MPC shell, annulus air and concrete temperatures. In the next step, the temperature of stored fuel in a pressurized helium canister (thermosiphon model) is determined using the overpack thermal solution in the first step to fashion a bounding MPC shell temperature profile for the MPC thermal model. The modeling details are provided in the Holtec benchmarking report [4.1.5]. A summary of the essential features of this model is presented in the following:

- A conservatively lower bound canister pressure of 5 atm is postulated for the thermosiphon modeling.

- Heat input due to insolation is applied to the top surface and the cylindrical surface of the overpack with a bounding maximum solar absorbtivity equal to 1.0.

- The heat generation in the MPC is assumed to be uniform in each horizontal plane, but to vary in the axial direction to correspond to the axial power distribution listed in Chapter 2.

- The most disadvantageously placed cask (i.e., the one subjected to maximum radiative blockage), is modeled.

- The bottom surface of the overpack, in contact with the ISFSI pad, rejects heat through the pad to the constant temperature (77°F) earth below. For some scenarios, the bottom surface of the overpack is conservatively assumed to be adiabatic.

The finite-volume model constructed in this manner will produce an axisymmetric temperature distribution. The peak temperature will occur at the centerline and is expected to be above the axial

HOLTEC INTERNATIONAL COPYRIGHTED MATERIAL

location of peak heat generation. As will be shown in Subsection 4.4.2, the results of the finite-volume solution bear out these observations.

The HI-STORM 100 System is evaluated for two fuel storage scenarios. In one scenario, designated as uniform loading, every basket cell is assumed to be occupied with fuel producing heat at the maximum rate. Storage of moderate burnup and high burnup fuels are analyzed for this loading scenario. In another scenario, denoted as regionalized loading, a two-region fuel loading configuration is stipulated. The two regions are defined as an inner region (for storing hot fuel) and an outer region with low decay heat fuel physically enveloping the inner region. This scenario is depicted in Figure 4.4.25. The inner region is shown populated with fuel having a heat load of q_1 and the outer region with fuel of heat load q_2, where $q_1 > q_2$. To permit hot fuel storage in the inner region, a uniform low decay heat rate is stipulated for the outer region fuel. In the HI-STORM 100 System, four central locations in the MPC-24 and MPC-24E, twelve inner cells in MPC-32 and 32 in MPC-68 are designated as inner region locations in the regionalized fuel-loading scenario. Results of thermal evaluations for both scenarios are present in Subsection 4.4.2.

4.4.1.1.10 Effect of Fuel Cladding Crud Resistance

In this subsection, a conservatively bounding estimate of temperature drop across a crud film adhering to a fuel rod during dry storage conditions is determined. The evaluation is performed for a BWR fuel assembly based on an upper bound crud thickness obtained from the PNL-4835 report ([4.3.2], Table 3). The crud present on the fuel assemblies is predominately iron oxide mixed with small quantities of other metals such as cobalt, nickel, chromium, etc. Consequently, the effective conductivity of the crud mixture is expected to be in the range of typical metal alloys. Metals have thermal conductivities several orders of magnitude larger than that of helium. In the interest of extreme conservatism, however, a film of helium with the same thickness replaces the crud layer. The calculation is performed in two steps. In the first step, a crud film resistance is determined based on a bounding maximum crud layer thickness replaced with a helium film on the fuel rod surfaces. This is followed by a peak local cladding heat flux calculation for the GE 7×7 array fuel assembly postulated to emit a conservatively bounding decay heat equal to 0.5kW. The temperature drop across the crud film obtained as a product of the heat flux and crud resistance terms is determined to be less than 0.1°F. The calculations are presented below.

Bounding Crud Thickness(s) = 130μm (4.26×10^{-4} ft) (PNL-4835)
Crud Conductivity (K) = 0.1 Btu/ft-hr-°F (conservatively assumed as helium)
GE 7×7 Fuel Assembly:

Rod O.D.	=	0.563"
Active Fuel Length	=	150"
Heat Transfer Area	=	$(7\times7) \times (\pi\times0.563) \times (150/144) = 90.3$ ft^2
Axial Peaking Factor	=	1.195 (Burnup distribution Table 2.1.11)
Decay Heat	=	500W (conservative assumption)

HOLTEC INTERNATIONAL COPYRIGHTED MATERIAL

$$\text{Crud Resistance} = \frac{\delta}{K} = \frac{4.26\times10^{-4}}{0.1} = 4.26\times10^{-3}\,\frac{\text{ft}^2\text{-hr-}^\circ\text{F}}{\text{Btu}}$$

$$\text{Peak Heat Flux} = \frac{(500\times3.417)\,\text{Btu/hr}}{90.3\,\text{ft}^2}\times1.195$$

$$= 18.92\times1.195 = 22.6\,\frac{\text{Btu}}{\text{ft}^2\,\text{hr}}$$

Temperature drop (ΔT_c) across crud film

$$= 4.26\times10^{-3}\,\frac{\text{ft}^2\text{-hr-}^\circ\text{F}}{\text{Btu}}\times22.6\,\frac{\text{Btu}}{\text{ft}^2\text{-hr}}$$

$$= 0.096^\circ\text{F}$$

(i.e., less than 0.1°F)

Therefore, it is concluded that deposition of crud does not materially change the SNF cladding temperature.

4.4.1.1.11 Thermal Conductivity Calculations with Diluted Backfill Helium

In this subsection, the thermal conductivities of mixtures of the helium backfill gas and the gaseous fission products released from a hypothetical rupture of 10% of the stored fuel rods are evaluated. The gaseous fission products release fractions are stipulated in NUREG-1536. The released gases will mix with the helium backfill gas and reduce its thermal conductivity. These reduced thermal conductivities are applied to determine fuel assembly, and MPC fuel basket and basket periphery effective conductivities for thermal evaluation of the HI-STORM System.

Appendix C of NUREG/CR-0497 [4.4.7] describes a method for calculating the effective thermal conductivity of a mixture of gases. The same method is also described by Rohsenow and Hartnett [4.2.2]. The following expression is provided by both references:

$$k_{mix} = \sum_{i=1}^{n}\left(\frac{k_i x_i}{x_i + \sum_{\substack{j=1\\ j\neq i}}^{n}\varphi_{ij}x_j}\right)$$

where:

k_{mix} = thermal conductivity of the gas mixture (Btu/hr-ft-°F)
n = number of gases
k_i = thermal conductivity of gas component i (Btu/hr-ft-°F)
x_i = mole fraction of gas component i

In the preceding equation, the term φ_{ij} is given by the following:

$$\varphi_{ij} = \varphi_{ij}\left[1 + 2.41\frac{(M_i - M_j)(M_i - 0.142 \cdot M_j)}{(M_i + M_j)^2}\right]$$

where M_i and M_j are the molecular weights of gas components i and j, and ϕ_{ij} is:

$$\varphi_{ij} = \frac{\left[1 + \left(\frac{k_i}{k_j}\right)^{\frac{1}{2}}\left(\frac{M_i}{M_j}\right)^{\frac{1}{4}}\right]^2}{2^{\frac{3}{2}}\left(1 + \frac{M_i}{M_j}\right)^{\frac{1}{2}}}$$

Table 4.4.7 presents a summary of the gas mixture thermal conductivity calculations for the MPC-24 and MPC-68 MPC designs containing design basis fuel assemblies.

Having calculated the gas mixture thermal conductivities, the effective thermal conductivities of the design basis fuel assemblies are calculated using the finite-volume model described in Subsection 4.4.1.1.2. Only the helium gas conductivity is changed, all other modeling assumptions are the same. The fuel assembly effective thermal conductivities with diluted helium are compared to those with undiluted helium in Table 4.4.8. From this table, it is observed that a 10% rod rupture condition has a relatively minor impact on the fuel assembly effective conductivity. Because the fuel regions comprise only a portion of the overall fuel basket thermal conductivity, the 10% rod rupture condition will have an even smaller impact on the basket effective conductivity.

4.4.1.1.12 Effects of Hypothetical Low Fuel Rod Emissivity

The value of emissivity (ε) utilized in this FSAR was selected as 0.8 based on:

i. the recommendation of an EPRI report [4.1.3]

ii. Holtec's prior licensing experience with the HI-STAR 100 System

iii. other vendors' cask licensing experience with the NRC

iv. authoritative literature citations

The table below provides relevant third party information to support the emissivity value utilized in this FSAR.

Source	Reference	Zircaloy Emissivity
EPRI	[4.1.3]	0.8
TN-68 TSAR	Docket 72-1027	0.8
TN-40	Prairie Island Site Specific ISFSI	0.8
TN-32	Docket 72-1021	0.8
Todreas & Mantuefel	[4.4.8]	0.8
DOE SNF Report	[4.4.9]	0.8

The appropriateness of the selected value of ε is further supported by the information provided by PNL-4835 [4.3.2] and NUREG/CR-0497 [4.4.7]. PNL-4835 reports cladding oxidation thickness in U.S. Zircaloy LWR SNF assemblies (20 μm for PWR and 30 μm for BWR fuel). If these oxide thickness values are applied to the mathematical formulas presented for emissivity determination in [4.4.7], then the computed values are slightly higher than our assumed value of 0.8. It should be recognized that the formulas in [4.4.7] include a conservative assumption that depresses the value of computed emissivity, namely, absence of crud. Significant crud layers develop on fuel cladding surfaces during in-core operation. Crud, which is recognized by the above-mentioned NUREG document as having a boosting effect on ε, is completely neglected.

The above discussion provides a reasonable rationale for our selection of 0.8 as the value for ε. However, to determine the effect of a hypothetical low emissivity of 0.4, an additional thermal analysis adopting this value has been performed. In this analysis, each fuel rod of a fuel assembly is stipulated to have this uniformly low $\varepsilon = 0.4$ and the effective fuel thermal conductivity is recalculated. In the next step, all cells of an MPC basket are assumed to be populated with this low ε fuel that is further assumed to be emitting decay heat at design basis level. The effective conductivity of this basket populated with low ε fuel is recalculated. Using the recalculated fuel basket conductivity, the HI-STORM system temperature field is recomputed. This exercise is performed for the MPC-24 basket because, as explained in the next paragraph, this basket design, which accommodates a fewer number of fuel assemblies (compared to the MPC-68 and MPC-32) has a higher sensitivity to the emissivity parameter. This analysis has determined that the impact of a low ε assumption on the peak cladding temperature is quite small (about 5°C). It is noted that these sensitivity calculations were performed under the completely suppressed helium thermosiphon cooling assumption. Consequently, as the burden of heat dissipation shouldered by radiation heat transfer under this assumption is much greater, the resultant computed sensitivity is a conservative upper bound for the HI-STORM system.

The relatively insignificant increase in the computed peak clad temperature as a result of applying a large penalty in ε (50%) is consistent with the findings in a German Ph.D. dissertation [4.4.11]. Dr. Anton's study consisted of analyzing a cask containing 4 fuel assemblies with a total heat load of 17 kW and helium inside the fuel cavity. For an emissivity of 0.8, the calculated peak cladding temperature was 337°C. In a sensitivity study, wherein the emissivity was varied from 0.7 to 0.9, the temperature changed only by 5°C, i.e. to 342°C and 332°C. Dr. Anton ascribed two reasons for this

low impact of emissivity on computed temperatures. Although the radiative heat emission by a surface decreases with lower emissivity, the fraction of heat reflected from other surfaces increases. In other words, the through-assembly heat dissipation by this means increases thereby providing some compensation for the reduced emission. Additionally, the fourth power of temperature dependence of thermal radiation heat transfer reduces the impact of changes in the coefficients on computed temperatures. For storage containers with larger number of fuel assemblies (like the HI-STORM System), an even smaller impact would be expected, since a larger fraction of the heat is dissipated via the basket conduction heat transfer.

4.4.1.1.13 HI-STORM Temperature Field with Low Heat Emitting Fuel

The HI-STORM 100 thermal evaluations for BWR fuel are grouped in two categories of fuel assemblies proposed for storage in the MPC-68. The two groups are classified as Low Heat Emitting (LHE) fuel assemblies and Design Basis (DB) fuel assemblies. The LHE group of fuel assemblies are characterized by low burnup, long cooling time, and short active fuel lengths. Consequently, their heat loads are dwarfed by the DB group of fuel assemblies. The Dresden-1 (6x6 and 8x8), Quad+, and Humboldt Bay (7x7 and 6x6) fuel assemblies are grouped as the LHE fuel. This fuel is evaluated when encased in Damaged Fuel Containers (DFC). As a result of interruption of radiation heat exchange between the fuel assembly and the fuel basket by the DFC boundary, this configuration is bounding for thermal evaluation. In Table 4.4.2, two canister types for encasing LHE fuel are evaluated – a Holtec design and an existing canister in which some of the Dresden-1 fuel is currently stored (Transnuclear D-1 canister). The most resistive LHE fuel assembly (Dresden-1 8x8) is considered for thermal evaluation (see Table 4.4.2) in a DFC container. The MPC-68 basket effective conductivity, loaded with the most resistive fuel assembly (encased in a canister) is provided in Table 4.4.3. To this basket, LHE decay heat is applied and a HI-STORM 100 System thermal solution computed. The peak cladding temperature is computed as 513°F, which is substantially below the temperature limit (752°F).

A thoria rod canister designed for holding a maximum of twenty fuel rods arrayed in a 5x4 configuration is currently stored at the Dresden-1 spent fuel pool. The fuel rods were originally constituted as part of an 8x8 fuel assembly and used in the second and third cycle of Dresden-1 operation. The maximum fuel burnup of these rods is quite low (~14,400 MWD/MTU). The thoria rod canister internal design is a honeycomb structure formed from 12-gage stainless steel plates. The rods are loaded in individual square cells. This long cooled, part assembly (18 fuel rods) and very low fuel burnup thoria rod canister renders it a miniscule source of decay heat. The canister all-metal internal honeycomb construction serves as an additional means of heat dissipation in the fuel cell space. In accordance with fuel loading stipulation in the Technical Specifications, long cooled fuel is loaded toward the basket periphery (i.e., away from the hot centrol core of the fuel basket). All these considerations provide ample assurance that these fuel rods will be stored in a benign thermal environment and, therefore, remain protected during long-term storage.

4.4.1.2 Test Model

A detailed analytical model for thermal design of the HI-STORM System was developed using the FLUENT CFD code and the industry standard ANSYS modeling package, as discussed in

Subsection 4.4.1.1. As discussed throughout this chapter and specifically in Section 4.4.6, the analysis incorporates significant conservatisms so as to compute bounding fuel cladding temperatures. Furthermore, compliance with specified limits of operation is demonstrated with adequate margins. In view of these considerations, the HI-STORM System thermal design complies with the thermal criteria set forth in the design basis (Sections 2.1 and 2.2) for long-term storage under normal conditions. Additional experimental verification of the thermal design is therefore not required.

4.4.2 Maximum Temperatures

All four MPC-basket designs developed for the HI-STORM System have been analyzed to determine temperature distributions under long-term normal storage conditions, and the results summarized in this subsection. A cross-reference of HI-STORM thermal analyses at other conditions with associated subsection of the FSAR summarizing obtained results is provided in Table 4.4.22. The MPC baskets are considered to be fully loaded with design basis PWR or BWR fuel assemblies, as appropriate. The systems are arranged in an ISFSI array and subjected to design basis normal ambient conditions with insolation.

As discussed in Subsection 4.4.1.1.1, the thermal analysis is performed using a submodeling process where the results of an analysis on an individual component are incorporated into the analysis of a larger set of components. Specifically, the submodeling process yields directly computed fuel temperatures from which fuel basket temperatures are then calculated. This modeling process differs from previous analytical approaches wherein the basket temperatures were evaluated first and then a basket-to-cladding temperature difference calculation by Wooten-Epstein or other means provided a basis for cladding temperatures. Subsection 4.4.1.1.2 describes the calculation of an effective fuel assembly thermal conductivity for an equivalent homogenous region. It is important to note that the result of this analysis is a function of thermal conductivity versus temperature. This function for fuel thermal conductivity is then input to the fuel basket effective thermal conductivity calculation described in Subsection 4.4.1.1.4. This calculation uses a finite-element methodology, wherein each fuel cell region containing multiple finite-elements has temperature-varying thermal conductivity properties. The resultant temperature-varying fuel basket thermal conductivity computed by this basket-fuel composite model is then input to the fuel basket region of the FLUENT cask model.

Because the FLUENT cask model incorporates the results of the fuel basket submodel, which in turn incorporates the fuel assembly submodel, the peak temperature reported from the FLUENT model is the peak temperature in any component. In a dry storage cask, the hottest components are the fuel assemblies. It should be noted that, because the fuel assembly models described in Subsection 4.4.1.1.2 include the fuel pellets, the FLUENT calculated peak temperatures reported in Tables 4.4.9 and 4.4.10 are actually peak pellet centerline temperatures which bound the peak cladding temperatures, and are therefore conservatively reported as the cladding temperatures.

Applying the radiative blocking factor applicable for the worst case cask location, conservatively bounding axial temperatures at the most heated fuel cladding are shown in Figures 4.4.16 and 4.4.17 for MPC-24 and MPC-68 to depict the thermosiphon effect in PWR and BWR SNF. From these plots, the upward movement of the hot spot is quite evident. As discussed in this chapter, these

HOLTEC INTERNATIONAL COPYRIGHTED MATERIAL

calculated temperature distributions incorporate many conservatisms. The maximum fuel clad temperatures for zircaloy clad fuel assemblies are listed in Tables 4.4.9, 4.4.10, 4.4.26, and 4.4.27, which also summarize maximum calculated temperatures in different parts of the MPCs and HI-STORM overpack (Table 4.4.36).

Figures 4.4.19 and 4.4.20, respectively, depict radial temperature distribution in the PWR (MPC-24) and the BWR (MPC-68) at the horizontal plane where maximum fuel cladding temperature occurs. Finally, axial variations of the ventilation air temperatures and that of the inner shell surface are depicted in Figure 4.4.26 for a bounding heat load.

The following additional observations can be derived by inspecting the temperature field obtained from the finite volume analysis:

- The fuel cladding temperatures are below the regulatory limit (ISG-11 [4.1.4]) under all storage scenarios (uniform and regionalized) in all MPCs.
- The maximum temperature of the basket structural material is within the stipulated design temperature.
- The maximum temperature of the neutron absorber is below the design temperature limit.
- The maximum temperatures of the MPC pressure boundary materials are well below their respective ASME Code limits.
- The maximum temperatures of concrete are within the guidance of the governing ACI Code (See Table 4.3.1).

For the regionalized loading scenario as depicted in Figure 4.4.25, outer region decay heat limits are stipulated in Table 4.4.30. The inner region heat load limits are provided in Table 4.4.31.

The calculated temperatures are based on a series of analyses, described previously in this chapter, that incorporate many conservatisms. A list of the significant conservatisms is provided in Subsection 4.4.6. As such, the calculated temperatures are upper bound values that would exceed actual temperatures.

The above observations lead us to conclude that the temperature field in the HI-STORM System with a fully loaded MPC containing design-basis heat emitting SNF complies with all regulatory and industry temperature limits. In other words, the thermal environment in the HI-STORM System will be conducive to long-term safe storage of spent nuclear fuel.

4.4.3 Minimum Temperatures

In Table 2.2.2 of this report, the minimum ambient temperature condition for the HI-STORM storage overpack and MPC is specified to be -40°F. If, conservatively, a zero decay heat load with

no solar input is applied to the stored fuel assemblies, then every component of the system at steady state would be at a temperature of -40°F. All HI-STORM storage overpack and MPC materials of construction will satisfactorily perform their intended function in the storage mode at this minimum temperature condition. Structural evaluations in Chapter 3 show the acceptable performance of the overpack and MPC steel and concrete materials at low service temperatures. Criticality and shielding evaluations (Chapters 5 and 6) are unaffected by temperature.

4.4.4 Maximum Internal Pressure

The MPC is initially filled with dry helium after fuel loading and drying prior to installing the MPC closure ring. During normal storage, the gas temperature within the MPC rises to its maximum operating basis temperature as determined based on the thermal analysis methodology described earlier. The gas pressure inside the MPC will also increase with rising temperature. The pressure rise is determined based on the ideal gas law, which states that the absolute pressure of a fixed volume of gas is proportional to its absolute temperature. Tables 4.4.12, 4.4.13, 4.4.24, and 4.4.25 present summaries of the calculations performed to determine the net free volume in the MPC-24, MPC-68, MPC-32, and MPC-24E, respectively.

The MPC maximum gas pressure is considered for a postulated accidental release of fission product gases caused by fuel rod rupture. For these fuel rod rupture conditions, the amounts of each of the release gas constituents in the MPC cavity are summed and the resulting total pressures determined from the Ideal Gas Law. Based on fission gases release fractions (per NUREG 1536 criteria [4.4.10]), net free volume and initial fill gas pressure, the bounding maximum gas pressures with 1% (normal), 10% (off-normal) and 100% (accident condition) rod rupture are given in Table 4.4.14. The maximum gas pressures listed in Table 4.4.14 are all below the MPC internal design pressure listed in Table 2.2.1.

The inclusion of PWR non-fuel hardware (BPRA control elements and thimble plugs) to the PWR baskets influences the MPC internal pressure through two distinct effects. The presence of non-fuel hardware increases the effective basket conductivity, thus enhancing heat dissipation and lowering fuel temperatures as well as the temperature of the gas filling the space between fuel rods. The gas volume displaced by the mass of non-fuel hardware lowers the cavity free volume. These two effects, namely, temperature lowering and free volume reduction, have opposing influence on the MPC cavity pressure. The first effect lowers gas pressure while the second effect raises it. In the HI-STORM thermal analysis, the computed temperature field (with non-fuel hardware excluded) has been determined to provide a conservatively bounding temperature field for the PWR baskets (MPC-24, MPC-24E, and MPC-32). The MPC cavity free space is computed based on volume displacement by the heaviest fuel (bounding weight) with non-fuel hardware included. This approach ensures conservative bounding pressures.

During in-core irradiation of BPRAs, neutron capture by the B-10 isotope in the neutron absorbing material produces helium. Two different forms of the neutron absorbing material are used in BPRAs: Borosilicate glass and B_4C in a refractory solid matrix (At_2O_3). Borosilicate glass (primarily a constituent of Westinghouse BPRAs) is used in the shape of hollow pyrex glass tubes sealed within

HOLTEC INTERNATIONAL COPYRIGHTED MATERIAL

steel rods and supported on the inside by a thin-walled steel liner. To accommodate helium diffusion from the glass rod into the rod internal space, a relatively high void volume (~40%) is engineered in this type of rod design. The rod internal pressure is thus designed to remain below reactor operation conditions (2,300 psia and approximately 600°F coolant temperature). The B_4C- Al_2O_3 neutron absorber material is principally used in B&W and CE fuel BPRA designs. The relatively low temperature of the poison material in BPRA rods (relative to fuel pellets) favor the entrapment of helium atoms in the solid matrix.

Several BPRA designs are used in PWR fuel that differ in the number, diameter, and length of poison rods. The older Westinghouse fuel (W-14x14 and W-15x15) has used 6, 12, 16, and 20 rods per assembly BPRAs and the later (W-17x17) fuel uses up to 24 rods per BPRA. The BPRA rods in the older fuel are much larger than the later fuel and, therefore, the B-10 isotope inventory in the 20-rod BPRAs bounds the newer W-17x17 fuel. Based on bounding BPRA rods internal pressure, a large hypothetical quantity of helium (7.2 g-moles/BPRA) is assumed to be available for release into the MPC cavity from each fuel assembly in the PWR baskets. The MPC cavity pressures (including helium from BPRAs) are summarized in Table 4.4.14.

4.4.5 Maximum Thermal Stresses

Thermal stress in a structural component is the resultant sum of two factors, namely: (i) restrain of free end expansion and (ii) non-uniform temperature distribution. To minimize thermal stresses in load bearing members, the HI-STORM System is engineered with adequate gaps to permit free thermal expansion of the fuel basket and MPC in axial and radial directions. In this subsection, differential thermal expansion calculations are performed to demonstrate that engineered gaps in the HI-STORM System are adequate to accommodate thermal expansion. To facilitate structural integrity evaluations, temperature distributions are provided herein (Tables 4.4.9, 4.4.10, 4.4.26 and 4.4.27).

As stated above, the HI-STORM System is engineered with gaps for the fuel basket and MPC to thermally expand without restraint of free end expansion. Differential thermal expansion of the following gaps are evaluated:

a. Fuel Basket-to-MPC Radial Gap
b. Fuel Basket to MPC Axial Gap
c. MPC-to-Overpack Radial Gap
d. MPC-to-Overpack Axial Gap

To demonstrate that the fuel basket and MPC are free to expand without restraint, it is required to show that differential thermal expansion from fuel heatup is less than the as-built gaps that exist in the HI-STORM System. For this purpose a suitably bounding temperature profile (T(r)) for the fuel basket is established in Figure 4.4.27 wherein the center temperature (TC) is set at the limit (752°F) for fuel cladding (conservatively bounding assumption) and the basket periphery (TP) conservatively postulated at an upperbound of 600°F (see Tables 4.4.9, 4.4.10, 4.4.26 and 4.4.27 for the maximum computed basket periphery temperatures). To maximize the fuel basket differential thermal expansion, the basket periphery-to-MPC shell temperature difference is conservatively maximized

HOLTEC INTERNATIONAL COPYRIGHTED MATERIAL

($\Delta T = 175°F$). From the bounding temperature profile T(r) and ΔT, the mean fuel basket temperature (T1) and MPC shell temperature (T2) are computed as follows:

$$T1 = \frac{\int_0^1 rT(r)dr}{\int_0^1 rdr} = 676°F$$

$$T2 = TP - \Delta T = 425°F$$

The differential radial growth of the fuel basket (Y1) from an initial reference temperature (To = 70°F) is computed as:

$$Y1 = R \times [A1 \times (T1 - To) - A2 \times (T2 - To)]$$

where:

R = Basket radius (conservatively assumed to be the MPC radius)
A1, A2 = Coefficients of thermal expansion for fuel basket and MPC shell at T1 and T2 respectively for Alloy X (Chapter 1 and Table 3.3.1)

For computing the relative axial growth of the fuel basket in the MPC, bounding temperatures for the fuel basket (TC) and MPC shell temperature T2 computed above (assuming a maximum basket periphery-to-MPC shell temperature differential) are adopted. The differential expansion is computed by a formula similar to the one for radial growth after replacing R with basket height (H), which is conservatively assumed to be that of the MPC cavity.

For computing the radial and axial MPC-to-overpack differential expansions, the MPC shell is postulated at its design temperature (Chapter 2, Table 2.2.3) and thermal expansion of the overpack is ignored. Even with the conservative computation of the differential expansions in the manner of the foregoing, it is evident from the data compiled in Table 4.4.37 that the differential expansions are a fraction of their respective gaps.

4.4.6 Evaluation of System Performance for Normal Conditions of Storage

The HI-STORM System thermal analysis is based on a detailed and complete heat transfer model that conservatively accounts for all modes of heat transfer in various portions of the MPC and overpack. The thermal model incorporates many conservative features that render the results for long-term storage to be extremely conservative:

1. The most severe levels of environmental factors for long-term normal storage, which are an ambient temperature of 80°F and 10CFR71 insolation levels, were coincidentally imposed on the system.

2. A hypothetical rupture of 10% of the stored fuel rods was conservatively considered for determining the thermal conductivity of the diluted helium backfill gas.

3. The most adversely located* HI-STORM System in an ISFSI array was considered for analysis.

4. A conservative assessment of thermosiphon effect in the MPC, which is intrinsic to the HI-STORM fuel basket design is included in the thermal analyses.

5. The MPC internal pressure is conservatively understated for performing temperature calculations. This maximizes calculated temperatures.

6. No credit was considered for contact between fuel assemblies and the MPC basket wall or between the MPC basket and the basket supports. The fuel assemblies and MPC basket were conservatively considered to be in concentric alignment.

7. The MPC is assumed to be loaded with the SNF type which has the maximum equivalent thermal resistance of all fuel types in its category (BWR or PWR), as applicable.

8. The design basis maximum decay heat loads are used for all thermal-hydraulic analyses. For casks loaded with fuel assemblies having decay heat generation rates less than design basis, additional thermal margins of safety will exist. This is assured by defining the burnup limits for the fuel assemblies based on the bounding (i.e., most heat emissive) fuel assembly types within each class (PWR or BWR). For all other fuel types, the heat emission rates at the design-basis burnup levels will be below the design-basis heat emission rate.

9. Not Used

Temperature distribution results obtained from this highly conservative thermal model show that the maximum fuel cladding temperature limits are met with adequate margins. Expected margins during normal storage will be much greater due to the many conservative assumptions incorporated in the analysis. The long-term impact of decay heat induced temperature levels on the HI-STORM System structural and neutron shielding materials is considered to be negligible. The maximum local MPC basket temperature level is below the recommended limits for structural materials in terms of susceptibility to stress, corrosion and creep-induced degradation. Furthermore, stresses induced due to imposed temperature gradients are within Code limits. Therefore, it is concluded that the HI-STORM System thermal design is in compliance with 10CFR72 requirements.

---

* In an ISFSI array, HI-STORM overpacks at interior locations are relatively more disadvantaged in their lateral access to ambient air and in their effectiveness to radiate heat to the environment. To bound these effects, a reference cask is enclosed in a hypothetical reflecting cylinder as described in Section 4.4.1.1.9.

HOLTEC INTERNATIONAL COPYRIGHTED MATERIAL

Table 4.4.1

SUMMARY OF PWR FUEL ASSEMBLY EFFECTIVE THERMAL CONDUCTIVITIES

Fuel	**@ 200°F (Btu/ft-hr-°F)**	**@ 450°F (Btu/ft-hr-°F)**	**@ 700°F (Btu/ft-hr-°F)**
W - 17×17 OFA	0.182	0.277	0.402
W - 17×17 Standard	0.189	0.286	0.413
W - 17×17 Vantage	0.182	0.277	0.402
W - 15×15 Standard	0.191	0.294	0.430
W - 14×14 Standard	0.182	0.284	0.424
W - 14×14 OFA	0.175	0.275	0.413
B&W - 17×17	0.191	0.289	0.416
B&W - 15×15	0.195	0.298	0.436
CE - 16×16	0.183	0.281	0.411
CE - 14×14	0.189	0.293	0.435
HN† - 15×15 SS	0.180	0.265	0.370
W - 14×14 SS	0.170	0.254	0.361
B&W-15x15 Mark B-11	0.187	0.289	0.424
CE-14x14 (MP2)	0.188	0.293	0.434
IP-1 (14x14) SS	0.125	0.197	0.293

† Haddam Neck Plant B&W or Westinghouse stainless steel clad fuel assemblies.

HOLTEC INTERNATIONAL COPYRIGHTED MATERIAL

Table 4.4.2

SUMMARY OF BWR FUEL ASSEMBLY EFFECTIVE THERMAL CONDUCTIVITIES

Fuel	**@ 200°F (Btu/ft-hr-°F)**	**@ 450°F (Btu/ft-hr-°F)**	**@ 700°F (Btu/ft-hr-°F)**
Dresden 1 - 8×8†	0.119	0.201	0.319
Dresden 1 - 6×6†	0.126	0.215	0.345
GE - 7×7	0.171	0.286	0.449
GE - 7×7R	0.171	0.286	0.449
GE - 8×8	0.168	0.278	0.433
GE - 8×8R	0.166	0.275	0.430
GE10 - 8×8	0.168	0.280	0.437
GE11 - 9×9	0.167	0.273	0.422
AC††-10×10 SS	0.152	0.222	0.309
Exxon-10×10 SS	0.151	0.221	0.308
Damaged Dresden-1 8×8† (in a Holtec damaged fuel container)	0.107	0.169	0.254
Humboldt Bay-7x7†	0.127	0.215	0.343
Dresden-1 Thin Clad 6x6†	0.124	0.212	0.343
Damaged Dresden-1 8x8 (in TN D-1 canister)†	0.107	0.168	0.252
8x8 Quad+ Westinghouse†	0.164	0.276	0.435

† Cladding temperatures of low heat emitting Dresden (intact and damaged) SNF in the HI-STORM System will be bounded by design basis fuel cladding temperatures. Therefore, these fuel assembly types are excluded from the list of fuel assemblies (zircaloy clad) evaluated to determine the most resistive SNF type.

†† Allis-Chalmers stainless steel clad fuel assemblies.

Table 4.4.3

MPC BASKET EQUIVALENT ISOTROPIC THERMAL CONDUCTIVITY VALUES††

Basket	@200°F (Btu/ft-hr-°F)	@450°F (Btu/ft-hr-°F)	@700°F (Btu/ft-hr-°F)
MPC-24 (Zircaloy Clad Fuel)	1.109	1.495	1.955
MPC-68 (Zircaloy Clad Fuel)	1.111	1.347	1.591
MPC-24 (Stainless Steel Clad Fuel) †	0.897	1.213	1.577(a)
MPC-68 (Stainless Steel Clad Fuel)†	1.070	1.270	1.451(b)
MPC-32 (Zircaloy Clad Fuel)	1.015	1.271	1.546
MPC-32 (Stainless Steel Clad Fuel)†	0.806	0.987	1.161 (c)
MPC-24E (Zircaloy Clad Fuel)	1.216	1.637	2.133
MPC-24E (Stainless Steel Clad fuel)†	0.991	1.351	1.766 (d)

(a) Conductivity is 19% less than corresponding zircaloy fueled basket.
(b) Conductivity is 9% less than corresponding zircaloy fueled basket.
(c) Conductivity is 25% less than corresponding zircaloy fueled basket.
(d) Conductivity is 17% less than corresponding zircaloy fueled basket.

†† The values reported in this table are conservatively understated.
† Evaluated in a damaged fuel canister (conservatively bounding)

Table 4.4.4

[INTENTIONALLY DELETED]

HOLTEC INTERNATIONAL COPYRIGHTED MATERIAL

Table 4.4.5

SUMMARY OF 10×10 ARRAY TYPE BWR FUEL ASSEMBLY
EFFECTIVE THERMAL CONDUCTIVITIES[†]

Fuel Assembly	**@ 200°F (Btu/ft-hr-°F)**	**@ 450°F (Btu/ft-hr-°F)**	**@ 700°F (Btu/ft-hr-°F)**
GE-12/14	0.166	0.269	0.412
Atrium-10	0.164	0.266	0.409
SVEA-96	0.164	0.269	0.416

[†] The conductivities reported in this table are obtained by the simplified method described in the beginning of Subsection 4.4.1.1.2.

HOLTEC INTERNATIONAL COPYRIGHTED MATERIAL

Table 4.4.6

COMPARISON OF ATRIUM-10 BWR FUEL ASSEMBLY CONDUCTIVITY[†] WITH THE BOUNDING[††] BWR FUEL ASSEMBLY CONDUCTIVITY

Temperature (°F)	Atrium-10 BWR Assembly		Bounding BWR Assembly	
	(Btu/ft-hr-°F)	(W/m-K)	(Btu/ft-hr-°F)	(W/m-K)
200	0.225	0.389	0.171	0.296
450	0.345	0.597	0.271	0.469
700	0.504	0.872	0.410	0.710

[†] The reported effective conductivity has been obtained from a rigorous finite-element model.

[††] The bounding BWR fuel assembly conductivity applied in the MPC-68 basket thermal analysis.

HOLTEC INTERNATIONAL COPYRIGHTED MATERIAL

Table 4.4.7

SUMMARY OF THERMAL CONDUCTIVITY CALCULATIONS
FOR MPC HELIUM DILUTED BY RELEASED ROD GASES

Component Gas	**Molecular Weight (g/mole)**	**Component Gas Mole Fractions and Mixture Conductivity (Btu/hr-ft-°F)**	
		MPC-24	**MPC-68**
MPC Backfill Helium	4	0.951	0.962
Fuel Rod Backfill Helium	4	0.023	5.750×10^{-3}
Rod Tritium	3	1.154×10^{-5}	4.483×10^{-5}
Rod Krypton	85	2.372×10^{-3}	2.905×10^{-3}
Rod Xenon	131	0.024	0.030
Rod Iodine	129	1.019×10^{-3}	1.273×10^{-3}
Mixture of Gases (diluted helium)	N/A	0.088 at 200°F 0.116 at 450°F 0.142 at 700°F	0.086 at 200°F 0.113 at 450°F 0.139 at 700°F

Table 4.4.8

COMPARISON OF COMPONENT THERMAL CONDUCTIVITIES
WITH AND WITHOUT BACKFILL HELIUM DILUTION

	@ 200°F (Btu/hr-ft-°F)	**@ 450°F (Btu/hr-ft-°F)**	**@ 700°F (Btu/hr-ft-°F)**
GE-11 9×9 Fuel Assembly with Undiluted Helium	0.171	0.271	0.410
GE-11 9×9 Fuel Assembly with Diluted Helium	0.158	0.254	0.385
W 17×17 OFA Fuel Assembly with Undiluted Helium	0.257	0.406	0.604
W 17×17 OFA Fuel Assembly with Diluted Helium	0.213	0.347	0.537

HOLTEC INTERNATIONAL COPYRIGHTED MATERIAL

Table 4.4.9

HI-STORM† SYSTEM LONG-TERM NORMAL
STORAGE MAXIMUM TEMPERATURES
(MPC-24 BASKET)

Component	Normal Condition Temp. (°F)	Long-Term Temperature Limit (°F)
HI-STORM		
Fuel Cladding	691	752††
MPC Basket	650	725†††
Basket Periphery	486	725†††
MPC Outer Shell	344	500
HI-STORM 100S Version B		
Fuel Cladding	612	752
MPC Basket	571	725
Basket Periphery	487	725
MPC Outer Shell	400	500

† Bounding overpack temperatures are provided in Table 4.4.36.

†† This temperature limit is in accordance with ISG-11 [4.1.4].

††† The ASME Code allowable temperature of the fuel basket Alloy X materials is 800°F. This lower temperature limit is imposed to add additional conservatism to the analysis of the HI-STORM System.

HOLTEC INTERNATIONAL COPYRIGHTED MATERIAL

Table 4.4.10

HI-STORM† SYSTEM LONG-TERM NORMAL
STORAGE MAXIMUM TEMPERATURES
(MPC-68 BASKET)

Component	Normal Condition Temp. (°F)	Long-Term Temperature Limit (°F)
HI-STORM 100		
Fuel Cladding	740	752††
MPC Basket	720	725†††
Basket Periphery	501	725†††
MPC Outer Shell	347	500
HI-STORM 100S Version B		
Fuel Cladding	673	752
MPC Basket	653	725
Basket Periphery	499	725
MPC Outer Shell	405	500

† Bounding overpack temperatures are provided in Table 4.4.36.

†† This temperature limit is in accordance with ISG-11 [4.1.4].

††† The ASME Code allowable temperature of the fuel basket Alloy X materials is 800°F. This lower temperature limit is imposed to add additional conservatism to the analysis of the HI-STORM System.

Table 4.4.11

INTENTIONALLY DELETED

HOLTEC INTERNATIONAL COPYRIGHTED MATERIAL

Table 4.4.12

SUMMARY OF MPC-24 FREE VOLUME CALCULATIONS

Item	Volume (ft^3)
Cavity Volume	367.9
Basket Metal Volume	39.7
Bounding Fuel Assemblies Volume	78.8
Basket Supports and Fuel Spacers Volume	6.1
Net Free Volume	243.3 (6,889 liters)*

* A conservative lowerbound value of 237.5 ft^3 (6,724 liters) is used for subsequent MPC internal pressure calculations.

Table 4.4.13

SUMMARY OF MPC-68 FREE VOLUME CALCULATIONS

Item	Volume (ft^3)
Cavity Volume	367.3
Basket Metal Volume	34.8
Bounding Fuel Assemblies Volume	93.0
Basket Supports and Fuel Spacers Volume	11.3
Aluminum Conduction Elements	5.9†
Net Free Volume	222.3 (6,294 liters)

† Bounding 1,000 lbs weight assumed. Included herein to bound early production units with these optional items installed.

Table 4.4.14
SUMMARY OF MPC CONFINEMENT BOUNDARY PRESSURES[†]
FOR LONG-TERM STORAGE

Condition	Pressure (psig)[‡]
MPC-24:	
Initial backfill (at 70°F)	31.3
Normal condition	66.4
With 1% rods rupture	66.1
With 10% rods rupture	72.2
With 100% rods rupture	132.5
MPC-68:	
Initial backfill (at 70°F)	31.3
Normal condition	67.1
With 1% rods rupture	67.5
With 10% rods rupture	71.1
With 100% rods rupture	107.6
MPC-32:	
Initial backfill (at 70°F)	31.3
Normal Condition	65.6
With 1% rods rupture	66.5
With 10% rods rupture	75.0
With 100% rods rupture	160.1
MPC-24E:	
Initial backfill (at 70°F)	31.3
Normal Condition	65.8
With 1% rods rupture	66.4
With 10% rods rupture	72.5
With 100% rods rupture	133.5

† Per NUREG-1536, pressure analyses with ruptured fuel rods (including BPRA rods for PWR fuel) is performed with release of 100% of the ruptured fuel rod fill gas and 30% of the significant radioactive gaseous fission products.

‡ All pressures reported in this table are calculated for MPCs in the HI-STORM 100 System. Bulk MPC cavity gas temperartures in the HI-STORM 100S Version B are lower than in the HI-STORM 100. As a consequence of the ideal gas law, the pressures in this table are therefore bounding for the HI-STORM 100S Version B.

Table 4.4.15

SUMMARY OF HI-STORM SYSTEM COMPONENT TEMPERATURES
FOR LONG-TERM STORAGE (°F)

Location	MPC-24	MPC-68	MPC-32	MPC-24E
HI-STORM 100				
MPC Basket Top:				
Basket periphery	485	501	496	488
MPC shell	344	348	351	346
Overpack Inner Shell	199	199	199	199
Overpack Outer Shell	124	124	124	124
MPC Basket Bottom:				
Basket periphery	281	280	290	284
MPC shell	256	258	261	258
Overpack Inner Shell	106	106	106	106
Overpack Outer Shell	107	107	107	107
HI-STORM 100S Version B				
MPC Basket Top:				
Basket periphery	487	500	487	See Note
MPC shell	401	407	403	See Note
Overpack Inner Shell	241	243	243	See Note
Overpack Outer Shell	123	124	129	See Note
MPC Basket Bottom:				
Basket periphery	238	207	247	See Note
MPC shell	186	167	191	See Note
Overpack Inner Shell	104	101	107	See Note
Overpack Outer Shell	93	92	101	See Note

Note: In the HI-STORM 100S Version B, the MPC-24E temperatures are essentially the same as those for the MPC-24.

HOLTEC INTERNATIONAL COPYRIGHTED MATERIAL

Table 4.4.16

INTENTIONALLY DELETED

HOLTEC INTERNATIONAL COPYRIGHTED MATERIAL

Table 4.4.17

INTENTIONALLY DELETED

HOLTEC INTERNATIONAL COPYRIGHTED MATERIAL

Table 4.4.18

INTENTIONALLY DELETED

HOLTEC INTERNATIONAL COPYRIGHTED MATERIAL

Table 4.4.19

SUMMARY OF MPC CONFINEMENT BOUNDARY
TEMPERATURE DISTRIBUTIONS

Location	MPC-24 (°F)	MPC-68 (°F)	MPC-32 (°F)	MPC-24E (°F)
HI-STORM 100				
MPC Lid Inside Surface at Centerline	463	502	487	462
MPC Lid Outside Surface at Centerline	427	454	447	425
MPC Lid Inside Surface at Periphery	371	381	383	372
MPC Lid Outside Surface at Periphery	360	375	372	358
MPC Baseplate Inside Surface at Centerline	207	209	214	209
MPC Baseplate Outside Surface at Centerline	200	203	208	202
MPC Baseplate Inside Surface at Periphery	243	246	249	245
MPC Baseplate Outside Surface at Periphery	194	196	199	195
HI-STORM 100S Version B				
MPC Lid Inside Surface at Centerline	472	492	479	See Note
MPC Lid Outside Surface at Centerline	440	456	445	See Note
MPC Lid Inside Surface at Periphery	395	403	387	See Note
MPC Lid Outside Surface at Periphery	375	382	378	See Note
MPC Baseplate Inside Surface at Centerline	171	161	181	See Note
MPC Baseplate Outside Surface at Centerline	170	160	179	See Note
MPC Baseplate Inside Surface at Periphery	169	157	177	See Note
MPC Baseplate Outside Surface at Periphery	164	153	172	See Note

Note: In the HI-STORM 100S Version B, the MPC-24E temperatures are essentially the same as those for the MPC-24.

Table 4.4.20

MPC-24 DESIGN-BASIS MAXIMUM HEAT LOAD

Permissible Heat Load (kW)
27.77

Table 4.4.21

MPC-68 DESIGN-BASIS MAXIMUM HEAT LOAD

Permissible Heat Load (kW)
28.19

HOLTEC INTERNATIONAL COPYRIGHTED MATERIAL

Table 4.4.22
MATRIX OF HI-STORM SYSTEM THERMAL EVALUATIONS

Scenario	Description	Ultimate Heat Sink	Analysis Type	Principal Input Parameters	Results in FSAR Subsection
1	Long Term Normal	Ambient	SS	N_T, Q_D, ST, SC, I_O	4.4.2
2	Off-Normal Environment	Ambient	SS(B)	O_T, Q_D, ST, SC, I_O	11.1.2
3	Extreme Environment	Ambient	SS(B)	E_T, Q_D, ST, SC, I_O	11.2.15
4	Partial Ducts Blockage	Ambient	SS(B)	N_T, Q_D, ST, SC, $I_{1/2}$	11.1.4
5	Ducts Blockage Accident	Overpack	TA	N_T, Q_D, ST, SC, I_C	11.2.13
6	Fire Accident	Overpack	TA	Q_D, F	11.2.4
7	Tip Over Accident	Overpack	AH	Q_D	11.2.3
8	Debris Burial Accident	Overpack	AH	Q_D	11.2.14

Legend:
N_T - Maximum Annual Average (Normal) Temperature (80°F)
O_T - Off-Normal Temperature (100°F)
E_T - Extreme Hot Temperature (125°F)
Q_D - Design Basis Maximum Heat Load
SS - Steady State
SS(B) - Bounding Steady State
TA - Transient Analysis
AH - Adiabatic Heating
I_O - All Inlet Ducts Open
$I_{1/2}$ - Half of Inlet Ducts Open
I_C - All Inlet Ducts Closed
ST - Insolation Heating (Top)
SC - Insolation Heating (Curved)
F - Fire Heating (1475°F)

HOLTEC INTERNATIONAL COPYRIGHTED MATERIAL

Table 4.4.23

PLANT SPECIFIC BWR FUEL TYPES EFFECTIVE CONDUCTIVITY†

Fuel	@200°C [Btu/ft-hr-°F]	@450°F [Btu/ft-hr-°F]	@700°F [Btu/ft-hr-°F]
Oyster Creek (7x7)	0.161	0.269	0.422
Oyster Creek (8x8)	0.162	0.266	0.413
TVA Browns Ferry (8x8)	0.160	0.264	0.411
SPC-5 (9x9)	0.149	0.245	0.380
ANF 8x8	0.167	0.277	0.433
ANF-9X (9x9)	0.165	0.272	0.423

† The conductivities reported in this table are obtained by a simplified analytical method in Subsection 4.4.1.1.2.

Table 4.4.24

SUMMARY OF MPC-32 FREE VOLUME CALCULATIONS

Item	Volume (ft^3)
Cavity Volume	367.9
Basket Metal Volume	27.4
Bounding Free Assemblies Volume	105.0
Basket Supports and Fuel Spacers Volume	9.0
Net Free Volume	226.5 (6,414 liters)*

* A conservative lowerbound value of 220.6 ft^3 (6,247 liters) is used for subsequent MPC internal pressure calculations.

Table 4.4.25

SUMMARYOF MPC-24E FREE VOLUME CALCULATIONS

Item	Volume (ft^3)
Cavity Volume	367.9
Basket Metal Volume	51.2
Bounding Fuel Assemblies Volume	78.8
Basket Supports and Fuel Spacers Volume	6.1
Net Free Volume	231.8 (6,564 liters)*

* A conservative lowerbound value of 225.9 ft^3 (6,398 liters) is used for subsequent MPC internal pressure calculations.

Table 4.4.26

HI-STORM† SYSTEM LONG-TERM NORMAL STORAGE MAXIMUM TEMPERATURES
(MPC-32 BASKET)

Component	Normal Condition Temp. (°F)	Long-Term Temperature Limit (°F)
HI-STORM 100		
Fuel Cladding	691	752††
MPC Basket	660	725†††
Basket Periphery	496	725†††
MPC Outer Shell	351	500
HI-STORM 100S Version B		
Fuel Cladding	595	752
MPC Basket	564	725
Basket Periphery	487	725
MPC Outer Shell	403	500

† Bounding overpack temperatures are provided in Table 4.4.36.

†† This temperature limit is in accordance with ISG-11 [4.1.4].

††† The ASME Code allowable temperature of the fuel basket Alloy X materials is 800°F. This lower temperature limit is imposed to add additional conservatism in the analysis of the HI-STORM Systems.

HOLTEC INTERNATIONAL COPYRIGHTED MATERIAL

Table 4.4.27

HI-STORM† SYSTEM LONG-TERM NORMAL STORAGE MAXIMUM TEMPERATURES
(MPC-24E BASKET)

Component	Normal Condition Temp. (°F)	Long-Term Temperature Limit (°F)
Fuel Cladding	691	752††
MPC Basket	650	725†††
Basket Periphery	492	725†††
MPC Outer Shell	347	500

Note: Values presented in this table are all for the HI-STORM 100. In the HI-STORM 100S Version B, the MPC-24E temperatures are essentially the same as those for the MPC-24 (See Table 4.4.9).

† Bounding overpack temperatures are provided in Table 4.4.36.

†† This temperature limit is in accordance with ISG-11 [4.1.4].

††† The ASME Code allowable temperature of the fuel basket Alloy X materials is 800°F. This lower temperature limit is imposed to add additional conservatism to the analysis of the HI-STORM System.

HOLTEC INTERNATIONAL COPYRIGHTED MATERIAL

Table 4.4.28

MPC-32 DESIGN BASIS MAXIMUM HEAT LOAD

Permissible Heat Load (kW)
28.74

Table 4.4.28

MPC-32 DESIGN BASIS MAXIMUM HEAT LOAD

Permissible Heat Load (kW)
28.74

HOLTEC INTERNATIONAL COPYRIGHTED MATERIAL

Table 4.4.29

MPC-24E DESIGN BASIS MAXIMUM HEAT LOAD

Permissible Heat Load (kW)
28.17

Table 4.4.30

REGIONALIZED LOADING OUTER REGION HEAT LOAD LIMITS

MPC Type	Inner Region Assemblies	Outer Region Assemblies	Outer Region Heat Load (kW)
MPC-24	4	20	18
MPC-24E	4	20	18
MPC-32	12	20	12
MPC-68	32	36	9.9

HOLTEC INTERNATIONAL COPYRIGHTED MATERIAL

Table 4.4.31

REGIONALIZED LOADING INNER REGION HEAT LOAD LIMITS (kW)

MPC-24	MPC-24E	MPC-32	MPC-68
5.88†	6.16†	13.58	16.02

† Inner region heat load governed by interface cladding temperature limit.

Table 4.4.32

[INTENTIONALLY DELETED]

HOLTEC INTERNATIONAL COPYRIGHTED MATERIAL

Table 4.4.33

[INTENTIONALLY DELETED]

HOLTEC INTERNATIONAL COPYRIGHTED MATERIAL

Table 4.4.34

[INTENTIONALLY DELETED]

HOLTEC INTERNATIONAL COPYRIGHTED MATERIAL

Table 4.4.35

[INTENTIONALLY DELETED]

HOLTEC INTERNATIONAL COPYRIGHTED MATERIAL

Table 4.4.36

BOUNDING LONG-TERM NORMAL STORAGE
HI-STORM OVERPACK TEMPERATURES

Component†	Local Section Temperature†† (°F)	Long-Term Temperature Limit (°F)
HI-STORM 100		
Inner shell	199	350
Outer shell	145	350
Lid bottom plate	339	450
Lid top plate	196	450
MPC pedestal plate	208	350
Baseplate	111	350
Overpack Body Concrete	172	300
Overpack Lid Concrete	268	300
Overpack Pedestal Concrete	160	300
Air outlet†††	206	
HI-STORM 100S Version B		
Inner shell	246	350
Outer shell	140	350
Lid bottom plate	393	450
Lid top plate	201	450
MPC pedestal plate	179	350
Baseplate	89	350
Overpack Body Concrete	193	300
Overpack Lid Concrete	297	300
Air outlet	200	

Note: These lid bottom plate, lid top plate and lid concrete temperatures are calculated without crediting the heat shield on the underside of the HI-STORM 100 lid, shown on the drawings in Section 1.5. Actual temperatures will be lower if the heat shield is installed. Local areas of the overpack lid concrete exceed 300°F, with a maximum local value of 339°F. A discussion of the impact of these elevated local temperatures on the shielding performance of the lid concrete is presented in Section 5.3.2. All areas of the overpack body and pedestal concrete are below 300 °F.

† See Figure 1.2.8 for a description of HI-STORM components.
†† Section temperature is defined as the through-thickness average temperature.
††† Reported herein for the option of temperature measurement surveillance of outlet ducts air temperature as set forth in the Technical Specifications.

Table 4.4.37

SUMMARY OF HI-STORM DIFFERENTIAL THERMAL EXPANSIONS

Gap Description	Cold Gap U (in)	Differential Expansion V (in)	Is Free Expansion Criterion Satisfied (i.e., U > V)
Fuel Basket-to-MPC Radial Gap	0.1875	0.096	Yes
Fuel Basket-to-MPC Axial Gap	1.25	0.499	Yes
MPC-to-Overpack Radial Gap	0.5	0.139	Yes
MPC-to-Overpack Axial Gap	1.0	0.771	Yes

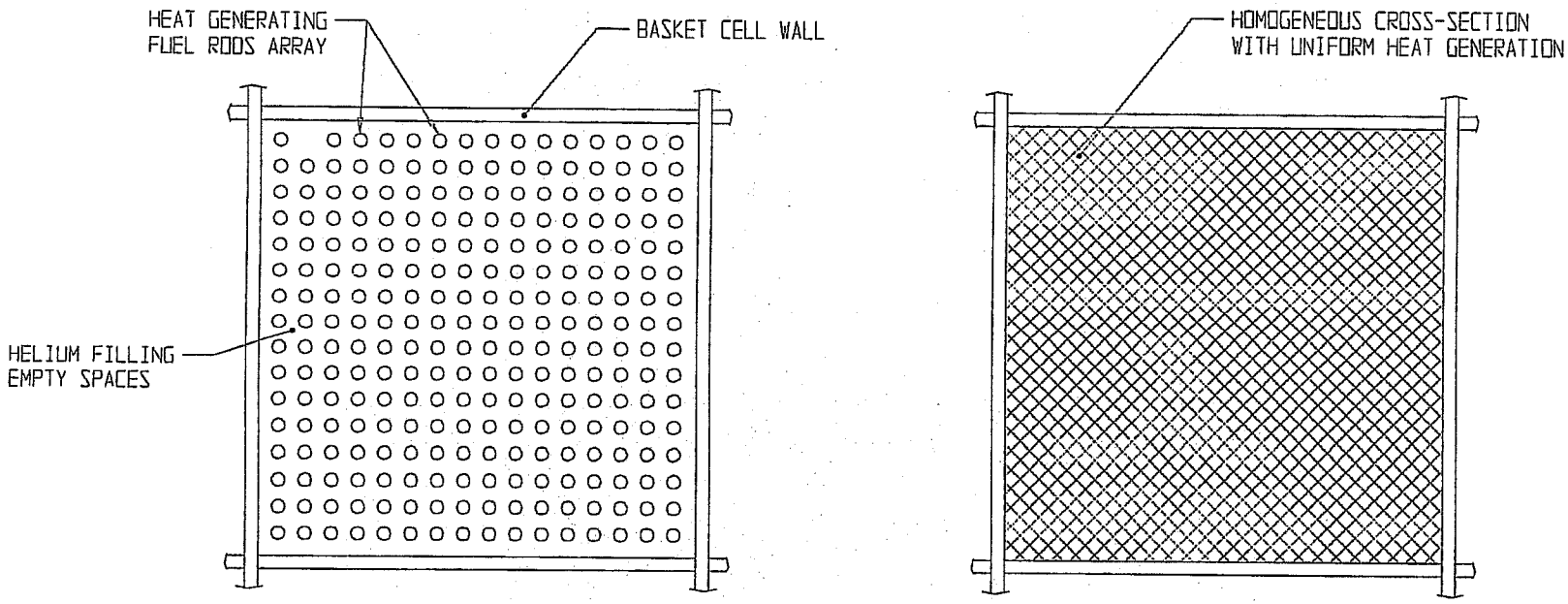

FIGURE 4.4.1; HOMOGENIZATION OF THE STORAGE CELL CROSS-SECTION

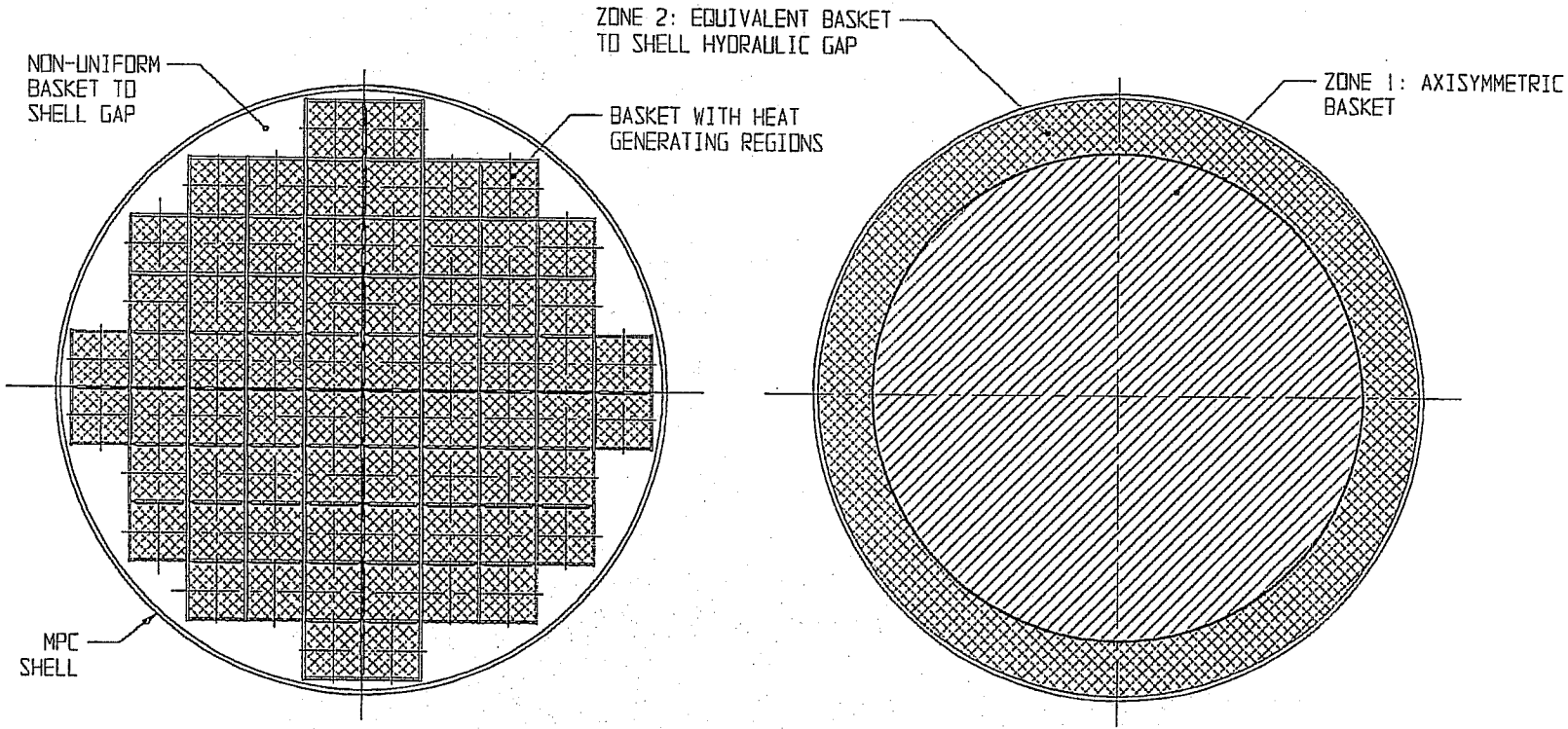

(a) TYPICAL MPC CROSS-SECTION

(b) EQUIVALENT TWO ZONE MODEL

FIGURE 4.4.2; MPC CROSS-SECTION REPLACED WITH AN EQUIVALENT TWO ZONE AXISYMMETRIC BODY

\PROJECTS\5014\HI951312\CH_4\4_4_2

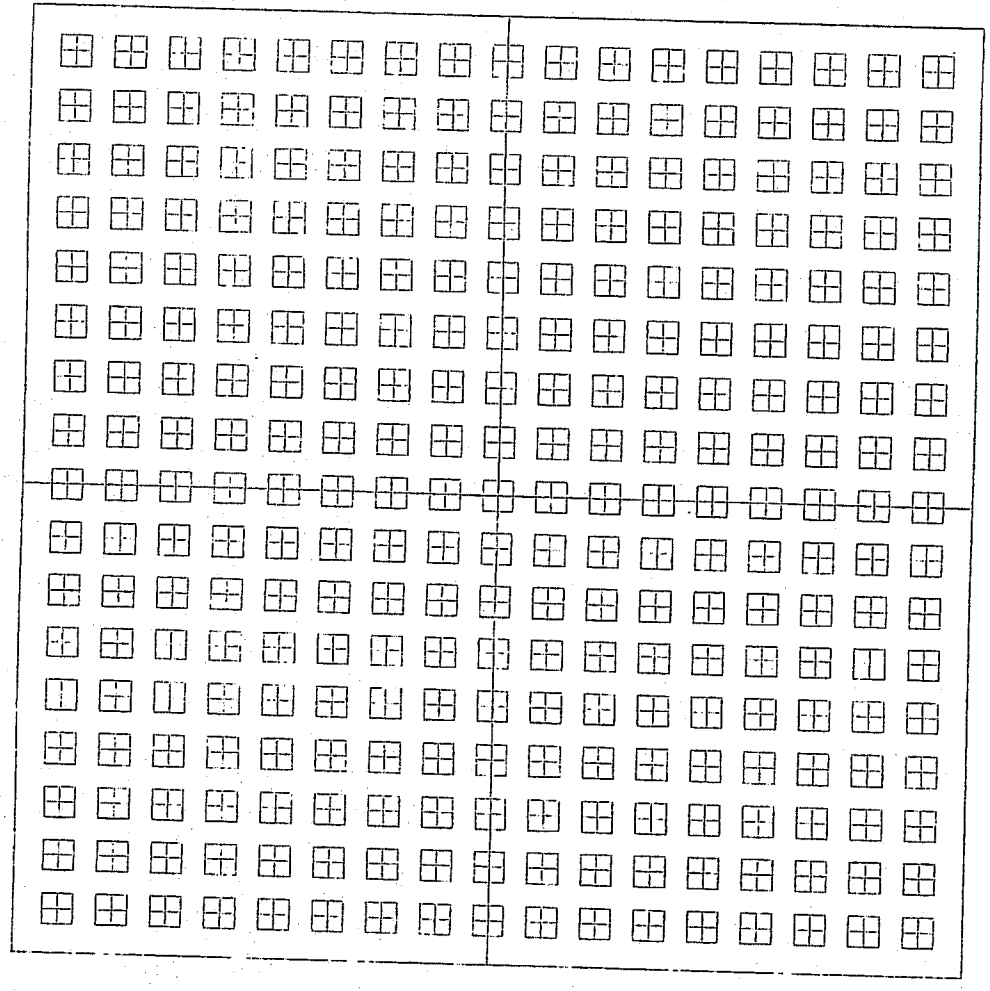

W17X17 OFA FUEL ASSEMBLY MODEL

Nov 11 1997
Fluent 4.32
Fluent Inc.

FIGURE 4.4.3: WESTINGHOUSE 17x17 OFA PWR FUEL ASSEMBLY MODEL

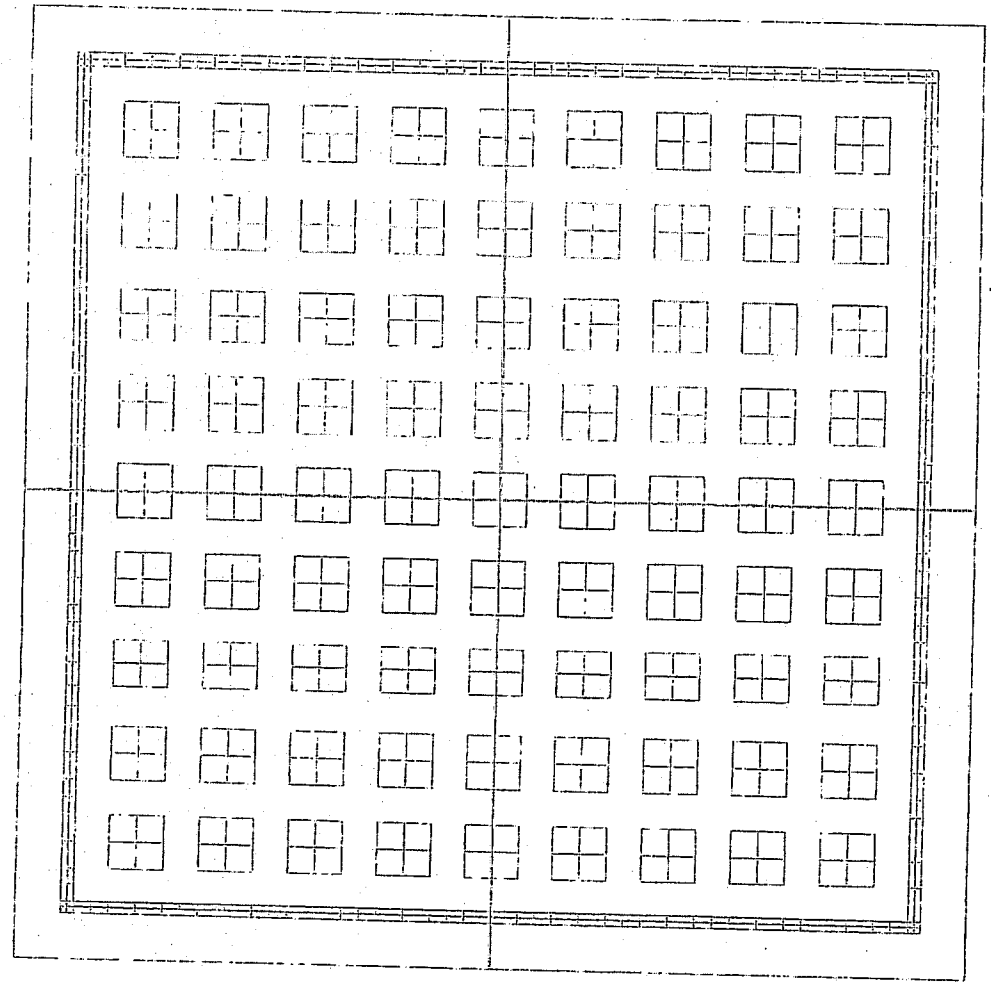

GE11-9X9 CHANNELED FUEL ASSEMBLY MODEL

Nov 11 1997
Fluent 4.32
Fluent Inc.

FIGURE 4.4.4: GENERAL ELECTRIC 9x9 BWR FUEL ASSEMBLY MODEL

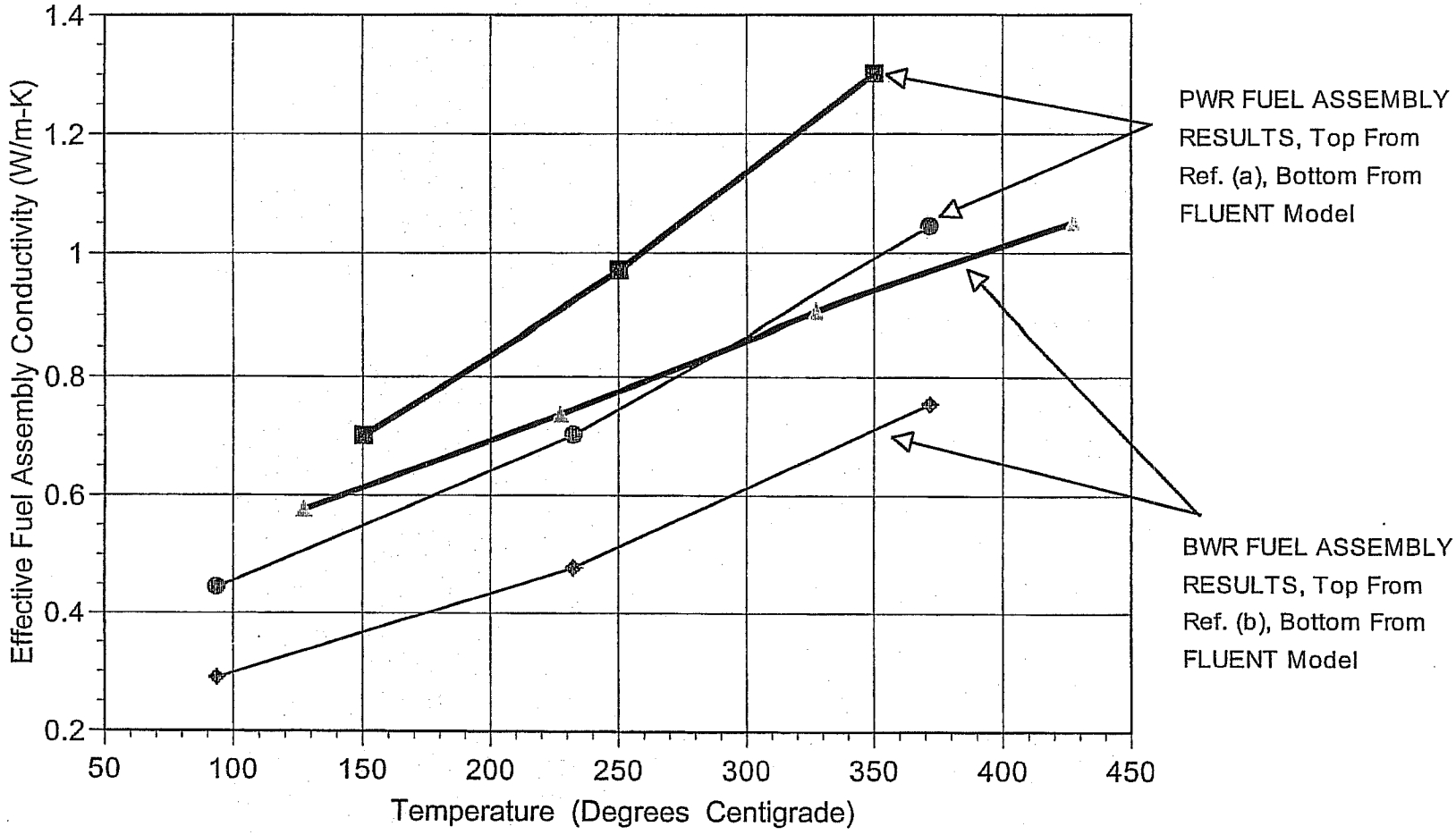

(a) "Determination of SNF Peak Temperatures in the Waste Package", Bahney & Doering, *HLRWM Sixth Annual Conf.*, Pages 671-673, (April 30 - May 5, 1995).

(b) "A Method for Determining the Spent-Fuel Contribution to Transport Cask Containment Requirements", *Sandia Report SAND90-2406*, page II-132, (1992).

FIGURE 4.4.5; COMPARISON OF FLUENT CALCULATED FUEL ASSEMBLY CONDUCTIVITY RESULTS WITH PUBLISHED TECHNICAL DATA

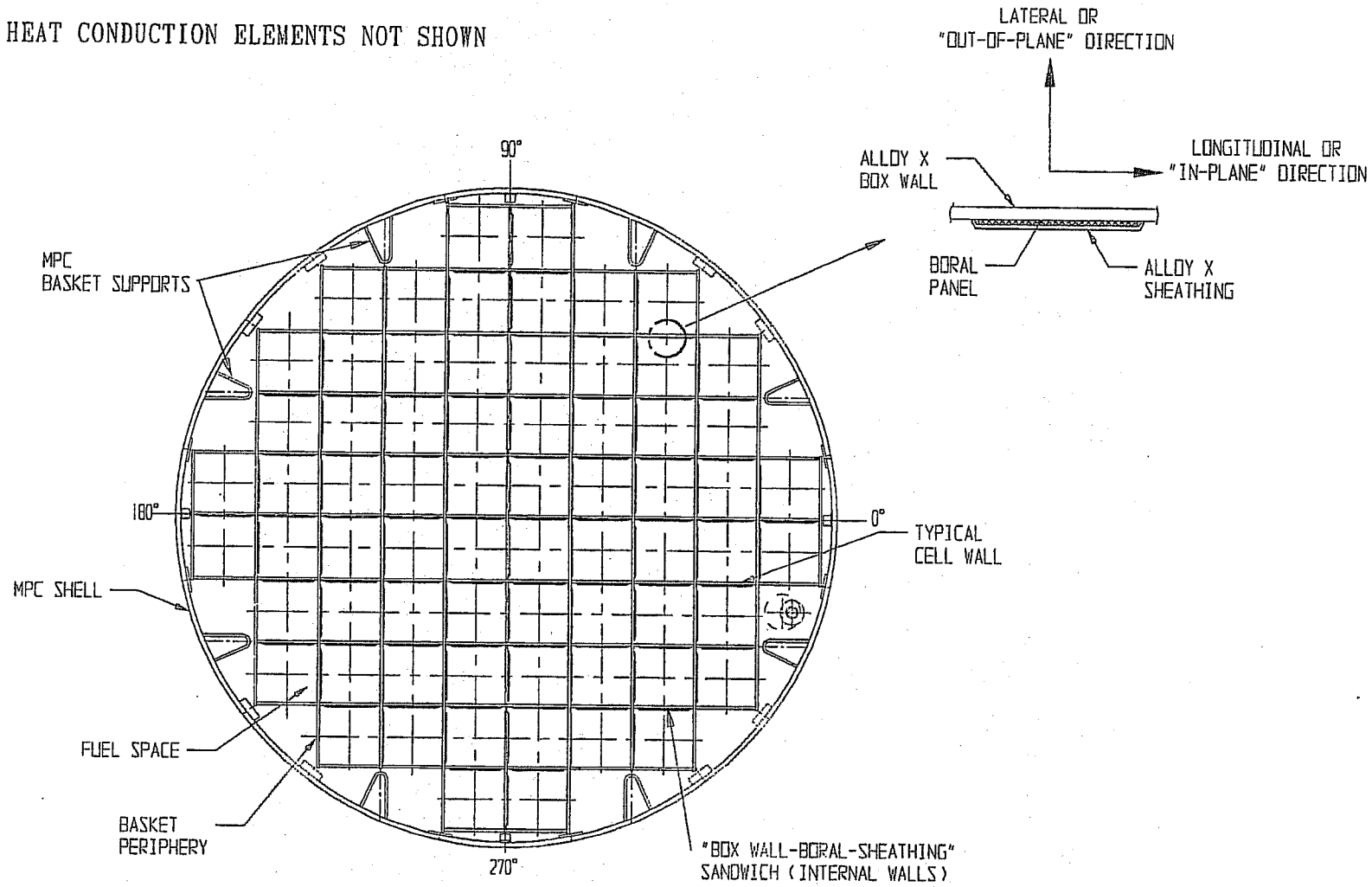

FIGURE 4.4.6; TYPICAL MPC BASKET PARTS IN A CROSS-SECTIONAL VIEW

\PROJECTS\5014\HI951312\CH_4\4_4_6

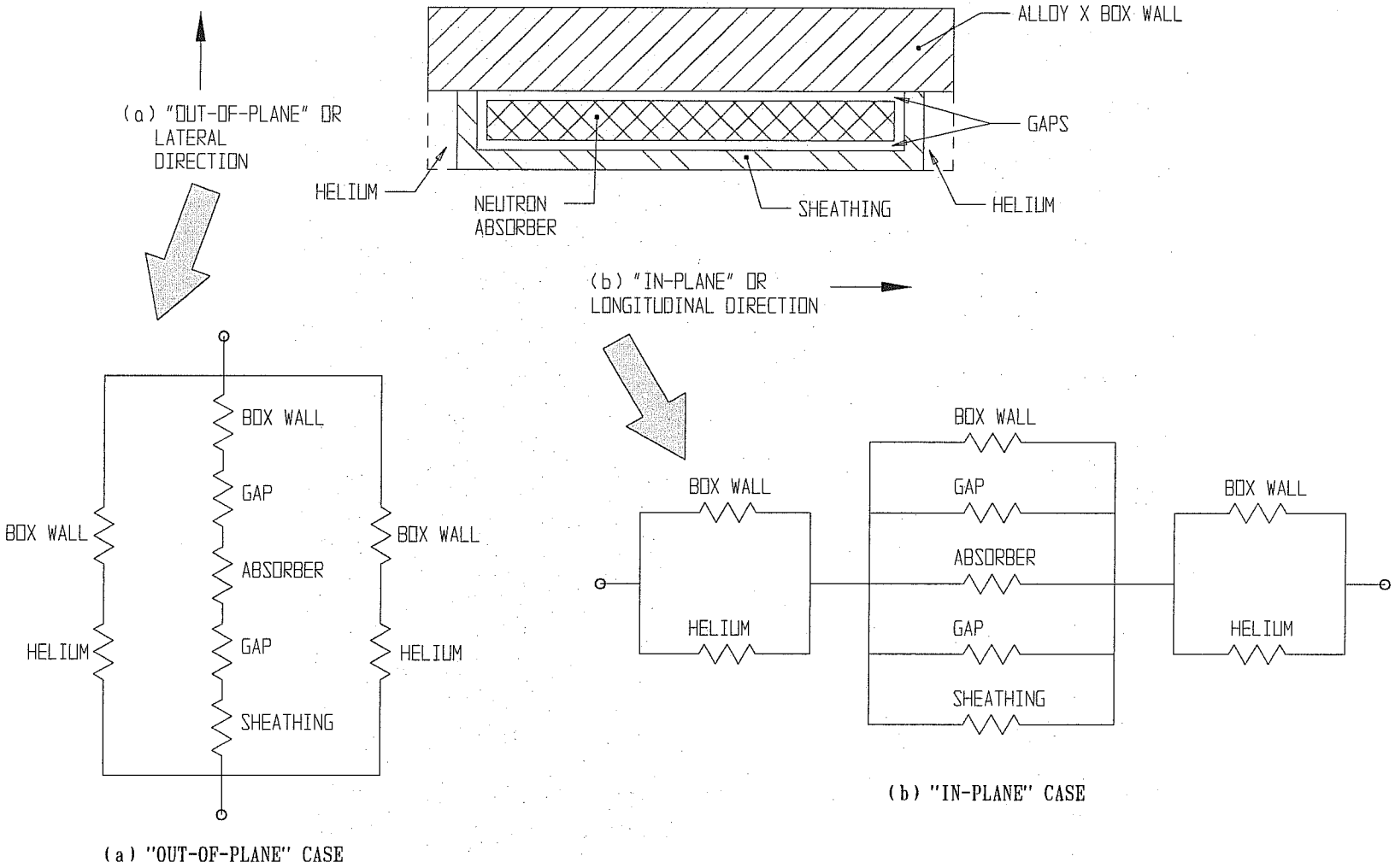

FIGURE 4.4.7; RESISTANCE NETWORK MODEL OF A "BOX WALL-NEUTRON ABSORBER-SHEATHING" SANDWICH

FIGURE 4.4.8

THIS FIGURE INTENTIONALLY DELETED.

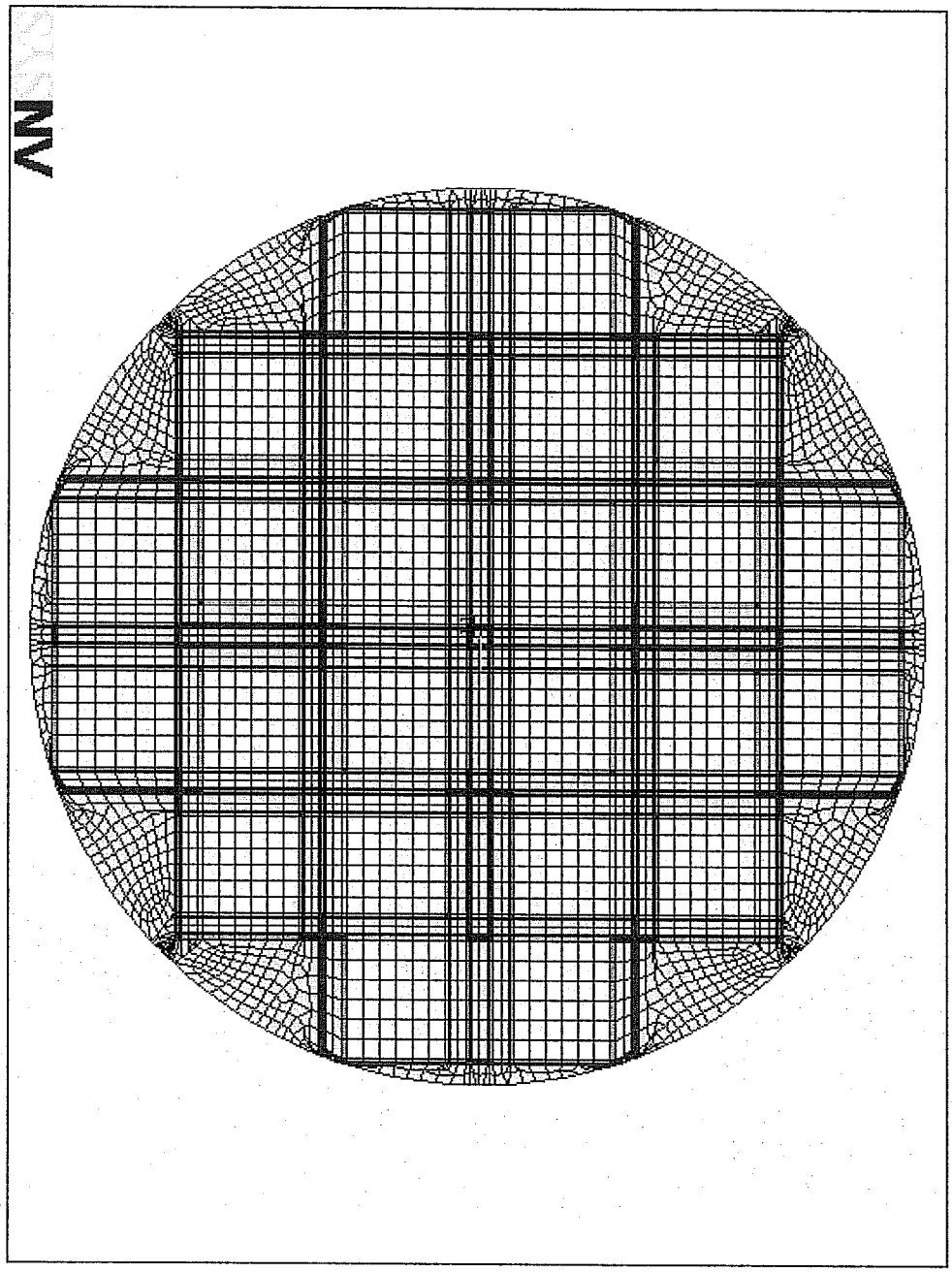

FIGURE 4.4.9; MPC-24 BASKET CROSS-SECTION ANSYS FINITE-ELEMENT MODEL

FIGURE 4.4.10; MPC-68 BASKET CROSS-SECTION ANSYS FINITE ELEMENT MODEL

FIGURE 4.4.11

INTENTIONALLY DELETED

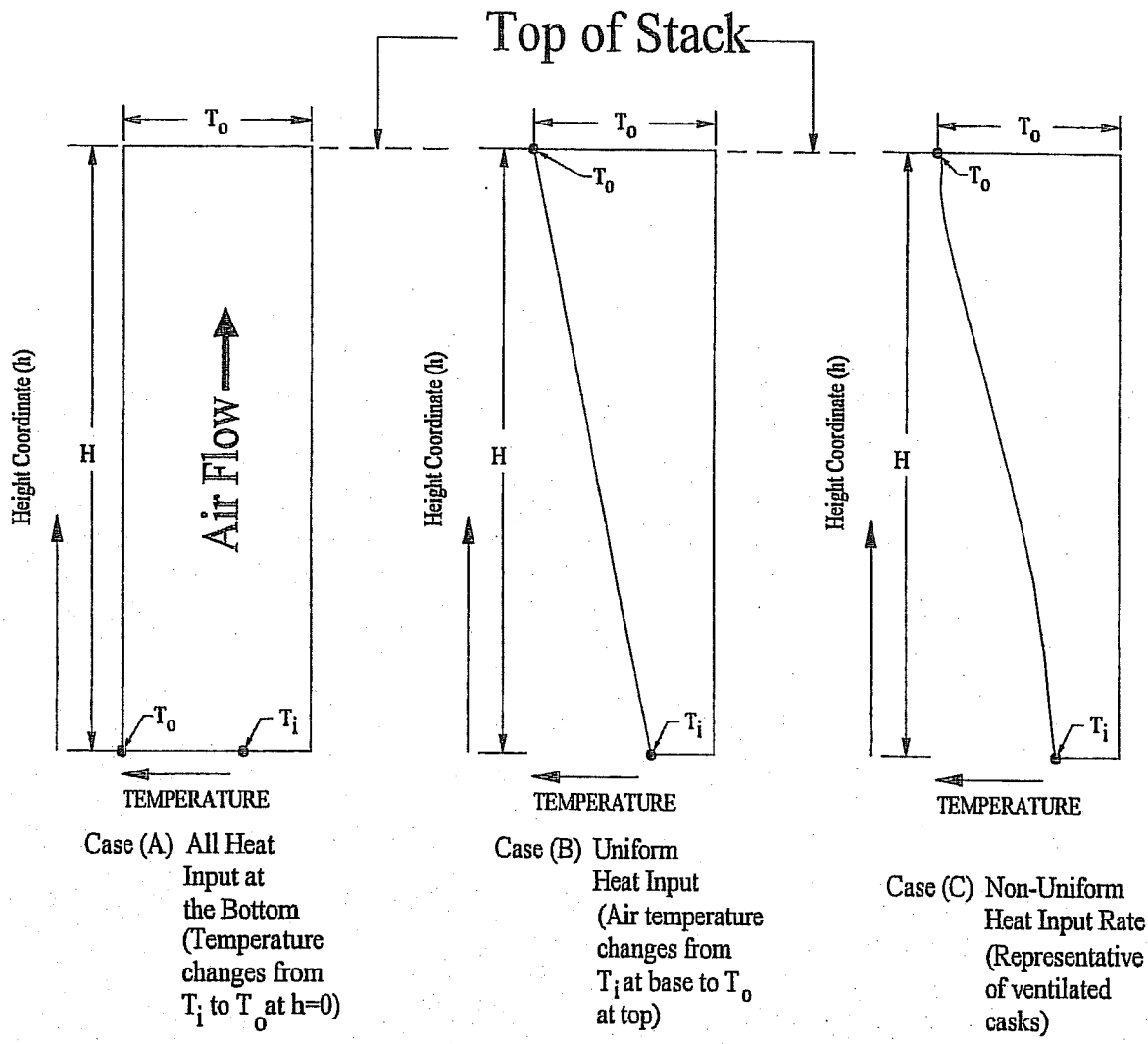

Case (A) All Heat Input at the Bottom (Temperature changes from T_i to T_o at h=0)

Case (B) Uniform Heat Input (Air temperature changes from T_i at base to T_o at top)

Case (C) Non-Uniform Heat Input Rate (Representative of ventilated casks)

Figure 4.4.12; Stack Air Temperature as a Function of Height

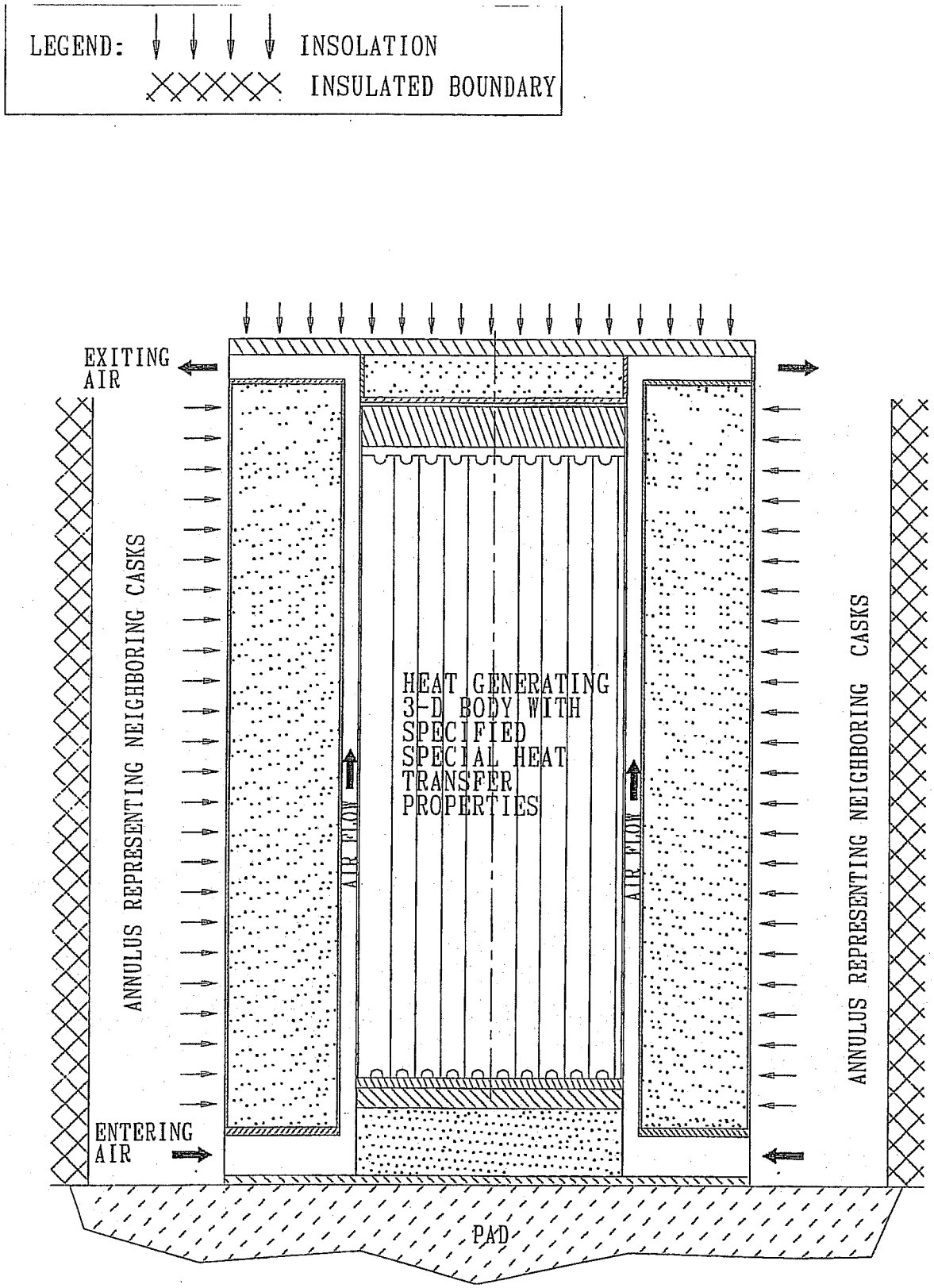

FIGURE 4.4.13; SCHEMATIC DEPICTION OF THE HI-STORM THERMAL ANALYSIS

FIGURE 4.4.14

INTENTIONALLY DELETED

FIGURE 4.4.15

THIS FIGURE INTENTIONALLY DELETED.

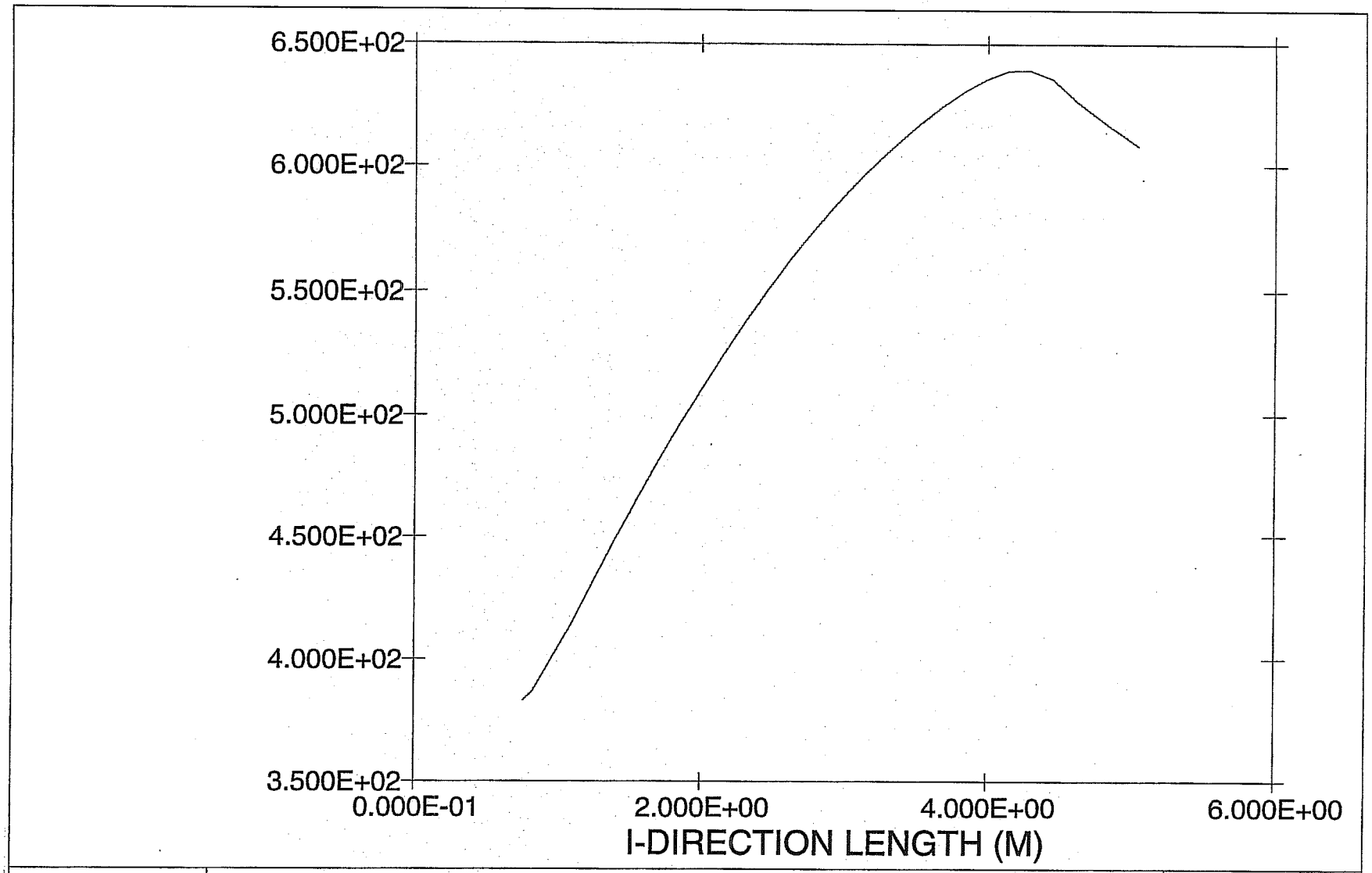

FIGURE 4.4.16: MPC-24 Peak Rod Axial Temperature Profile

Aug 22 2000
Fluent 4.48
Fluent Inc.

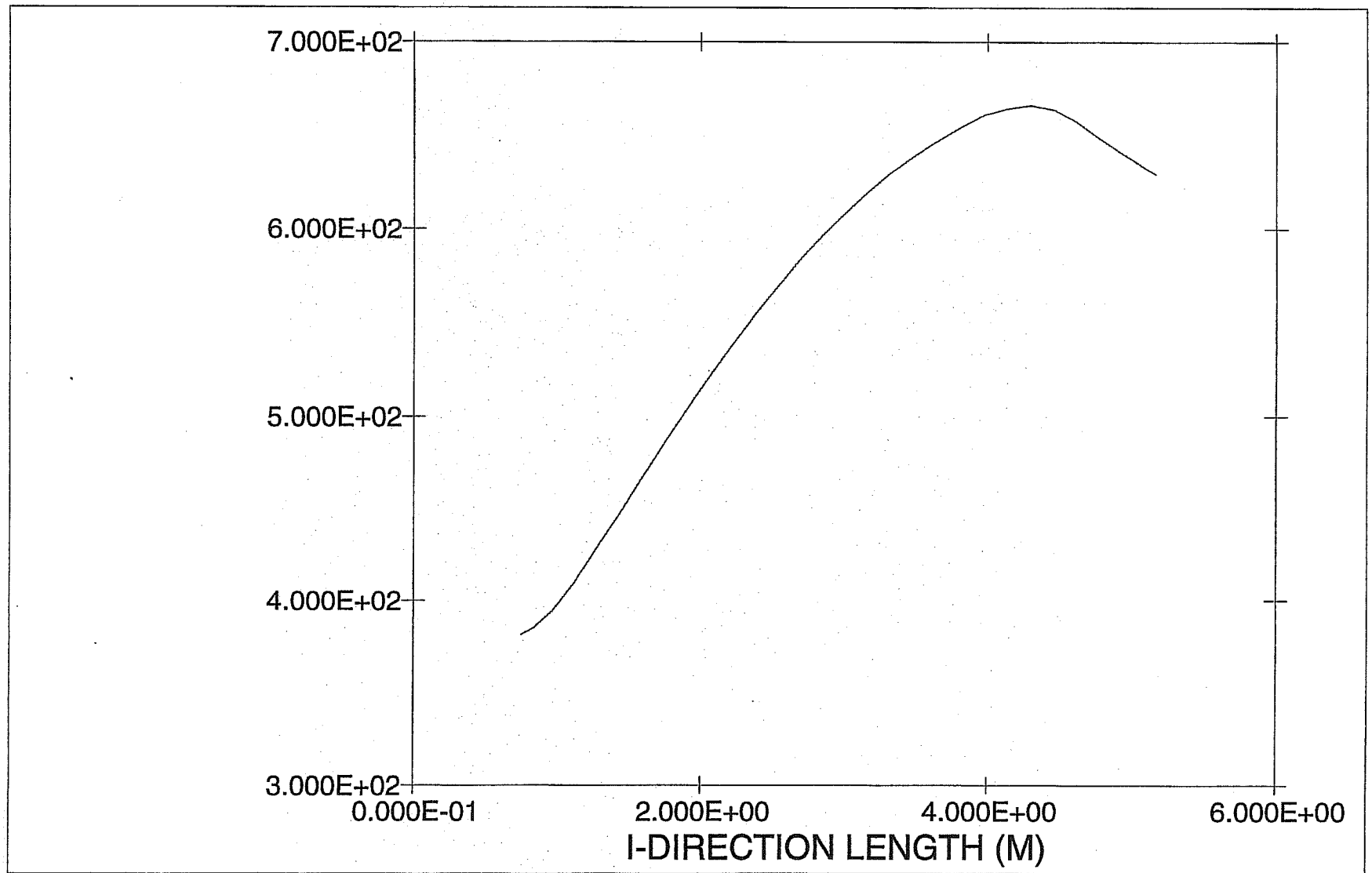

Y Z X	FIGURE 4.4.17: MPC-68 Peak Rod Axial Temperature Profile	Aug 22 2000 Fluent 4.48 Fluent Inc.

FIGURE 4.4.18

THIS FIGURE INTENTIONALLY DELETED.

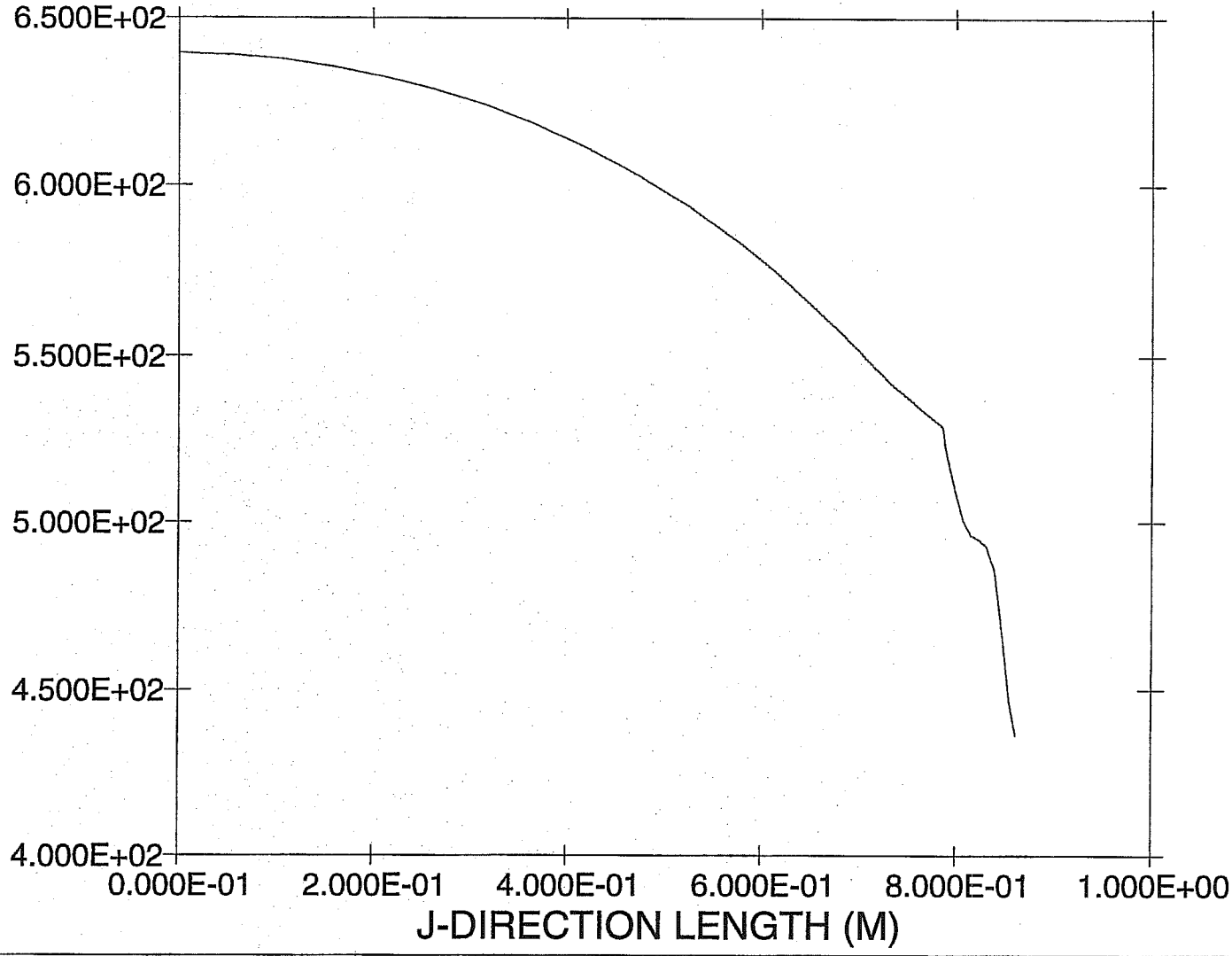

FIGURE 4.4.19: MPC-24 Radial Temperature Profile
(Hottest Basket Cross-Section)

Aug 23 2000
Fluent 4.48
Fluent Inc.

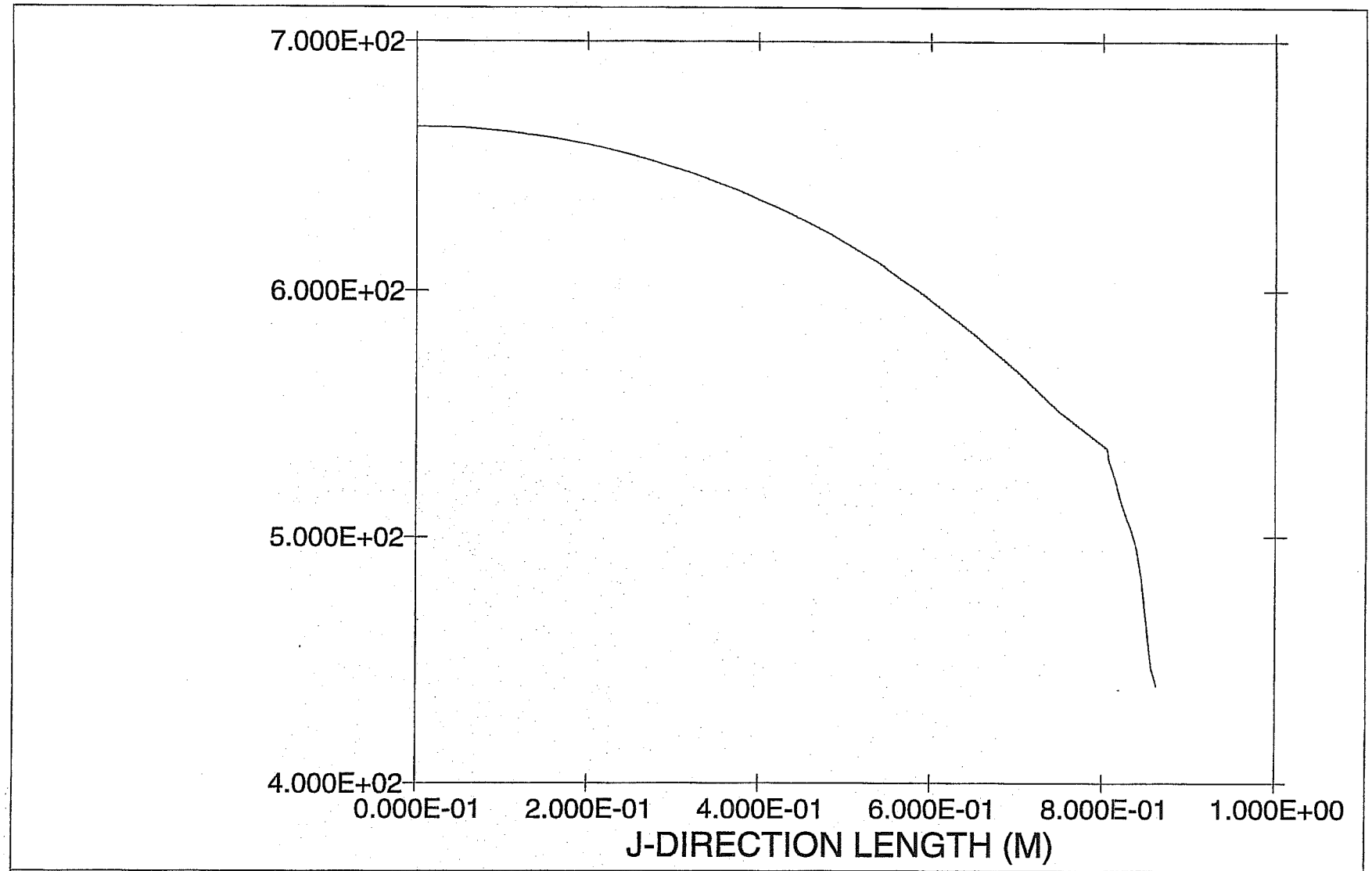

FIGURE 4.4.20: MPC-68 Radial Temperature Profile
(Hottest Basket Cross-section)

Aug 23 2000
Fluent 4.48
Fluent Inc.

FIGURE 4.4.21

THIS FIGURE INTENTIONALLY DELETED.

FIGURE 4.4.22

INTENTIONALLY DELETED

FIGURE 4.4.23

INTENTIONALLY DELETED

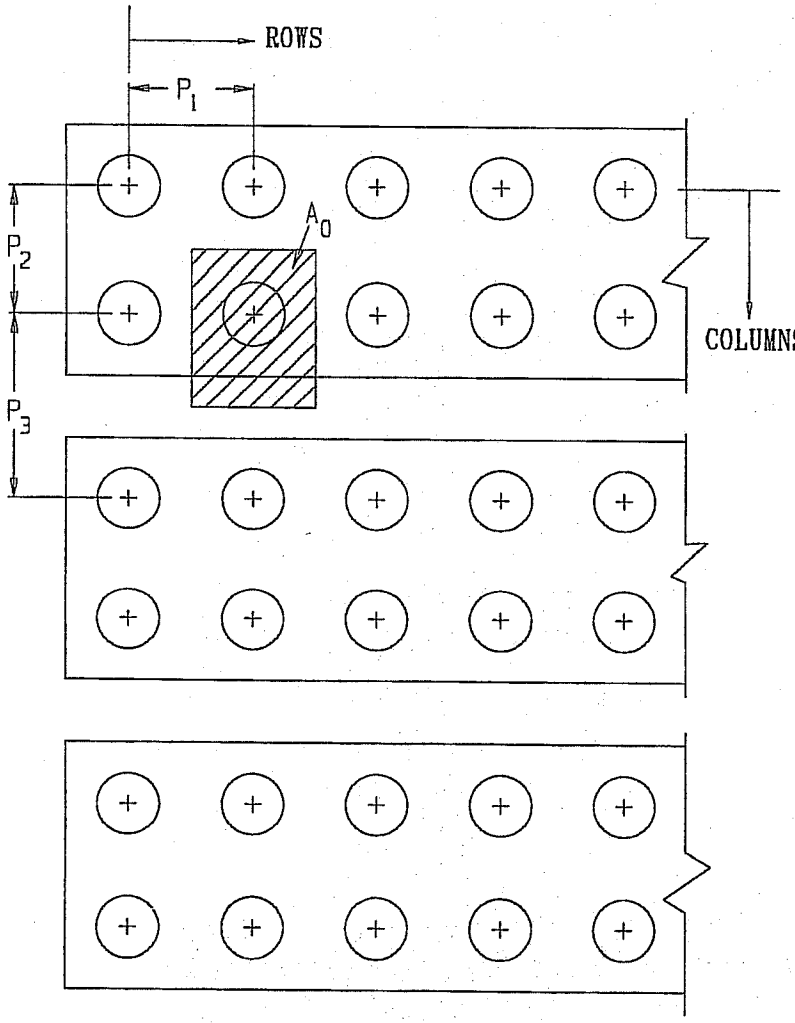

CASE (i) LAYOUT ON A RECTANGULAR PITCH

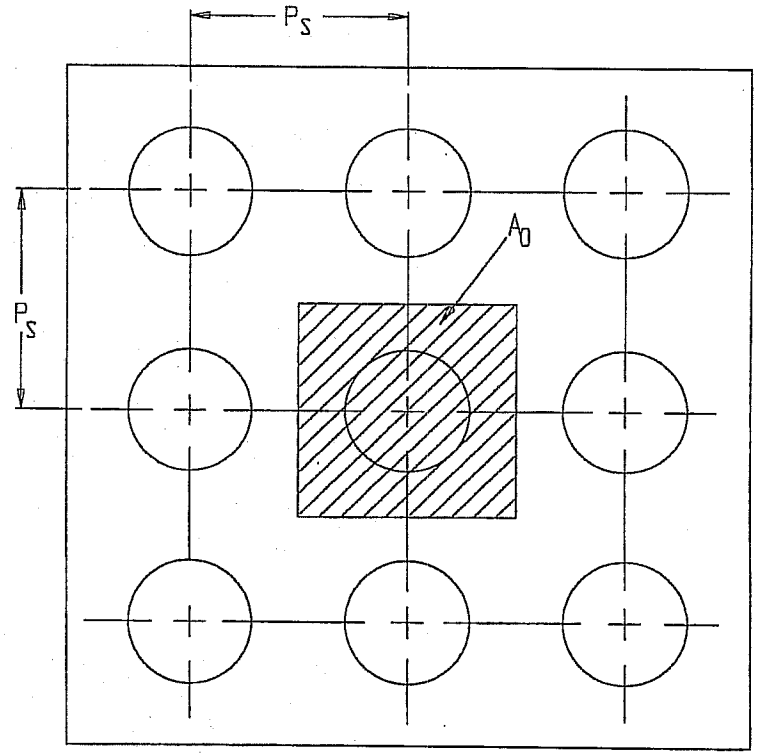

CASE (ii) LAYOUT ON A SQUARE PITCH

LEGEND:

$A_0 = P_1 \times (P_2 + P_3)/2$ CASE (i)

$A_0 = P_S \times P_S$ CASE (ii)

FIGURE 4.4.24; ILLUSTRATION OF MINIMUM AVAILABLE PLANAR AREA PER HI-STORM MODULE AT AN ISFSI.

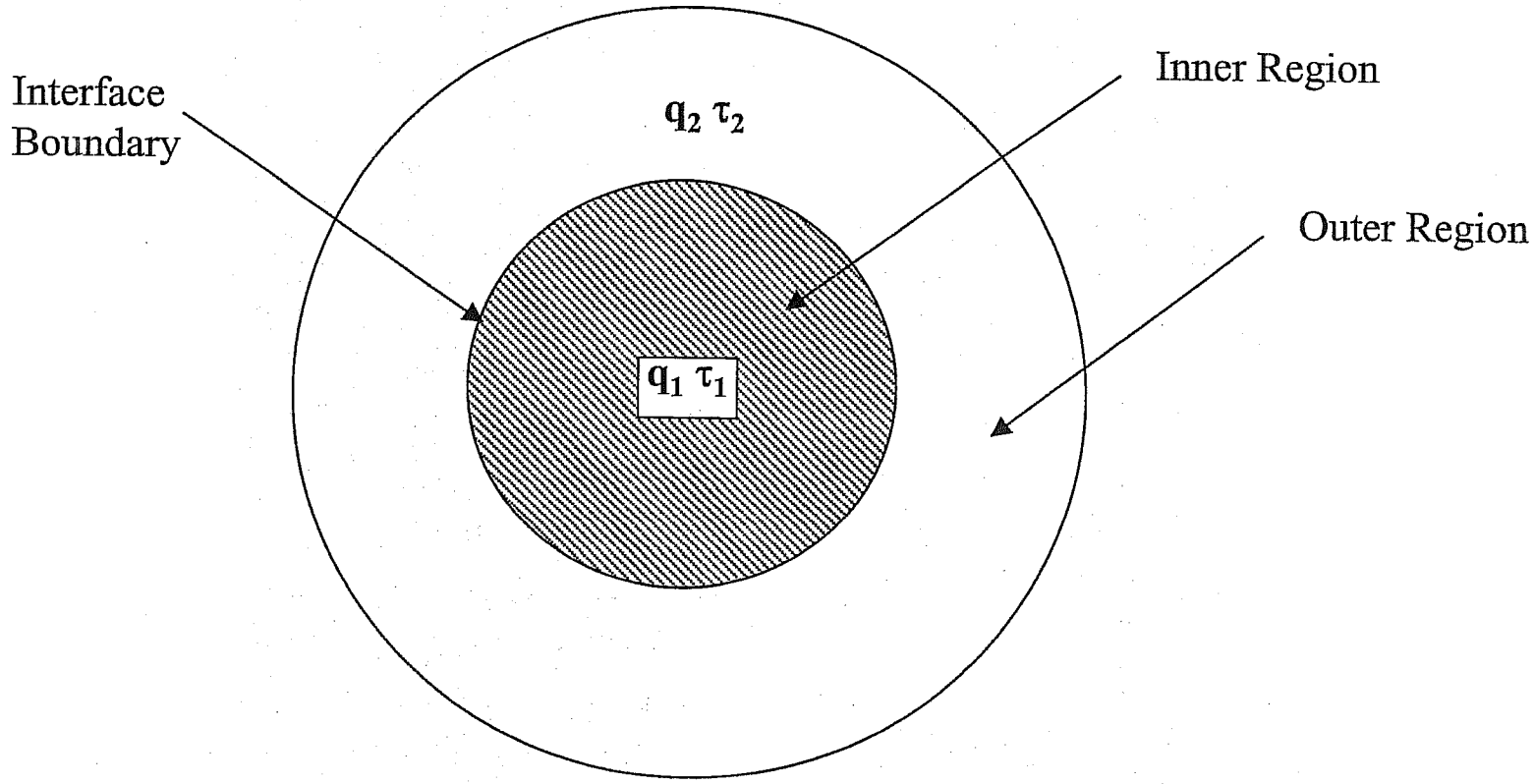

FIGURE 4.4.25: FUEL BASKET REGIONALIZED LOADING SCENARIO

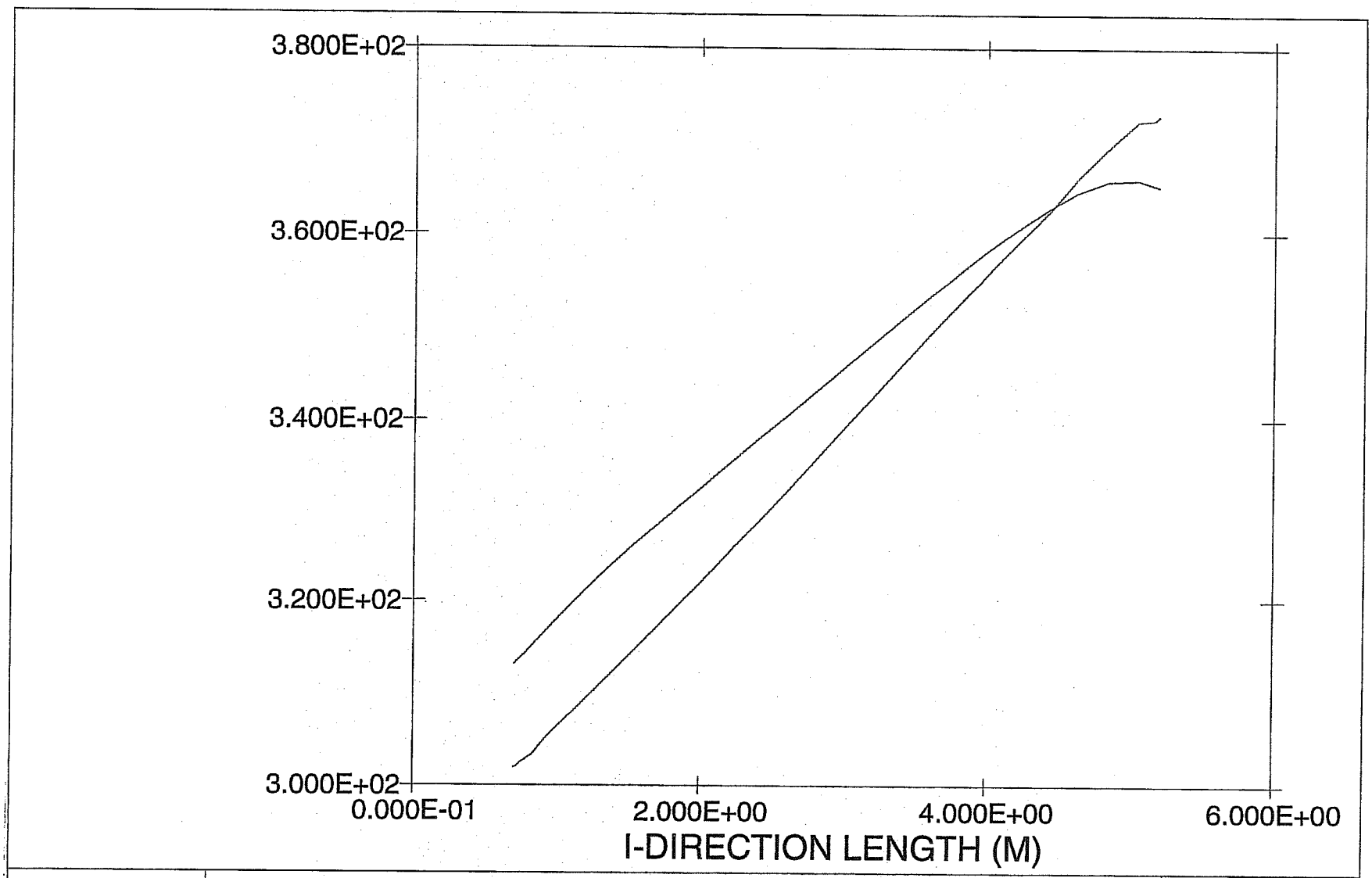

FIGURE 4.4.26: Bounding Overpack Annulus Axial Profiles

Aug 23 2000
Fluent 4.48
Fluent Inc.

HOLTEC INTERNATIONAL COPYRIGHTED MATERIAL

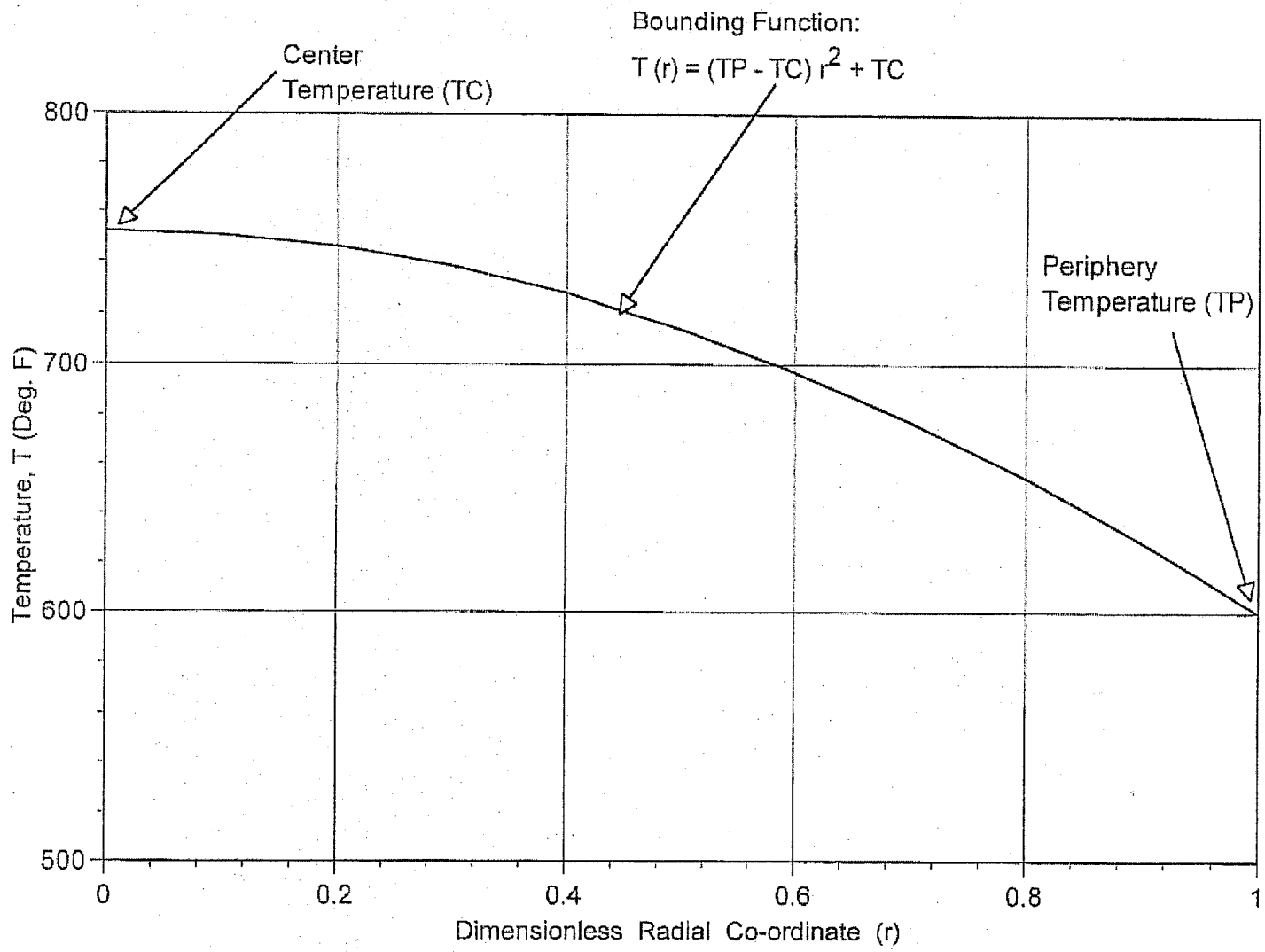

FIGURE 4.4.27: BOUNDING BASKET TEMPERATURE PROFILE FOR DIFFERENTIAL EXPANSION

4.5 THERMAL EVALUATION OF SHORT TERM OPERATIONS

Prior to placement in a HI-STORM overpack, an MPC must be loaded with fuel, outfitted with closures, dewatered, dried, backfilled with helium and transported to the HI-STORM module. In the unlikely event that the fuel needs to be returned to the spent fuel pool, these steps must be performed in reverse. Finally, if required, transfer of a loaded MPC between HI-STORM overpacks or between a HI-STAR transport overpack and a HI-STORM storage overpack must be carried out in an assuredly safe manner. All of the above operations are short duration events that would likely occur no more than once or twice for an individual MPC.

The device central to all of the above operations is the HI-TRAC transfer cask that, as stated in Chapter 1, is available in two anatomically identical weight ratings (100- and 125-ton). Two different versions of the 100 ton and the 125 ton HI-TRAC, a classical design and an operationally enhanced version D, are available for use during fuel transfer operations. The HI-TRAC transfer cask is a short-term host for the MPC; therefore it is necessary to establish that, during all thermally challenging operation events involving either the 100-ton or 125-ton versions of the HI-TRAC, the permissible temperature limits presented in Section 4.3 are not exceeded. The following discrete thermal scenarios, all of short duration, involving the HI-TRAC transfer cask have been identified as warranting thermal analysis.

i. Normal Onsite Transport
ii. MPC Cavity Drying
iii. Post-Loading Wet Transfer Operations
iv. MPC Cooldown and Reflood for Unloading Operations

Onsite transport of the MPC generally occurs with the HI-TRAC in the vertical orientation, which preserves the thermosiphon action within the MPC. However, there may be a scenario where onsite transport of an MPC must occur with the HI-TRAC in the horizontal configuration. Both orientations are evaluated in this section.

The fuel handling operations listed above place a certain level of constraint on the dissipation of heat from the MPC relative to the normal storage condition. Consequently, for some scenarios, it is necessary to provide additional cooling. For such situations, a new ancillary henceforth referred to as the Supplemental Cooling System (SCS) is required to provide additional cooling during short term operations. The specific design of an SCS must accord with site-specific needs and resources, including the availability of plant utilities. However, a set of specifications to ensure that the performance objectives of the SCS will be satisfied by any plant-specific design are set forth in Appendix 2.C.

The above listed conditions are described and evaluated in the following subsections. Subsection 4.5.1 describes the individual analytical models used to evaluate these conditions. Due to the simplicity of the conservative evaluation of wet transfer operations, Subsection 4.5.1.1.5 includes both the analysis model and analysis results discussions. The maximum temperature analyses for onsite transport and vacuum drying are discussed in Subsection 4.5.2. Subsections

HOLTEC INTERNATIONAL COPYRIGHTED MATERIAL

4.5.3, 4.5.4 and 4.5.5, respectively, discuss minimum temperature, MPC maximum internal pressure and thermal data for stress analyses during onsite transport.

4.5.1 Thermal Model

The HI-TRAC transfer cask is used to load and unload the HI-STORM concrete storage overpack, including onsite transport of the MPCs from the loading facility to an ISFSI pad. Section views of the HI-TRAC have been presented in Chapter 1. Within a loaded HI-TRAC, heat generated in the MPC is transported from the contained fuel assemblies to the MPC shell in the manner described in Section 4.4. From the outer surface of the MPC to the ambient air, heat is transported by a combination of conduction, thermal radiation and natural convection. Analytical modeling details of all the various thermal transport mechanisms are provided in the following subsection.

All of the HI-TRAC transfer cask designs, are developed for onsite handling and transport, as discussed in Chapter 1. From a thermal performance standpoint, the designs are principally different in terms of lead thickness and the number and thickness of radial connectors in the water jacket region. The analytical model developed for HI-TRAC thermal characterization conservatively accounts for these differences by applying the higher shell and lead thicknesses, lowest number of radial connectors and thinner radial connectors' thickness to the model. In this manner, the HI-TRAC overpack resistance to heat transfer is overestimated, resulting in higher predicted MPC internals and fuel cladding temperature levels.

4.5.1.1 Analytical Model

From the outer surface of the MPC to the ambient atmosphere, heat is transported within HI-TRAC through multiple concentric layers of air, steel and shielding materials. Heat must be transported across a total of six concentric layers, representing the air gap, the HI-TRAC inner shell, the lead shielding, the HI-TRAC outer shell, the water jacket and the enclosure shell. From the surface of the enclosure shell heat is rejected to the atmosphere by natural convection and radiation.

A small diametral air gap exists between the outer surface of the MPC and the inner surface of the HI-TRAC overpack. Heat is transported across this gap by the parallel mechanisms of conduction and thermal radiation. Assuming that the MPC is centered and does not contact the transfer overpack walls conservatively minimizes heat transport across this gap. Additionally, thermal expansion that would minimize the gap is conservatively neglected. Heat is transported through the cylindrical wall of the HI-TRAC transfer overpack by conduction through successive layers of steel, lead and steel. A water jacket, which provides neutron shielding for the HI-TRAC overpack, surrounds the cylindrical steel wall. The water jacket is composed of carbon steel channels with welded, connecting enclosure plates. Conduction heat transfer occurs through both the water cavities and the channels. While the water jacket channels are sufficiently large for natural convection loops to form, this mechanism is conservatively neglected. Heat is

HOLTEC INTERNATIONAL COPYRIGHTED MATERIAL

passively rejected to the ambient from the outer surface of the HI-TRAC transfer overpack by natural convection and thermal radiation.

In the vertical position, the bottom face of the HI-TRAC is in contact with a supporting surface. This face is conservatively modeled as an insulated surface. Because the HI-TRAC is not used for long-term storage in an array, radiative blocking does not need to be considered. The HI-TRAC top lid is modeled as a surface with convection, radiative heat exchange with air and a constant maximum incident solar heat flux load. Insolation on cylindrical surfaces is conservatively based on 12-hour levels prescribed in 10CFR71 averaged on a 24-hour basis. Concise descriptions of these models are given below.

4.5.1.1.1 Effective Thermal Conductivity of Water Jacket

The classical versions of the HI-TRAC water jacket is composed of an array of radial ribs equispaced along the circumference of the HI-TRAC and welded along their length to the HI-TRAC outer shell. Enclosure plates are welded to these ribs, creating an array of water compartments. The version D HI-TRAC water jackets have an array of radial ribs connected to enclosure plates with an array of plug welds to form multiple water compartments. Holes in the radial ribs connect all the individual compartments in the water jacket. Any combination of rib number and thickness that yields an equal or larger heat transfer area is bounded by the calculation. Thus, the annular region between the HI-TRAC outer shell and the enclosure shell can be considered as an array of steel ribs and water spaces.

The effective radial thermal conductivity of this array of steel ribs and water spaces is determined by combining the heat transfer resistance of individual components in a parallel network. A bounding calculation is assured by using the minimum number of ribs and rib thickness as input values. The thermal conductivity of the parallel steel ribs and water spaces is given by the following formula:

$$K_{ne} = \frac{K_r N_r t_r \ln\left(\frac{r_o}{r_i}\right)}{2\pi L_R} + \frac{K_w N_r t_w \ln\left(\frac{r_o}{r_i}\right)}{2\pi L_R}$$

where:

K_{ne} = effective radial thermal conductivity of water jacket
r_i = inner radius of water spaces
r_o = outer radius of water spaces
K_r = thermal conductivity of carbon steel ribs
N_r = minimum number of radial ribs (equal to number of water spaces)
t_r = minimum (nominal) rib thickness (lower of 125-ton and 100-ton designs)
L_R = effective radial heat transport length through water spaces
K_w = thermal conductivity of water
t_w = water space width (between two carbon steel ribs)

HOLTEC INTERNATIONAL COPYRIGHTED MATERIAL

Figure 4.5.1 depicts the resistance network to combine the resistances to determine an effective conductivity of the water jacket. The effective thermal conductivity is computed in the manner of the foregoing, and is provided in Table 4.5.1.

4.5.1.1.2 Heat Rejection from Overpack Exterior Surfaces

The following relationship for the surface heat flux from the outer surface of an isolated cask to the environment is applied to the thermal model:

$$q_s = 0.19\,(T_s - T_A)^{4/3} + 0.1714\varepsilon\left[\left(\frac{T_s + 460}{100}\right)^4 - \left(\frac{T_A + 460}{100}\right)^4\right]$$

where:

T_S = cask surface temperatures (°F)
T_A = ambient atmospheric temperature (°F)
q_s = surface heat flux (Btu/ft^2×hr)
ε = surface emissivity

The second term in this equation the Stefan-Boltzmann formula for thermal radiation from an exposed surface to ambient. The first term is the natural convection heat transfer correlation recommended by Jacob and Hawkins [4.2.9]. This correlation is appropriate for turbulent natural convection from vertical surfaces, such as the vertical overpack wall. Although the ambient air is conservatively assumed to be quiescent, the natural convection is nevertheless turbulent.

Turbulent natural convection correlations are suitable for use when the product of the Grashof and Prandtl (Gr×Pr) numbers exceeds 10^9. This product can be expressed as $L^3 \times \Delta T \times Z$, where L is the characteristic length, ΔT is the surface-to-ambient temperature difference, and Z is a function of the surface temperature. The characteristic length of a vertically oriented HI-TRAC is its height of approximately 17 feet. The value of Z, conservatively taken at a surface temperature of 340°F, is 2.6×10^5. Solving for the value of ΔT that satisfies the equivalence $L^3 \times \Delta T \times Z = 10^9$ yields $\Delta T = 0.78$°F. For a horizontally oriented HI-TRAC the characteristic length is the diameter of approximately 7.6 feet (minimum of 100- and 125-ton designs), yielding $\Delta T = 8.76$°F. The natural convection will be turbulent, therefore, provided the surface to air temperature difference is greater than or equal to 0.78°F for a vertical orientation and 8.76°F for a horizontal orientation.

4.5.1.1.3 Determination of Solar Heat Input

As discussed in Section 4.4.1.1.8, the intensity of solar radiation incident on an exposed surface depends on a number of time varying terms. A twelve-hour averaged insolation level is prescribed in 10CFR71 for curved surfaces. The HI-TRAC cask, however, possesses a considerable thermal inertia. This large thermal inertia precludes the HI-TRAC from reaching a steady-state thermal condition during a twelve-hour period. Thus, it is considered appropriate to use the 24-hour averaged insolation level.

4.5.1.1.4 MPC Temperatures During Moisture Removal Operations

4.5.1.1.4.1 Vacuum Drying

The initial loading of SNF in the MPC requires that the water within the MPC be drained and replaced with helium. For MPCs containing moderate burnup fuel assemblies only, this operation may be carried out using the conventional vacuum drying approach. In this method, removal of the last traces of residual moisture from the MPC cavity is accomplished by evacuating the MPC for a short time after draining the MPC. Vacuum drying may not be performed on MPCs containing high burnup fuel assemblies. High burnup fuel drying is performed by a forced flow helium drying process as described in Section 4.5.1.1.4.2 and Appendix 2.B.

Prior to the start of the MPC draining operation, both the HI-TRAC annulus and the MPC are full of water. The presence of water in the MPC ensures that the fuel cladding temperatures are lower than design basis limits by large margins. As the heat generating active fuel length is uncovered during the draining operation, the fuel and basket mass will undergo a gradual heat up from the initially cold conditions when the heated surfaces were submerged under water.

The vacuum condition effective fuel assembly conductivity is determined by procedures discussed earlier (Subsection 4.4.1.1.2) after setting the thermal conductivity of the gaseous medium to a small fraction (one part in one thousand) of helium conductivity. The MPC basket cross sectional effective conductivity is determined for vacuum conditions according to the procedure discussed in 4.4.1.1.4. Basket periphery-to-MPC shell heat transfer occurs through conduction and radiation.

For total decay heat loads up to and including 20.88 kW for the MPC-24 and 21.52 kW for the MPC-68, vacuum drying of the MPC is performed with the annular gap between the MPC and the HI-TRAC filled with water. The presence of water in this annular gap will maintain the MPC shell temperature approximately equal to the saturation temperature of the annulus water. Thus, the thermal analysis of the MPC during vacuum drying for these conditions is performed with cooling of the MPC shell with water at a bounding maximum temperature of 232°F.

For higher total decay heat loads in the MPC-24 and MPC-68 or for any decay heat load in an MPC-24E or MPC-32, vacuum drying of the MPC is performed with the annular gap between the MPC and the HI-TRAC continuously flushed with water. The water movement in this annular gap will maintain the MPC shell temperature at about the temperature of flowing water. Thus, the thermal analysis of the MPC during vacuum drying for these conditions is performed with cooling of the MPC shell with water at a bounding maximum temperature of 125°F.

An axisymmetric FLUENT thermal model of the MPC is constructed, employing the MPC in-plane conductivity as an isotropic fuel basket conductivity (i.e. conductivity in the basket radial and axial directions is equal), to determine peak cladding temperature at design basis heat loads.

To avoid excessive conservatism in the computed FLUENT solution, partial recognition for higher axial heat dissipation is adopted in the peak cladding calculations. The boundary conditions applied to this evaluation are:

i. A bounding steady-state analysis is performed with the MPC decay heat load set equal to the largest design-basis decay heat load. As discussed above, there are two different ranges for the MPC-24 and MPC-68 designs.

ii. The entire outer surface of the MPC shell is postulated to be at a bounding maximum temperature of 232°F or 125°F, as discussed above.

iii. The top and bottom surfaces of the MPC are adiabatic.

Results of vacuum condition analyses are provided in Subsection 4.5.2.2.

4.5.1.1.4.2 Forced Helium Dehydration

To reduce moisture to trace levels in the MPC using a Forced Helium Dehydration (FHD) system, a conventional, closed loop dehumidification system consisting of a condenser, a demoisturizer, a compressor, and a pre-heater is utilized to extract moisture from the MPC cavity through repeated displacement of its contained helium, accompanied by vigorous flow turbulation. A vapor pressure of 3 torr or less is assured by verifying that the helium temperature exiting the demoisturizer is maintained at or below the psychrometric threshold of 21°F for a minimum of 30 minutes. See Appendix 2.B for detailed discussion of the design criteria and operation of the FHD system.

The FHD system provides concurrent fuel cooling during the moisture removal process through forced convective heat transfer. The attendant forced convection-aided heat transfer occurring during operation of the FHD system ensures that the fuel cladding temperature will remain below the applicable peak cladding temperature limit for normal conditions of storage, which is well below the high burnup cladding temperature limit 752°F (400°C) for all combinations of SNF type, burnup, decay heat, and cooling time. Because the FHD operation induces a state of forced convection heat transfer in the MPC, (in contrast to the quiescent mode of natural convection in long term storage), it is readily concluded that the peak fuel cladding temperature under the latter condition will be greater than that during the FHD operation phase. In the event that the FHD system malfunctions, the forced convection state will degenerate to natural convection, which corresponds to the conditions of normal onsite transport. As a result, the peak fuel cladding temperatures will approximate the values reached during normal onsite transport as described elsewhere in this chapter.

4.5.1.1.5 Maximum Time Limit During Wet Transfer Operations

In accordance with NUREG-1536, water inside the MPC cavity during wet transfer operations is not permitted to boil. Consequently, uncontrolled pressures in the de-watering, purging, and

recharging system that may result from two-phase conditions are completely avoided. This requirement is accomplished by imposing a limit on the maximum allowable time duration for fuel to be submerged in water after a loaded HI-TRAC cask is removed from the pool and prior to the start of vacuum drying operations.

When the HI-TRAC transfer cask and the loaded MPC under water-flooded conditions are removed from the pool, the combined water, fuel mass, MPC, and HI-TRAC metal will absorb the decay heat emitted by the fuel assemblies. This results in a slow temperature rise of the entire system with time, starting from an initial temperature of the contents. The rate of temperature rise is limited by the thermal inertia of the HI-TRAC system. To enable a bounding heat-up rate determination for the HI-TRAC system, the following conservative assumptions are imposed:

i. Heat loss by natural convection and radiation from the exposed HI-TRAC surfaces to the pool building ambient air is neglected (i.e., an adiabatic temperature rise calculation is performed).

ii. Design-basis maximum decay heat input from the loaded fuel assemblies is imposed on the HI-TRAC transfer cask.

iii. The smaller of the two versions of the HI-TRAC transfer cask designs (i.e., 100-ton and 125-ton) is credited in the analysis. The 100-ton designs have a significantly smaller quantity of metal mass, which will result in a higher rate of temperature rise.

iv. The smallest of the minimum MPC cavity-free volumes among the two MPC types is considered for flooded water mass determination.

v. Only fifty percent of the water mass in the MPC cavity is credited towards water thermal inertia evaluation.

Table 4.5.5 summarizes the weights and thermal inertias of several components in the loaded HI-TRAC transfer cask. The rate of temperature rise of the HI-TRAC transfer cask and contents during an adiabatic heat-up is governed by the following equation:

$$\frac{dT}{dt} = \frac{Q}{C_h}$$

where:

Q = decay heat load (Btu/hr) [Design Basis maximum 28.74 kW = 98,205 Btu/hr]
C_h = combined thermal inertia of the loaded HI-TRAC transfer cask (Btu/°F)
T = temperature of the contents (°F)
t = time after HI-TRAC transfer cask is removed from the pool (hr)

A bounding heat-up rate for the HI-TRAC transfer cask contents is determined to be equal to 3.77°F/hr. From this adiabatic rate of temperature rise estimate, the maximum allowable time duration (t_{max}) for fuel to be submerged in water is determined as follows:

$$t_{max} = \frac{T_{boil} - T_{initial}}{(dT/dt)}$$

where:

T_{boil} = boiling temperature of water (equal to 212°F at the water surface in the MPC cavity)

$T_{initial}$ = initial temperature of the HI-TRAC contents when the transfer cask is removed from the pool

Table 4.5.6 provides a summary of t_{max} at several representative HI-TRAC contents starting temperature.

As set forth in the HI-STORM operating procedures, in the unlikely event that the maximum allowable time provided in Table 4.5.6 is found to be insufficient to complete all wet transfer operations, a forced water circulation shall be initiated and maintained to remove the decay heat from the MPC cavity. In this case, relatively cooler water will enter via the MPC lid drain port connection and heated water will exit from the vent port. The minimum water flow rate required to maintain the MPC cavity water temperature below boiling with an adequate subcooling margin is determined as follows:

$$M_W = \frac{Q}{C_{pW}(T_{max} - T_{in})}$$

where:

M_W = minimum water flow rate (lb/hr)

C_{pw} = water heat capacity (Btu/lb-°F)

T_{max} = maximum MPC cavity water mass temperature

T_{in} = temperature of pool water supply to MPC

With the MPC cavity water temperature limited to 150°F, MPC inlet water maximum temperature equal to 125°F and at the design basis maximum heat load, the water flow rate is determined to be 3928 lb/hr (7.9 gpm).

4.5.1.1.6 Cask Cooldown and Reflood Analysis During Fuel Unloading Operation

NUREG-1536 requires an evaluation of cask cooldown and reflood procedures to support fuel unloading from a dry condition. Past industry experience generally supports cooldown of cask internals and fuel from hot storage conditions by direct water quenching. Direct MPC cooldown is effectuated by introducing water through the lid drain line. From the drain line, water enters the MPC cavity near the MPC baseplate. Steam produced during the direct quenching process will be vented from the MPC cavity through the lid vent port. To maximize venting capacity, both vent port RVOA connections must remain open for the duration of the fuel unloading

operations. As direct water quenching of hot fuel results in steam generation, it is necessary to limit the rate of water addition to avoid MPC overpressurization. For example, steam flow calculations using bounding assumptions (100% steam production and MPC at design pressure) show that the MPC is adequately protected upto a reflood rate of 3715 lb/hr. Limiting the water reflood rate to this amount or less would prevent exceeding the MPC design pressure.

4.5.1.1.7 Study of Lead-to-Steel Gaps on Predicted Temperatures

Lead, poured between the inner and outer shells, is utilized as a gamma shield material in the HI-TRAC on-site transfer cask designs. Lead shrinks during solidification requiring the specification and implementation of appropriate steps in the lead installation process so that the annular space is free of gaps. Fortunately, the lead pouring process is a mature technology and proven methods to insure that radial gaps do not develop are widely available. This subsection outlines such a method to achieve a zero-gap lead installation in the annular cavity of the HI-TRAC casks.

The 100-ton and 125-ton HI-TRAC designs incorporate a maximum of 2.875 inches and a 4.5 inches annular space, respectively, formed between a 3/4-inch thick steel inner shell and a 1-inch thick steel outer shell. The interior steel surfaces are cleaned, sandblasted and fluxed in preparation for the molten lead that will be poured in the annular cavity. The appropriate surface preparation technique is essential to ensure that molten lead sticks to the steel surfaces, which will form a metal to lead bond upon solidification. The molten lead is poured to fill the annular cavity. The molten lead in the immediate vicinity of the steel surfaces, upon cooling by the inner and outer shells, solidifies forming a melt-solid interface. The initial formation of a gap-free interfacial bond between the solidified lead and steel surfaces initiates a process of lead crystallization from the molten pool onto the solid surfaces. Static pressure from the column of molten lead further aids in retaining the solidified lead layer to the steel surfaces. The melt-solid interface growth occurs by freezing of successive layers of molten lead as the heat of fusion is dissipated by the solidified metal and steel structure enclosing it. This growth stops when all the molten lead is used up and the annulus is filled with a solid lead plug. The shop fabrication procedures, being developed in conjunction with the designated manufacturer of the HI-TRAC transfer casks, shall contain detailed step-by-step instructions devised to eliminate the incidence of annular gaps in the lead space of the HI-TRAC.

In the spirit of a defense-in-depth approach, however, a conservatively bounding lead-to-steel gap is assumed herein and the resultant peak cladding temperature under design basis heat load is computed. It is noted that in a non-bonding lead pour scenario, the lead shrinkage resulting from phase transformation related density changes introduces a tendency to form small gaps. This tendency is counteracted by gravity induced slump, which tends to push the heavy mass of lead against the steel surfaces. If the annular molten mass of lead is assumed to contract as a solid, in the absence of gravity, then a bounding lead-to-steel gap is readily computed from density changes. This calculation is performed for the 125-ton HI-TRAC transfer cask, which has a larger volume of lead and is thus subject to larger volume shrinkage relative to the 100-ton design, and is presented below.

The densities of molten (ρ_l) and solid (ρ_s) lead are given on page 3-96 of Perry's Handbook (6th Edition) as 10,430 kg/m^3 and 11,010 kg/m^3, respectively. The fractional volume contraction during solidification ($\delta v/v$) is calculated as:

$$\frac{\delta v}{v} = \frac{(\rho_s - \rho_l)}{\rho_l} = \frac{(11{,}010 - 10{,}430)}{10{,}430} = 0.0556$$

and the corresponding fractional linear contraction during solidification is calculated as:

$$\frac{\delta L}{L} = \left[1 + \frac{\delta v}{v}\right]^{1/3} - 1 = 1.0556^{1/3} - 1 = 0.0182$$

The bounding lead-to-steel gap, which is assumed filled with air, is calculated by multiplying the nominal annulus radial dimension (4.5 inches in the 125-ton HI-TRAC) by the fractional linear contraction as:

$$\delta = 4.5 \times \frac{\delta L}{L} = 4.5 \times 0.0182 = 0.082 \cdot \text{inches}$$

In this hypothetical lead shrinkage process, the annular lead cylinder will contract towards the inner steel shell, eliminating gaps and tightly compressing the two surfaces together. Near the outer steel cylinder, a steel-to-lead air gap will develop as a result of volume reduction in the liquid to solid phase transformation. The air gap is conservatively postulated to occur between the inner steel shell and the lead, where the heat flux is higher relative to the outer steel shell, and hence the computed temperature gradient is greater. The combined resistance of an annular lead cylinder with an air gap (R_{cyl}) is computed by the following formula:

$$R_{cyl} = \frac{\ln(R_o/R_i)}{2\pi K_{pb}} + \frac{\delta}{2\pi R_i [K_{air} + K_r]}$$

where:

R_i = inner radius (equal to 35.125 inches)
R_o = outer radius (equal to 39.625 inches)
K_{pb} = bounding minimum lead conductivity (equal to 16.9 Btu/ft-hr-°F, from Table 4.2.2)
δ = lead-to-steel air gap, computed above
K_{air} = temperature dependent air conductivity (see Table 4.2.2)
K_r = effective thermal conductivity contribution from radiation heat transfer across air gap

The effective thermal conductivity contribution from radiation heat transfer (K_r) is defined by the following equation:

$$K_r = 4 \times \sigma \times F_\varepsilon \times T^3 \times \delta$$

HOLTEC INTERNATIONAL COPYRIGHTED MATERIAL

where:

σ = Stefan-Boltzmann constant
F_ε = $(1/\varepsilon_{cs} + 1/\varepsilon_{pb} - 1)^{-1}$
ε_{cs} = carbon steel emissivity (equal to 0.66, HI-STORM FSAR Table 4.2.4)
ε_{pb} = lead emissivity (equal to 0.63 for oxidized surfaces at 300°F from McAdams, Heat Transmission, 3rd Ed.)
T = absolute temperature

Based on the total annular region resistance (R_{cyl}) computed above, equivalent annulus conductivity is readily computed. This effective temperature-dependent conductivity results are tabulated below:

Temperature (°F)	Effective Annulus Conductivity (Btu/ft-hr-°F)
200	1.142
450	1.809

The results tabulated above confirm that the assumption of a bounding annular air gap grossly penalizes the heat dissipation characteristics of lead filled regions. Indeed, the effective conductivity computed above is an order of magnitude lower than that of the base lead material. To confirm the heat dissipation adequacy of HI-TRAC casks under the assumed overly pessimistic annular gaps, the HI-TRAC thermal model described earlier is altered to include the effective annulus conductivity computed above for the annular lead region. The peak cladding temperature results are tabulated below:

Annular Gap Assumption	Peak Cladding Temperature (°F)	Cladding Temperature Limit (°F)
None	872	1058
Bounding Maximum	924	1058

From these results, it is readily apparent that the stored fuel shall be maintained within safe temperature limits by a substantial margin of safety (in excess of 100°F).

4.5.1.2 Test Model

A detailed analytical model for thermal design of the HI-TRAC transfer cask was developed using the FLUENT CFD code, the industry standard ANSYS modeling package and conservative adiabatic calculations, as discussed in Subsection 4.5.1.1. Furthermore, the analyses incorporate many conservative assumptions in order to demonstrate compliance to the specified short-term limits with adequate margins. In view of these considerations, the HI-TRAC transfer cask thermal design complies with the thermal criteria established for short-term handling and

onsite transport. Additional experimental verification of the thermal design is therefore not required.

4.5.2 Maximum Temperatures

4.5.2.1 Maximum Temperatures Under Onsite Transport Conditions

An axisymmetric FLUENT thermal model of an MPC inside a HI-TRAC transfer cask was developed to evaluate temperature distributions for onsite transport conditions. A bounding steady-state analysis of the HI-TRAC transfer cask has been performed using the hottest MPC, the highest design-basis decay heat load (Table 2.1.6), and design-basis insolation levels. While the duration of onsite transport may be short enough to preclude the MPC and HI-TRAC from obtaining a steady-state, a steady-state analysis is conservative. Information listing all other thermal analyses pertaining to the HI-TRAC cask and associated subsection of the FSAR summarizing obtained results is provided in Table 4.5.8.

A converged temperature contour plot is provided in Figure 4.5.2. Maximum fuel clad temperatures are listed in Table 4.5.2, which also summarizes maximum calculated temperatures in different parts of the HI-TRAC transfer cask and MPC. As described in Subsection 4.4.2, the FLUENT calculated peak temperature in Table 4.5.2 is actually the peak pellet centerline temperature, which bounds the peak cladding temperature. We conservatively assume that the peak clad temperature is equal to the peak pellet centerline temperature.

The maximum computed temperatures listed in Table 4.5.2 are based on the HI-TRAC cask at Design Basis Maximum heat load, passively rejecting heat by natural convection and radiation to a hot ambient environment at 100°F in still air in a vertical orientation. In this orientation, there is apt to be a less of metal-to-metal contact between the physically distinct entitities, viz., fuel, fuel basket, MPC shell and HI-TRAC cask. For this reason, the gaps resistance between these parts is higher than in a horizontally oriented HI-TRAC. To bound gaps resistance, the various parts are postulated to be in a centered configuration. MPC internal convection at a postulated low cavity pressure of 5 atm is included in the thermal model. The peak cladding temperature computed under these adverse Ultimate Heat Sink (UHS) assumptions is 872°F which is substantially lower than the temperature limit of 1058°F for moderate burnup fuel (MBF). Consequently, cladding integrity assurance is provided by large safety margins (in excess of 100°F) during onsite transfer of an MPC containing MBF emplaced in a HI-TRAC cask.

As a defense-in-depth measure, cladding integrity is demonstrated for a theoretical bounding scenario. For this scenario, all means of convective heat dissipation within the canister are neglected in addition to the bounding relative configuration for the fuel, basket, MPC shell and HI-TRAC overpack assumption stated earlier for the vertical orientation. This means that the fuel is centered in the basket cells, the basket is centered in the MPC shell and the MPC shell is centered in the HI-TRAC overpack to maximize gaps thermal resistance. The peak cladding temperature computed for this scenario (1025°F) is below the short-term limit of 1058°F.

HOLTEC INTERNATIONAL COPYRIGHTED MATERIAL

For high burnup fuel (HBF), however, the maximum computed fuel cladding temperature reported in Table 4.5.2 is significantly greater than the temperature limit of 752°F for HBF. Consequently, it is necessary to utilize the SCS described at the beginning of this section and in Appendix 2.C during onsite transfer of an MPC containing HBF emplaced in a HI-TRAC transfer cask. As stated earlier, the exact design and operation of the SCS is necessarily site-specific. The design is required to satisfy the specifications and operational requirements of Appendix 2.C to ensure compliance with ISG-11 [4.1.4] temperature limits.

4.5.2.2 Maximum MPC Basket Temperature Under Vacuum Conditions

As stated in Subsection 4.5.1.1.4, above, an axisymmetric FLUENT thermal model of the MPC is developed for the vacuum condition. For the MPC-24E and MPC-32 designs, and for the higher heat load ranges in the MPC-24 and MPC-68 designs, the model also includes an isotropic fuel basket thermal conductivity. Each MPC is analyzed at its respective design maximum heat load. The steady-state peak cladding results, with partial recognition for higher axial heat dissipation where included, are summarized in Table 4.5.9. The peak fuel clad temperatures for moderate burnup fuel during short-term vacuum drying operations with design-basis maximum heat loads are calculated to be less than 1058°F for all MPC baskets by a significant margin.

4.5.3 Minimum Temperatures

In Table 2.2.2 and Chapter 12, the minimum ambient temperature condition required to be considered for the HI-TRAC design is specified as 0°F. If, conservatively, a zero decay heat load (with no solar input) is applied to the stored fuel assemblies then every component of the system at steady state would be at this outside minimum temperature. Provided an antifreeze is added to the water jacket (required for ambient temperatures below 32°F), all HI-TRAC materials will satisfactorily perform their intended functions at this minimum postulated temperature condition. Fuel transfer operations must be controlled to ensure that onsite transport operations are not performed at an ambient temperature less than 0°F.

4.5.4 Maximum Internal Pressure

After fuel loading and vacuum drying, but prior to installing the MPC closure ring, the MPC is initially filled with helium. During handling in the HI-TRAC transfer cask, the gas temperature within the MPC rises to its maximum operating temperature as determined based on the thermal analysis methodology described previously. The gas pressure inside the MPC will also increase with rising temperature. The pressure rise is determined based on the ideal gas law, which states that the absolute pressure of a fixed volume of gas is proportional to its absolute temperature. The net free volumes of the four MPC designs are determined in Section 4.4.

The maximum MPC internal pressure is determined for normal onsite transport conditions, as well as off-normal conditions of a postulated accidental release of fission product gases caused by fuel rod rupture. Based on NUREG-1536 [4.4.10] recommended fission gases release fraction data, net free volume and initial fill gas pressure, the bounding maximum gas pressures with 1% and 10% rod rupture are given in Table 4.5.3. The MPC maximum gas pressures listed in Table 4.5.3 are all below the MPC design internal pressure listed in Table 2.2.1.

4.5.5 Maximum Thermal Stresses

Thermal expansion induced mechanical stresses due to non-uniform temperature distributions are reported in Chapter 3. Tables 4.5.2 and 4.5.4 provide a summary of MPC and HI-TRAC transfer cask component temperatures for structural evaluation.

4.5.6 Evaluation of System Performance for Normal Conditions of Handling and Onsite Transport

The HI-TRAC transfer cask thermal analysis is based on a detailed heat transfer model that conservatively accounts for all modes of heat transfer in various portions of the MPC and HI-TRAC. The thermal model incorporates several conservative features, which are listed below:

i. The most severe levels of environmental factors - bounding ambient temperature (100°F) and constant solar flux - were coincidentally imposed on the thermal design. A bounding solar absorbtivity of 1.0 is applied to all insolation surfaces.

ii. The HI-TRAC cask-to-MPC annular gap is analyzed based on the nominal design dimensions. No credit is considered for the significant reduction in this radial gap that would occur as a result of differential thermal expansion with design basis fuel at hot conditions. The MPC is considered to be concentrically aligned with the cask cavity. This is a worst-case scenario since any eccentricity will improve conductive heat transport in this region.

iii. No credit is considered for cooling of the HI-TRAC baseplate while in contact with a supporting surface. An insulated boundary condition is applied in the thermal model on the bottom baseplate face.

Temperature distribution results (Tables 4.5.2 and 4.5.4, and Figure 4.5.2) obtained from this highly conservative thermal model show that the fuel cladding and cask component temperature limits are met with adequate margins for MBF. For HBF, supplemental cooling is required to comply with the applicable temperature limits. Expected margins during normal HI-TRAC use will be larger due to the many conservative assumptions incorporated in the analysis. Corresponding MPC internal pressure results (Table 4.5.3) show that the MPC confinement boundary remains well below the short-term condition design pressure. Stresses induced due to imposed temperature gradients are within ASME Code limits (Chapter 3). The maximum local axial neutron shield temperature is lower than design limits. Therefore, it is concluded that the

HOLTEC INTERNATIONAL COPYRIGHTED MATERIAL

HI-TRAC transfer cask thermal design is adequate to maintain fuel cladding integrity for short-term onsite handling and transfer operations.

The water in the water jacket of the HI-TRAC provides necessary neutron shielding. During normal handling and onsite transfer operations this shielding water is contained within the water jacket, which is designed for an elevated internal pressure. It is recalled that the water jacket is equipped with pressure relief valves set at 60 psig and 65 psig. This set pressure elevates the saturation pressure and temperature inside the water jacket, thereby precluding boiling in the water jacket under normal conditions. Under normal handling and onsite transfer operations, the bulk temperature inside the water jacket reported in Table 4.5.2 is less than the coincident saturation temperature at 60 psig (307°F), so the shielding water remains in its liquid state. The bulk temperature is determined via a conservative analysis, presented earlier, with design-basis maximum decay heat load. One of the assumptions that render the computed temperatures extremely conservative is the stipulation of a 100°F steady-state ambient temperature. In view of the large thermal inertia of the HI-TRAC, an appropriate ambient temperature is the "time-averaged" temperature, formally referred to in this FSAR as the normal temperature.

Note that during hypothetical fire accident conditions (see Section 11.2) these relief valves allow venting of any steam generated by the extreme fire flux, to prevent overpressurizing the water jacket. In this manner, a portion of the fire heat flux input to the HI-TRAC outer surfaces is expended in vaporizing a portion of the water in the water jacket, thereby mitigating the magnitude of the heat input to the MPC during the fire.

During vacuum drying operations, the annular gap between the MPC and the HI-TRAC is filled with water. The saturation temperature of the annulus water bounds the maximum temperatures of all HI-TRAC components, which are located radially outside the water-filled annulus. As previously stated (see Subsection 4.5.1.1.4) the maximum annulus water temperature is only 125°F, so the HI-TRAC water jacket temperature will be less than the 307°F saturation temperature.

Table 4.5.1

EFFECTIVE RADIAL THERMAL CONDUCTIVITY OF THE WATER JACKET

Temperature (°F)	**Thermal Conductivity (Btu/ft-hr-°F)**
200	1.376
450	1.408
700	1.411

Table 4.5.2

HI-TRAC TRANSFER CASK STEADY-STATE
MAXIMUM TEMPERATURES

Component	Temperature [°F]
Fuel Cladding	872*
MPC Basket	852
Basket Periphery	600
MPC Outer Shell Surface	455
HI-TRAC Inner Shell Inner Surface	322
Water Jacket Inner Surface	314
Enclosure Shell Outer Surface	224
Water Jacket Bulk Water	258
Axial Neutron Shield†	258

* This calculated value exceeds the allowable limit for high-burnup fuel. A Supplemental Cooling System that satisfies the criteria in Appendix 2.C shall be used to comply with applicable temperature limits when an MPC contains one or more high burnup fuel assemblies.

† Local neutron shield section temperature.

Table 4.5.3

SUMMARY OF MPC CONFINEMENT BOUNDARY PRESSURES[†] FOR NORMAL HANDLING AND ONSITE TRANSPORT

Condition	Pressure (psig)
MPC-24:	
Initial backfill (at 70°F)	31.3
Normal condition	76.0
With 1% rod rupture	76.8
With 10% rod rupture	83.7
MPC-68:	
Initial backfill (at 70°F)	31.3
Normal condition	76.0
With 1% rods rupture	76.5
With 10% rod rupture	80.6
MPC-32:	
Initial backfill (at 70°F)	31.3
Normal condition	76.0
With 1% rods rupture	77.1
With 10% rod rupture	86.7
MPC-24E:	
Initial backfill (at 70°F)	31.3
Normal condition	76.0
With 1% rods rupture	76.8
With 10% rod rupture	83.7

[†] Includes gas from BPRA rods for PWR MPCs

Table 4.5.4

SUMMARY OF HI-TRAC TRANSFER CASK AND MPC COMPONENTS
NORMAL HANDLING AND ONSITE TRANSPORT TEMPERATURES

Location	Temperature (°F)
MPC Basket Top:	
Basket periphery	590
MPC shell	445
O/P† inner shell	280
O/P enclosure shell	196
MPC Basket Bottom:	
Basket periphery	334
MPC shell	302
O/P inner shell	244
O/P enclosure shell	199

† O/P is an abbreviation for HI-TRAC overpack.

Table 4.5.5

SUMMARY OF LOADED 100-TON HI-TRAC TRANSFER CASK
BOUNDING COMPONENT
WEIGHTS AND THERMAL INERTIAS

Component	Weight (lbs)	Heat Capacity (Btu/lb-°F)	Thermal Inertia (Btu/°F)
Water Jacket	7,000	1.0	7,000
Lead	52,000	0.031	1,612
Carbon Steel	40,000	0.1	4,000
Alloy-X MPC (empty)	39,000	0.12	4,680
Fuel	40,000	0.056	2,240
MPC Cavity Water†	6,500	1.0	6,500
			26,032 (Total)

† Conservative lower bound water mass.

Table 4.5.6

MAXIMUM ALLOWABLE TIME DURATION FOR WET TRANSFER OPERATIONS

Initial Temperature (°F)	Time Duration (hr)
115	25.7
120	24.4
125	23.1
130	21.7
135	20.4
140	19.1
145	17.8
150	16.4

Table 4.5.7

INTENTIONALLY DELETED

HOLTEC INTERNATIONAL COPYRIGHTED MATERIAL

Table 4.5.8

MATRIX OF HI-TRAC TRANSFER CASK THERMAL EVALUATIONS

Scenario	Description	Ultimate Heat Sink	Analysis Type	Principal Input Parameters	Results in FSAR Subsection
1	Onsite Transport	Ambient	SS(B)	O_T, Q_D, ST, SC	4.5.2.1
2	Lead Gaps	Ambient	SS(B)	O_T, Q_D, ST, SC	4.5.1.1.7
3	Vacuum	HI-TRAC annulus water	SS(B)	Q_D	4.5.2.2
4	Wet Transfer Operation	Cavity water and Cask Internals	AH	Q_D	4.5.1.1.5
5	Deleted	Deleted	Deleted	Deleted	Deleted
6	Fire Accident	Jacket Water, Cask Internals	TA	Q_D, F	11.2.4
7	Jacket Water Loss Accident	Ambient	SS(B)	O_T, Q_D, ST, SC	11.2.1

Legend:
O_T - Off-Normal Temperature (100°F)
Q_D - Design Basis Maximum Heat Load

ST - Insolation Heating (Top)
SC - Insolation Heating (Curved)
F - Fire Heating (1475°F)

SS(B) - Bounding Steady State
TA - Transient Analysis
AH - Adiabatic Heating

Table 4.5.9

PEAK CLADDING TEMPERATURE IN VACUUM[†]
(MODERATE BURNUP FUEL ONLY)

MPC	Lower Decay Heat Load Range Temperatures (°F)	Higher Decay Heat Load Range Temperature (°F)
MPC-24	827	960
MPC-68	822	1014
MPC-32	n/a	1040
MPC-24E	n/a	942

[†] Steady state temperatures at the MPC design maximum heat load reported.

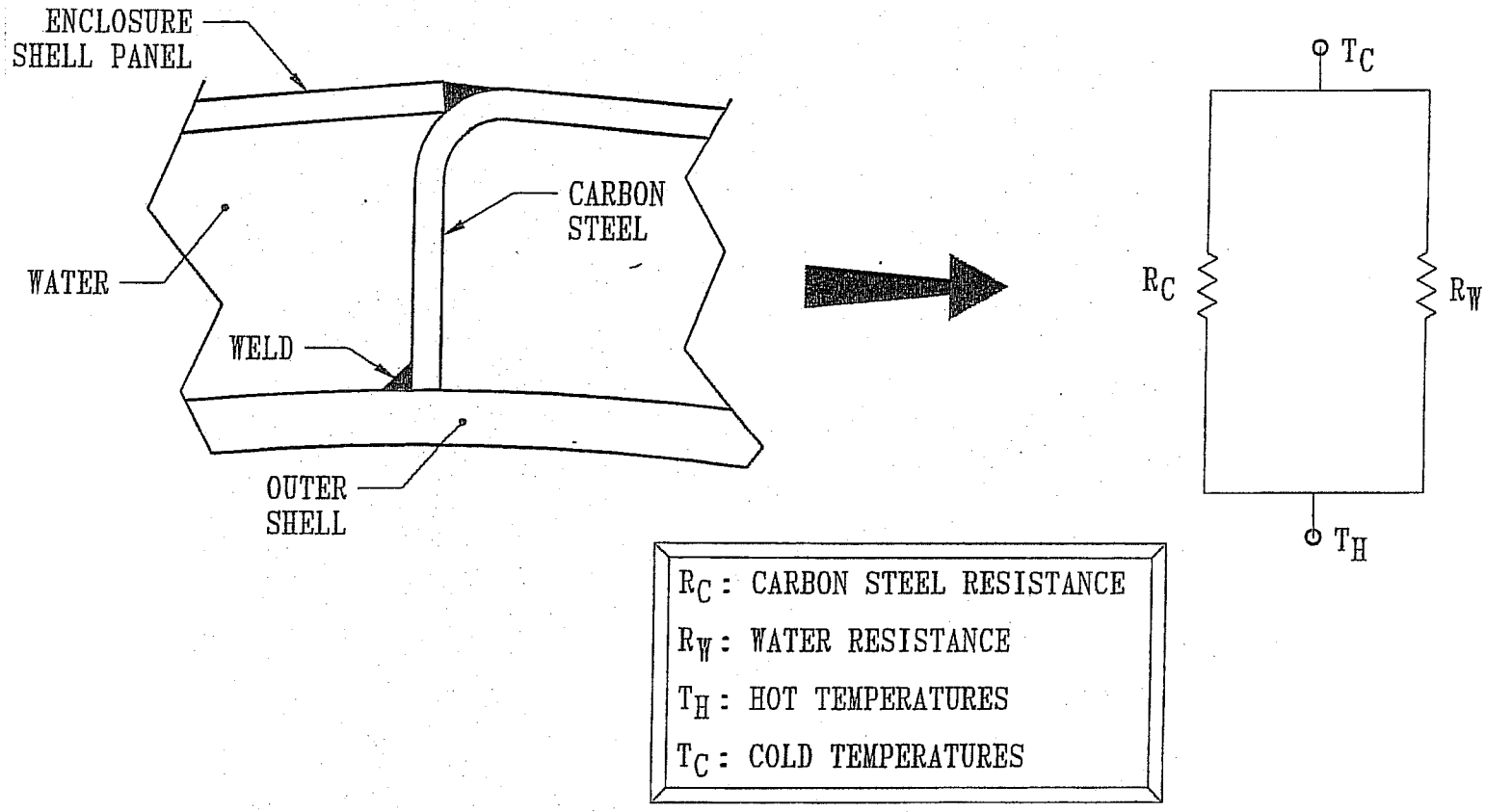

FIGURE 4.5.1; WATER JACKET RESISTANCE NETWORK ANALOGY FOR EFFECTIVE CONDUCTIVITY CALCULATION

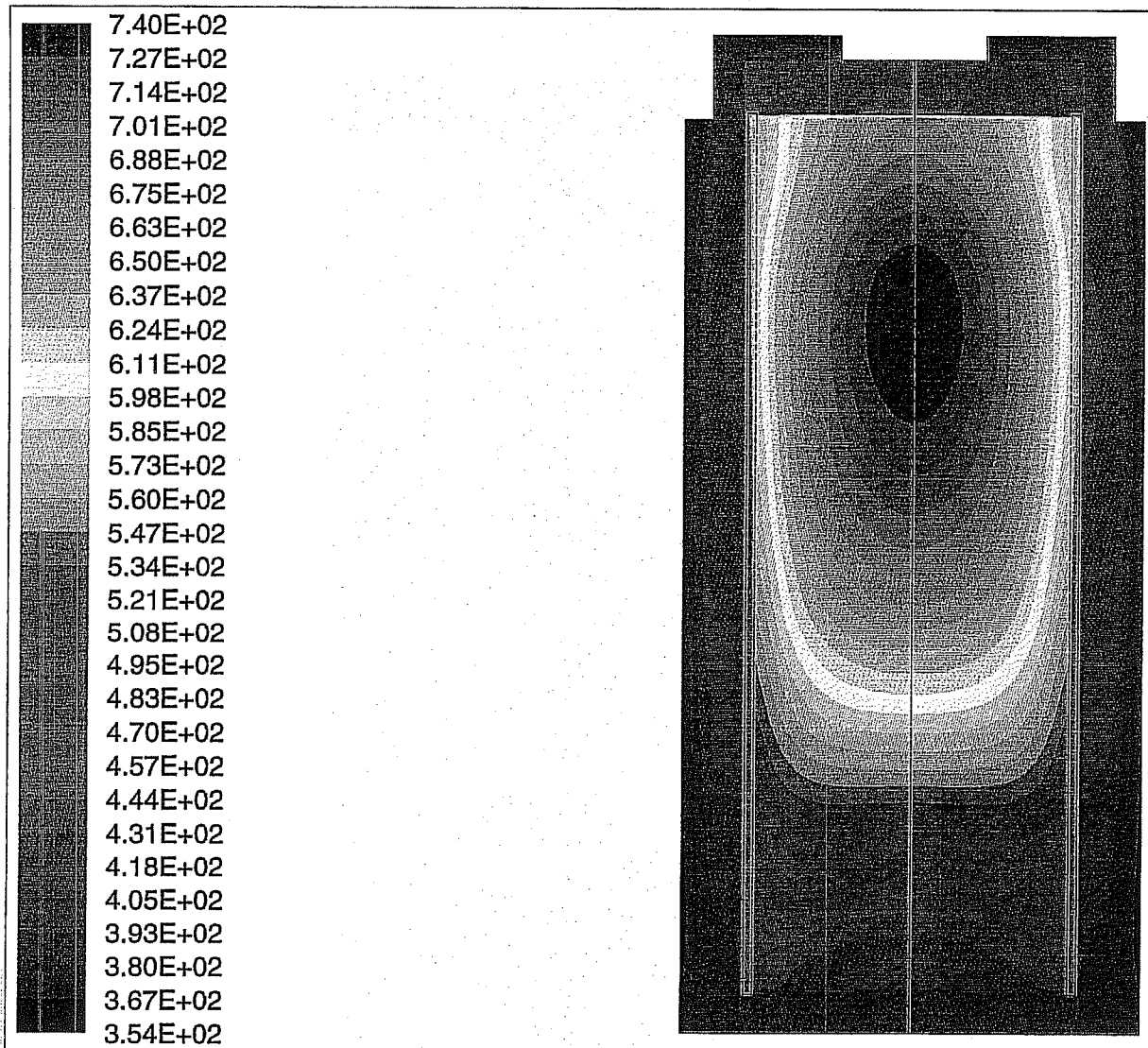

FIGURE 4.5.2: HI-TRAC Temperature Contours Plot
Temperature (Degrees Kelvin)
Max = 7.398E+02 Min = 3.540E+02

Aug 24 2000
Fluent 4.48
Fluent Inc.

4.6 REGULATORY COMPLIANCE

4.6.1 Normal Conditions of Storage

NUREG-1536 [4.4.10] and ISG-11 [4.1.4] define several thermal acceptance criteria that must be applied to evaluations of normal conditions of storage. These items are addressed in Sections 4.1 through 4.4.5 and results evaluated in Subsection 4.4.6. Each of the pertinent criteria and the conclusion of the evaluations are summarized here.

As required by ISG-11 [4.1.4], the fuel cladding temperature at the beginning of dry cask storage is maintained below the anticipated damage-threshold temperatures for normal conditions for the licensed life of the HI-STORM System. Maximum clad temperatures for long-term storage conditions are reported in Section 4.4.2.

As required by NUREG-1536 (4.0,IV,3), the maximum internal pressure of the cask remains within its design pressure for normal, off-normal, and accident conditions, assuming rupture of 1 percent, 10 percent, and 100 percent of the fuel rods, respectively. Assumptions for pressure calculations include release of 100 percent of the fill gas and 30 percent of the significant radioactive gases in the fuel rods. Maximum internal pressures are reported in Section 4.4.4. Design pressures are summarized in Table 2.2.1.

As required by NUREG-1536 (4.0,IV,4), all cask and fuel materials are maintained within their minimum and maximum temperature for normal and off-normal conditions in order to enable components to perform their intended safety functions. Maximum and minimum temperatures for long-term storage conditions are reported in Sections 4.4.2 and 4.4.3, respectively. Design temperature limits are summarized in Table 2.2.3. HI-STORM System components defined as important to safety are listed in Table 2.2.6.

As required by NUREG-1536 (4.0,IV,5), the cask system ensures a very low probability of cladding breach during long-term storage. For long-term normal conditions, the maximum CSF cladding temperature is below the ISG-11 [4.1.4] limit of 400°C (752°F).

As required by NUREG-1536 (4.0,IV,7), the cask system is passively cooled. All heat rejection mechanisms described in this chapter, including conduction, natural convection, and thermal radiation, are completely passive.

As required by NUREG-1536 (4.0,IV,8), the thermal performance of the cask is within the allowable design criteria specified in FSAR Chapters 2 and 3 for normal conditions. All thermal results reported in Sections 4.4.2 through 4.4.5 are within the design criteria allowable ranges for all normal conditions of storage.

4.6.2 Short Term Operations

As discussed ion Section 4.0, evaluation of short term operations is presented in Section 4.5. This section establishes complete compliance with the provisions of ISG-11 [4.1.4]. In particular, the ISG-11 requirement to ensure that maximum cladding temperatures under all fuel loading and short term operations be below 400°C (752°F) for high burnup fuel and below 570°C (1058°F) for moderate burnup fuel is demonstrated as stated below.

As required by ISG-11, the fuel cladding temperature is maintained below the applicable limits for HBF and MBF (Table 4.3.1) during short term operations.

As required by NUREG-1536 (4.0,IV,3), the maximum internal pressure of the cask remains within its design pressure for normal and off-normal conditions, assuming rupture of 1 percent and 10 percent of the fuel rods, respectively. Assumptions for pressure calculations include release of 100 percent of the fill gas and 30 percent of the significant radioactive gases in the fuel rods.

As required by NUREG-1536 (4.0,IV,4), all cask and fuel materials are maintained within their minimum and maximum temperature for all short term operations in order to enable components to perform their intended safety functions.

As required by NUREG-1536 (4.0,IV,8), the thermal performance of the cask is within the allowable design criteria specified in FSAR Chapters 2 and 3 for all short term operations.

HOLTEC INTERNATIONAL COPYRIGHTED MATERIAL

4.7 REFERENCES

[4.1.1] ANSYS Finite Element Modeling Package, Swanson Analysis Systems, Inc., Houston, PA, 1993.

[4.1.2] FLUENT Computational Fluid Dynamics Software, Fluent, Inc., Centerra Resource Park, 10 Cavendish Court, Lebanon, NH 03766.

[4.1.3] "The TN-24P PWR Spent-Fuel Storage Cask: Testing and Analyses," EPRI NP-5128, (April 1987).

[4.1.4] "Cladding Considerations for the Transportation and Storage of Spent Fuel," Interim Staff Guidance – 11, Revision 3.

[4.1.5] "Topical Report on the HI-STAR/HI-STORM Thermal Model and its Benchmarking with Full-Size Cask Test Data," Holtec Report HI-992252, Revision 1.

[4.2.1] Baumeister, T., Avallone, E.A. and Baumeister III, T., "Marks' Standard Handbook for Mechanical Engineers," 8th Edition, McGraw Hill Book Company, (1978).

[4.2.2] Rohsenow, W.M. and Hartnett, J.P., "Handbook of Heat Transfer," McGraw Hill Book Company, New York, (1973).

[4.2.3] Creer et al., "The TN-24P Spent Fuel Storage Cask: Testing and Analyses," EPRI NP-5128, PNL-6054, UC-85, (April 1987).

[4.2.4] Rust, J.H., "Nuclear Power Plant Engineering," Haralson Publishing Company, (1979).

[4.2.5] Kern, D.Q., "Process Heat Transfer," McGraw Hill Kogakusha, (1950).

[4.2.6] "A Handbook of Materials Properties for Use in the Analysis of Light Water Reactor Fuel Rod Behavior," NUREG/CR-0497, (August 1981).

[4.2.7] "Safety Analysis Report for the NAC Storable Transport Cask," Docket No. 71-9235.

[4.2.8] ASME Boiler and Pressure Vessel Code, Section II, Part D, (1995).

[4.2.9] Jakob, M. and Hawkins, G.A., "Elements of Heat Transfer," John Wiley & Sons, New York, (1957).

[4.2.10] ASME Steam Tables, 3rd Edition (1977).

HOLTEC INTERNATIONAL COPYRIGHTED MATERIAL

[4.3.1] Deleted

[4.3.2] Deleted

[4.3.3] Deleted

[4.3.4] Deleted

[4.3.5] Deleted

[4.3.6] Deleted

[4.3.7] Deleted

[4.3.8] Lanning and Beyer, "Estimated Maximum Cladding Stresses for Bounding PWR Fuel Rode During Short Term Operations for Dry Cask Storage," PNNL White Paper, (January 2004).

[4.4.1] Wooton, R.O. and Epstein, H.M., "Heat Transfer from a Parallel Rod Fuel Element in a Shipping Container," Battelle Memorial Institute, (1963).

[4.4.2] Rapp, D., "Solar Energy," Prentice-Hall, Inc., Englewood Cliffs, NJ, (1981).

[4.4.3] Siegel, R. and Howell, J.R., "Thermal Radiation Heat Transfer," 2nd Edition, McGraw Hill (1981).

[4.4.4] Deleted

[4.4.5] Sanders et al., "A Method for Determining the Spent-Fuel Contribution to Transport Cask Containment Requirements," Sandia Report SAND90-2406, TTC-1019, UC-820, page II-127, (November 1992).

[4.4.6] Deleted

[4.4.7] Hagrman, Reymann and Mason, "MATPRO-Version 11 (Revision 2) A Handbook of Materials Properties for Use in the Analysis of Light Water Reactor Fuel Rod Behavior," NUREG/CR-0497, Tree 1280, Rev. 2, EG&G Idaho, August 1981.

[4.4.8] "Effective Thermal Conductivity and Edge Conductance Model for a Spent-Fuel Assembly," R. D. Manteufel & N. E. Todreas, Nuclear Technology, 105, 421- 440, (March 1994).

HOLTEC INTERNATIONAL COPYRIGHTED MATERIAL

[4.4.9] "Spent Nuclear Fuel Effective Thermal Conductivity Report," US DOE Report BBA000000-01717-5705-00010 REV 0, (July 11, 1996).

[4.4.10] NUREG-1536, "Standard Review Plan for Dry Cask Storage Systems," USNRC, (January 1997).

[4.4.11] "Fuel Cladding Cladding Temperatures in Transport and Storage Casks Development and Validation of a Computation Method," S. Anton, Ph.D. Thesis (German) RWTH Aachen, Germany, 1997.

[4.4.12] Deleted

HOLTEC INTERNATIONAL COPYRIGHTED MATERIAL

APPENDIX 4.A:

INTENTIONALLY DELETED

APPENDIX 4.B: CONSERVATISMS IN THE THERMAL ANALYSIS OF THE HI-STORM 100 SYSTEM

4.B.1 OVERVIEW OF CASK HEAT REMOVAL SYSTEM

The HI-STORM 100 overpack is a large, cylindrical structure with an internal cavity suited for emplacement of a cylindrical canister containing spent nuclear fuel (SNF). The canister is arrayed in an upright manner inside the vertically oriented overpack. The design of the system provides for a small radial gap between the canister and the cylindrical overpack cavity. One principal function of a fuel storage system is to provide a means for ensuring fuel cladding integrity under long-term storage periods (20 years or more). The HI-STORM 100 overpack is equipped with four large ducts near its bottom and top extremities. The ducted overpack construction, together with an engineered annular space between the MPC cylinder and internal cavity in the HI-STORM 100 overpack structure, ensures a passive means of heat dissipation from the stored fuel via ventilation action (i.e., natural circulation of air in the canister-to-overpack annulus). In this manner a large structure physically interposed between the hot canister and ambient air (viz. the concrete overpack engineered for radiation protection) is rendered as an air flow device for convective heat dissipation. The pertinent design features producing the air ventilation ("chimney effect") in the HI-STORM 100 cask are shown in Figure 4.B.1.

A great bulk of the heat emitted by the SNF is rejected to the environment (Q_1) by convective action. A small quantity of the total heat rejection occurs by natural convection and radiation from the surface of the overpack (Q_2), and an even smaller amount is dissipated by conduction to the concrete pad upon which the HI-STORM 100 overpack is placed (Q_3). From the energy conservation principle, the sum of heat dissipation to all sinks (convective cooling (Q_1), surface cooling (Q_2) and cooling to pad (Q_3)) equals the sum of decay heat emitted from the fuel stored in the canister (Q_d) and the heat deposited by insolation, Q_s (i.e., $Q_d + Q_s = Q_1 + Q_2 + Q_3$). This situation is illustrated in Figure 4.B.2. In the HI-STORM 100 System, Q_1 is by far the dominant mode of heat removal, accounting for well over 80% of the decay heat conveyed to the external environment. Figure 4.B.3 shows the relative portions of Q_d transferred to the environs via Q_1, Q_2, and Q_3 in the HI-STORM 100 System under the design basis heat load.

The heat removal through convection, Q_1, is similar to the manner in which a fireplace chimney functions: Air is heated in the annulus between the canister and the overpack through contact with the canister's hot cylindrical surface causing it to flow upward toward the top (exit) ducts and inducing the suction of the ambient air through the bottom ducts. The flow of air sweeping past the cylindrical surfaces of the canister has sufficient velocity to create turbulence that aids in the heat extraction process. It is readily recognized that the chimney action relies on a fundamental and immutable property of air, namely that air becomes lighter (i.e., more buoyant) as it is heated. If the canister contained no heat emitting fuel, then there would be no means for the annulus air to heat and rise. Similarly, increasing the quantity of heat produced in the canister would make more heat available for heating of annulus air, resulting in a more vigorous chimney action. Because the heat energy of the spent nuclear fuel itself actuates the chimney action,

HOLTEC INTERNATIONAL COPYRIGHTED MATERIAL

ventilated overpacks of the HI-STORM 100 genre are considered absolutely safe against thermal malfunction. While the removal of heat through convective mass transport of air is the dominant mechanism, other minor components, labeled Q_2 and Q_3 in the foregoing, are recognized and quantified in the thermal analysis of the HI-STORM 100 System.

Heat dissipation from the exposed surfaces of the overpack, Q_2, occurs principally by natural convection and radiation cooling. The rate of decay heat dissipation from the external surfaces is, of course, influenced by several factors, some of which aid the process (e.g., wind, thermal turbulation of air), while others oppose it (for example, radiant heating by the sun or blocking of radiation cooling by surrounding casks). In this appendix, the relative significance of Q_2 and Q_3 and the method to conservatively simulate their effect in the HI-STORM 100 thermal model is discussed.

The thermal problem posed for the HI-STORM 100 System in the system's Final Safety Analysis Report (FSAR) is as follows: Given a specified maximum fuel cladding temperature, T_c, and a specified ambient temperature, T_a what is the maximum permissible heat generation rate Q_d, in the canister under steady state conditions? Of course, in the real world, the ambient temperature, T_a, varies continuously, and the cask system is rarely in a steady state (i.e., temperatures vary with time). Fortunately, fracture mechanics of spent fuel cladding instruct us that it is the time-integrated effect of elevated temperature, rather than an instantaneous peak value, that determines whether fuel cladding would rupture. The most appropriate reference ambient temperature for cladding integrity evaluation, therefore, is the average ambient temperature for the entire duration of dry storage. For conservatism, the reference ambient temperature is, however, selected to be the maximum yearly average for the ISFSI site. In the general certification of HI-STORM 100, the reference ambient temperature (formally referred to as the normal temperature) is set equal to 80°F, which is greater than the annual average for any power plant location in the U.S.*

The thermal analysis of the cask system leads to a computed value of the fuel cladding temperature greater than T_a by an amount C. In other words, $T_c = T_a + C$, where C decreases slightly as T_a (assumed ambient temperature) is increased. The thermal analysis of HI-STORM 100 is carried out to compute C in a most conservative manner. In other words, the mathematical model seeks to calculate an upper bound on the value of C.

Dry storage scenarios are characterized by relatively large temperature elevations (C) above ambient (650°F or so). The cladding temperature rise is the cumulative sum of temperature increments arising from individual elements of thermal resistance. To protect cladding from overheating, analytical assumptions adversely impacting heat transfer are chosen with particular attention given to those temperature increments which form the bulk of the temperature rise. In this appendix, the principal conservatisms in the thermal modeling of the HI-STORM 100 System and their underlying theoretical bases are presented. This overview is intended to provide

* According to the U.S. National Oceanic and Atmospheric Administration (NOAA) publication, "Comparative Climatic Data for the United States through 1998", the highest annual average temperature for any location in the continental U.S. is 77.8°F in Key West, Florida.

a physical understanding of the large margins buried in the HI-STORM 100 design which are summarized in Section 4.4.6 of this FSAR.

4.B.2 CONSERVATISM IN ENVIRONMENTAL CONDITION SPECIFICATION

The ultimate heat sink for decay heat generated by stored fuel is ambient air. The HI-STORM 100 System defines three ambient temperatures as the environmental conditions for thermal analysis. These are, the Normal (80°F), the Off-Normal (100°F) and Extreme Hot (125°F) conditions. Two factors dictate the stipulation of an ambient temperature for cladding integrity calculations. One factor is that ambient temperatures are constantly cycling on a daily basis (night and day). Furthermore, there are seasonal variations (summer to winter). The other factor is that cladding degradation is an incremental process that, over a long period of time (20 years), has an accumulated damage resulting from an "averaged-out" effect of the environmental temperature history. The 80°F normal temperature stated in the HI-STORM 100 FSAR is defined as the highest annual average temperature at a site established from past records. This is a principal design parameter in the HI-STORM 100 analysis because it establishes the basis for demonstrating long-term SNF integrity. The choice of maximum annual average temperature is conservative for a 20-year period. Based on meteorological data, the 80°F is chosen to bound annual average temperatures reported within the continental US.

For short periods, it is recognized that ambient temperature excursions above 80°F are possible. Two scenarios are postulated and analyzed in the FSAR to bound such transient events. The Off-Normal (100°F) and Extreme Hot (125°F)* cases are postulated as continuous (72-hour average) conditions. Both cases are analyzed as steady-state conditions (i.e., thermal inertia of the considerable concrete mass, fuel and metal completely neglected) occurring at the start of dry storage when the decay heat load to the HI-STORM 100 System is at its peak value with fuel emitting heat at its design basis maximum level.

4.B.3 CONSERVATISM IN MODELING THE ISFSI ARRAY

Traditionally, in the classical treatment of the ventilated storage cask thermal problem, the cask to be analyzed (the subject cask) is modeled as a stand-alone component that rejects heat to the ambient air through chimney action (Q_1) by natural convection to quiescent ambient air and radiation to the surrounding open spaces (Q_2), and finally, a small amount through the concrete pad into the ground (Q_3). The contributing effect of the sun (addition of heat) is considered, but the dissipative effect of wind is neglected. The interchange of radiative heat between proximate casks is also neglected (the so-called "cask-to-cask interactions"). In modeling the HI-STORM 100 System, Holtec International extended the classical cask thermal model to include the effect of the neighboring casks in a most conservative manner. This model represents the flow of supply air to the inlet ducts for the subject cask by erecting a cylinder around the subject cask. The model blocks all lateral flow of air from the surrounding space into the subject cask's inlet ducts. This mathematical artifice is illustrated in Figure 4.B.4, where the lateral air flow arrows

* According to NOAA, the highest daily mean temperature for any location in the continental U.S. is 93.7°F, which occurred in Yuma, Arizona.

are shown "dotted" to indicate that the mathematical cylinder constructed around the cask has blocked off the lateral flow of air. Consequently, the chimney air must flow down the annulus from the air plenum space above the casks, turn around at the bottom and enter the inlet ducts. Because the vertical downflow of air introduces additional resistance to flow, an obvious effect of the hypothetical enclosing cylinder construct is an increased total resistance to the chimney flow which, it is recalled, is the main heat conveyance mechanism in a ventilated cask. Throttling of the chimney flow by the hypothetical enclosing cylinder is an element of conservatism in the HI-STORM modeling.

Thus, whereas air flows toward the bottom ducts from areas of supply which are scattered in a three dimensional continuum with partial restriction from neighboring casks, the analytical model blocks the air flow completely from areas outside the hypothetical cylinder. This is illustrated in Figure 4.B.4 in which an impervious boundary is shown to limit HI-STORM 100 cask access to fresh air from an annular opening near the top.

Thus, in the HI-STORM model, the feeder air to the HI-STORM 100 System must flow down the hypothetical annulus sweeping past the external surface of the cask. The ambient air, assumed to enter this hypothetical annulus at the assumed environmental temperature, heats by convective heat extraction from the overpack before reaching the bottom (inlet) ducts. In this manner, the temperature of the feeder air into the ducts is maximized. In reality, the horizontal flow of air in the vicinity of the inlet ducts, suppressed by the enclosed cylinder construct (as shown in Figure 4.B.4) would act to mitigate the pre-heating of the feeder air. By maximizing the extent of air preheating, the computed value of ventilation flow is underestimated in the simulation.

4.B.4 CONSERVATISM IN RADIANT HEAT LOSS

In an array of casks, the external (exposed) cask surfaces have a certain "view" of each other. The extent of view is a function of relative geometrical orientation of the surfaces and presence of other objects between them. The extent of view influences the rate of heat exchange between surfaces by thermal radiation. The presence of neighboring casks also partially blocks the escape of radiant heat from a cask thus affecting its ability to dissipate heat to the environment. This aspect of Radiative Blocking (RB) is illustrated for a reference cask (shown shaded) in Figure 4.B.5. It is also apparent that a cask is a recipient of radiant energy from adjacent casks (Radiant Heating (RH)). Thus, a thermal model representative of a cask array must address the RB and RH effects in a conservative manner. To bound the physical situation, a Hypothetical Reflecting Boundary (HRB) modeling feature is introduced in the thermal model. The HRB feature surrounds the HI-STORM 100 overpack with a reflecting cylindrical surface with the boundaries insulated.

In Figures 4.B.6 and 4.B.7 the inclusion of RB and RH effects in the HI-STORM 100 modeling is graphically illustrated. Figure 4.B.6 shows that an incident ray of radiant energy leaving the cask surface bounces back from the HRB thus preventing escape (i.e., RB effect maximized). The RH effect is illustrated in Figure 4.B.7 by superimposing on the physical model reflected images of HI-STORM 100 cask surrounding the reference cask. A ray of radiant energy from an

HOLTEC INTERNATIONAL COPYRIGHTED MATERIAL

adjacent cask directed toward the reference cask (AA) is duplicated by the model via another ray of radiant energy leaving the cask (BB) and being reflected back by the HRB (BA'). A significant feature of this model is that the reflected ray (BA') initiated from a cask surface (reference cask) assumed to be loaded with design basis maximum heat (hottest surface temperature). As the strength of the ray is directly proportional to the fourth power of surface temperature, radiant energy emission from an adjacent cask at a lower heat load will be overestimated by the HRB construct. In other words, the reference cask is assumed to be in an array of casks all producing design basis maximum heat. Clearly, it is physically impossible to load every location of every cask with fuel emitting heat at design basis maximum. Such a spent fuel inventory does not exist. This bounding assumption has the effect of maximizing cask surface temperature as the possibility of "hot" (design basis) casks being radiatively cooled by adjacent casks is precluded. The HRB feature included in the HI-STORM 100 model thus provides a bounding effect of an infinite array of casks, all at design basis maximum heat loads. No radiant heat is permitted to escape the reference cask (bounding effect) and the reflecting boundary mimics incident radiation toward the reference casks around the 360° circumference (bounding effect).

4.B.5 CONSERVATISM IN REPRESENTING BASKET AXIAL RESISTANCE

As stated earlier, the largest fraction of the total resistance to the flow of heat from the spent nuclear fuel (SNF) to the ambient is centered in the basket itself. Out of the total temperature drop of approximately 650°F (C=650°F) between the peak fuel cladding temperature and the ambient, over 400°F occurs in the fuel basket. Therefore, it stands to reason that conservatism in the basket thermal simulation would have a pronounced effect on the conservatism in the final solution. The thermal model of the fuel basket in the HI-STORM 100 FSAR was accordingly constructed with a number of conservative assumptions that are described in the HI-STORM 100 FSAR. We illustrate the significance of the whole array of conservatisms by explaining one in some detail in the following discussion.

It is recognized that the heat emission from a fuel assembly is axially non-uniform. The maximum heat generation occurs at about the mid-height region of the enriched uranium column, and tapers off toward its extremities. The axial heat conduction in the fuel basket would act to diffuse and levelize the temperature field in the basket. The axial conductivity of the basket, quite clearly, is the key determinant in how well the thermal field in the basket would be homogenized. It is also evident that the conduction of heat along the length of the basket occurs in an uninterrupted manner in a HI-STORM 100 basket because of its continuously welded honeycomb geometry. On the other hand, the in-plane transfer of heat must occur through the physical gaps that exist between the fuel rods, between the fuel assembly and the basket walls and between the basket and the MPC shell. These gaps depress the in-plane conductivity of the basket. However, in the interest of conservatism, only a small fraction of the axial conductivity of the basket is included in the HI-STORM 100 thermal model. This assumption has the direct effect of throttling the axial flow of heat and thus of elevating the computed value of mid-height cladding temperature (where the peak temperature occurs) above its actual value. In actuality, the axial conductivity of the fuel basket is much greater than the in-plane conductivity due to the

HOLTEC INTERNATIONAL COPYRIGHTED MATERIAL

continuity of the fuel and basket structures in that direction. Had the axial conductivity of the basket been modeled less conservatively in the HI-STORM 100 thermal analysis, then the temperature distribution in the basket will be more uniform, i.e., the bottom region of the basket would be hotter than that computed. This means that the temperature of the MPC's external surface in the bottom region is hotter than computed in the HI-STORM 100 analysis. It is a well-known fact in ventilated column design that the lower the location in the column where the heat is introduced, the more vigorous the ventilation action. Therefore, the conservatism in the basket's axial conductivity assumption has the net effect of reducing the computed ventilation rate.

To estimate the conservatism in restricting the basket axial resistance, we perform a numerical exercise using mathematical perturbation techniques. The axial conductivity (K_z) of the MPC is, as explained previously, much higher than the in-plane (K_r) conductivity. The thermal solution to the MPC anisotropic conductivities problem (i.e. K_z and K_r are not equal) is mathematically expressed as a sum of a baseline isotropic solution T_o (setting $K_z = K_r$) and a perturbation T^* which accounts for anisotropic effects. From Fourier's Law of heat conduction in solids, the perturbation equation for T' is reduced to the following form:

$$K_z \frac{d^2T^*}{dz^2} = -\Delta K \frac{d^2T_o}{dz^2}$$

Where, ΔK is the perturbation parameter (i.e. axial conductivity offset $\Delta K = K_z - K_r$). The boundary conditions for the perturbation solution are zero slope at peak cladding temperature location ($dT^*/dz = 0$) (which occurs at about the top of the active fuel height) and $T^* = 0$ at the bottom of the active fuel length. The object of this calculation is to compute T^* where the peak fuel cladding temperature is reached. To this end, the baseline thermal solution T_o (i.e. HI-STORM isotropic modeling solution) is employed to compute an appropriate value for d^2T_o/dz^2 which characterizes the axial temperature rise over the height of the active fuel length in the hottest fuel cell. This is computed as $(-\Delta T_{ax}/L^2)$ where ΔT_{ax} is the fuel cell temperature rise and L is the active fuel length. Conservatively postulating a lower bound ΔT_{ax} of 200°F and L of 12 ft, d^2T_o/dz^2 is computed as $-1.39°F/ft^2$. Integrating the perturbation equation shown above, the following formula for T^* is obtained:

$$T^* = \left(\frac{\Delta K}{K_z}\right)\frac{d^2T_o}{dz^2}L^2$$

Employing a conservative low value for the $(\Delta K/K_z)$ parameter of 0.15, T^* is computed as –30°F. In other words, the baseline HI-STORM solution over predicts the peak cladding temperature by approximately 30°F.

4.B.6 HEAT DISSIPATION UNDERPREDICTION IN THE MPC DOWNCOMER

Internal circulation of helium in the sealed MPC is modeled as flow in a porous medium in the fueled region containing the SNF (including top and bottom plenums). The basket-to-MPC shell clearance space is modeled as a helium filled radial gap to include the downcomer flow in the thermal model. The downcomer region, as illustrated in Figure 4.4.2, consists of an azimuthally varying gap formed by the square-celled basket outline and the cylindrical MPC shell. At the

HOLTEC INTERNATIONAL COPYRIGHTED MATERIAL

locations of closest approach a differential expansion gap (a small clearance on the order of 1/10 of an inch) is engineered to allow free thermal expansion of the basket. At the widest locations, the gaps are on the order of the fuel cell opening (~6" (BWR) and ~9" (PWR) MPCs). It is heuristically evident that heat dissipation by conduction is maximum at the closest approach locations (low thermal resistance path) and that convective heat transfer is highest at the widest gap locations (large downcomer flow). In the FLUENT thermal model, a radial gap that is large compared to the basket-to-shell clearance and small compared to the cell opening is used. As a relatively large gap penalizes heat dissipation by conduction and a small gap throttles convective flow, the use of a single gap in the FLUENT model understates both conduction and convection heat transfer in the downcomer region.

Heat dissipation in the downcomer region is the sum of four elements, viz. convective heat transfer (C1), helium conduction heat transfer (C2), basket-to-shell contact heat transfer (C3), and radiation heat transfer (C4). In the HI-STORM thermal modeling, one element of heat transfer (C3) is completely neglected, C2 is severely penalized and C1 is underpredicted. In other words the HI-STORM thermosiphon model has choked the radial flow of heat in the downcomer space. This has the direct effect of raising the temperature of fuel in the thermal solutions.

4.B.7 CONSERVATISM IN MPC EXTERNAL HEAT DISSIPATION TO CHIMNEY AIR

The principle means of decay heat dissipation to the environment is by cooling of the MPC surface by chimney air flow. Heat rejection from the MPC surface is by a combination of convective heat transfer to a through flowing fluid medium (air), natural convection cooling at the outer overpack surface, and by radiation heat transfer. Because the temperature of the fuel stored in the MPC is directly affected by the rate of heat dissipation from the canister external surface, heat transfer correlations with robust conservatisms are employed in the HI-STORM simulations. The FLUENT computer code deployed for the modeling employs a so called "wall-functions" approach for computing the transfer of heat from solid surfaces to fluid medium. This approach has the desired effect of computing heat dissipation in a most conservative manner. As this default approach has been employed in the thermal modeling, it is contextually relevant to quantify the conservatism in a classical setting to provide an additional level of assurance in the HI-STORM results. To do this, we have posed a classical heat transfer problem of a heated square block cooled in a stream of upward moving air. The problem is illustrated in Figure 4.B.8. From the physics of the problem, the maximum steady state solid interior temperature (T_{max}) is computed as:

$$T_{max} = T_{sink} + \Delta T_{air} + \Delta T_s$$

where,
T_{sink} = Sink temperature (mean of inlet and outlet air temperature)
ΔT_{air} = Solid surface to air temperature difference
ΔT_s = Solid block interior temperature elevation

HOLTEC INTERNATIONAL COPYRIGHTED MATERIAL

The sink temperature is computed by first calculating the air outlet temperature from energy conservation principles. Solid-to-air heat transfer is computed using classical natural convection correlation proposed by Jakob and Hawkins ("Elements of Heat Transfer", John Wiley & Sons, 1957) and ΔTs is readily computed by an analytical solution to the equation of heat conduction in solids. By solving this same problem on the FLUENT computer code using the in-built "wall-functions", in excess of 100°F conservative margin over the classical result for T_{max} is established.

4.B.8 MISCELLANEOUS CONSERVATISMS

Section 4.4.6 of the FSAR lists eleven elements of conservatism, of which certain non-transparent and individually significant items are discussed in detail in this appendix. Out of the balance of conservatisms, the one of notable mention is the conservatism in fuel decay heat generation stipulation based on the most heat emissive fuel assembly type. This posture imputes a large conservatism for certain other fuel types, which have a much lower quantity of Uranium fuel inventory relative to the design basis fuel type. Combining this with other miscellaneous conservatisms, an aggregate effect is to overestimate cladding temperatures by about 15°F to 50°F.

4.B.9 CONCLUSIONS

The foregoing narrative provides a physical description of the many elements of conservatism in the HI-STORM 100 thermal model. The conservatisms may be broadly divided into two categories:

1. Those intrinsic to the FLUENT modeling process.

2. Those arising from the input data and on the HI-STORM 100 thermal modeling.

The conservatism in Category (1) may be identified by reviewing the Holtec International Benchmark Report [4.B.1], which shows that the FLUENT solution methodology, when applied to the prototype cask (TN 24P) over-predicts the peak cladding temperature by as much as 79 °F. and as much as 37°F relative to the PNNL results (see Attachment 1 to Reference [4.B.1]) from their COBRA SFS solution as compared against Holtec's FLUENT solution.

Category (2) conservatisms are those that we have deliberately embedded in the HI-STORM 100 thermal model to ensure that the computed value of the peak fuel cladding temperature is further over-stated. Table 4.B.1 contains a listing of the major conservatisms in the HI-STORM 100 thermal model, along with an estimate of the effect (increase) of each on the computed peak cladding temperature.

Table 4.B.1

Conservatism in the HI-STORM 100 Thermal Model

MODELING ELEMENT	CONSERVATISM [°F]
Long Term Ambient Temperature	2 to 30
Hypothetical Cylinder Construct	~5
Axial Heat Dissipation Restriction	30
MPC Downcomer Heat Dissipation Restriction	50
MPC External Heat Dissipation Under-prediction	50
Miscellaneous Conservatisms	15 to 50

4.B.9 REFERENCES

[4.B.1] "Topical Report on the HI-STAR/HI-STORM Thermal Model and its Benchmarking with Full-Size Cask Test Data", Holtec Report HI-992252, Rev. 1.

HOLTEC INTERNATIONAL COPYRIGHTED MATERIAL

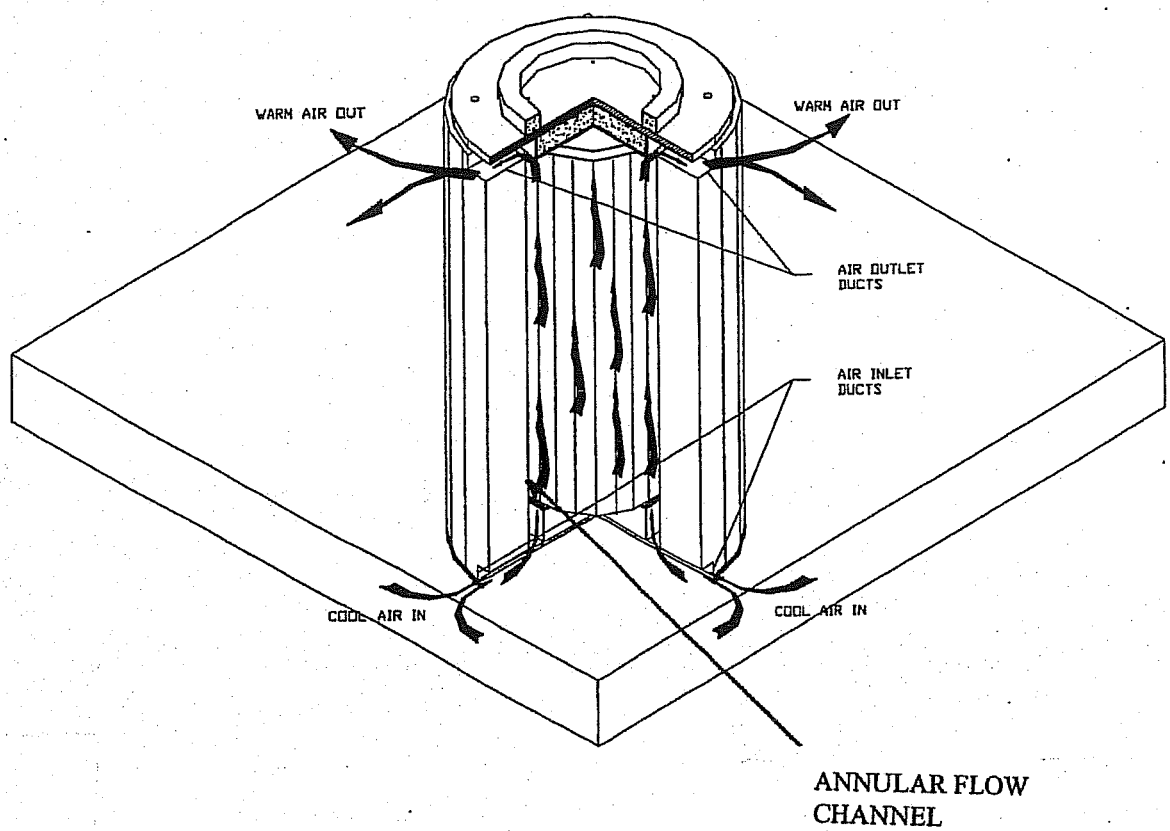

FIGURE 4.B.1: CUTAWAY VIEW OF A HI-STORM OVERPACK STANDING ON AN ISFSI PAD

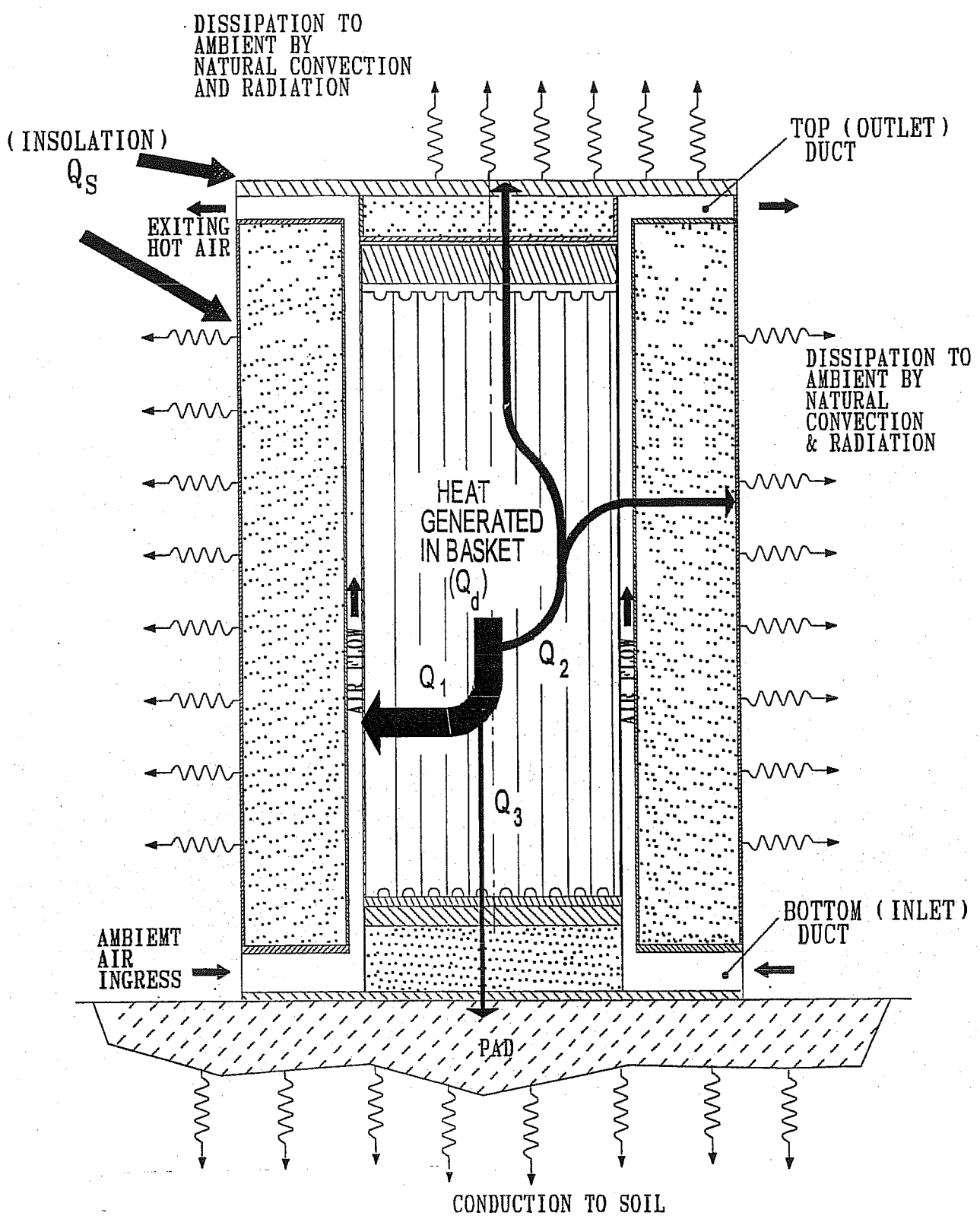

FIGURE 4.B.2: DEPICTION OF THE HI-STORM VENTILATED CASK HEAT DISSIPATION ELEMENTS

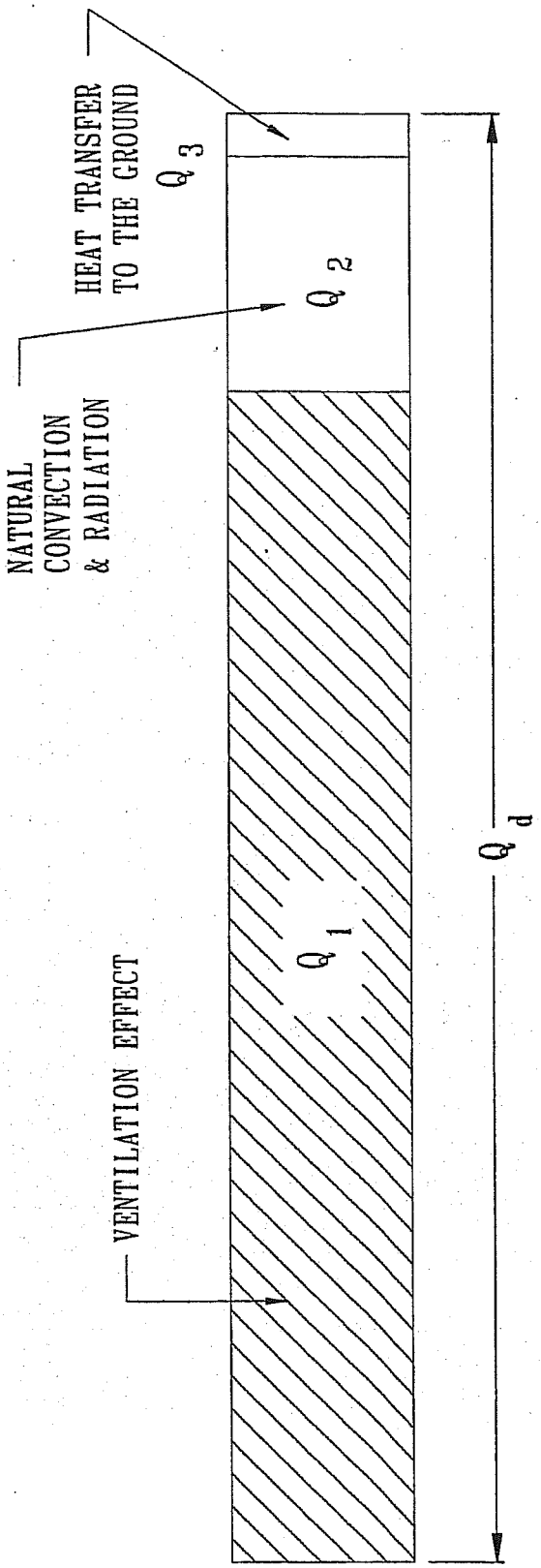

FIGURE 4.B.3: RELATIVE SIGNIFICANCE OF HEAT DISSIPATION ELEMENTS IN THE HI-STORM 100

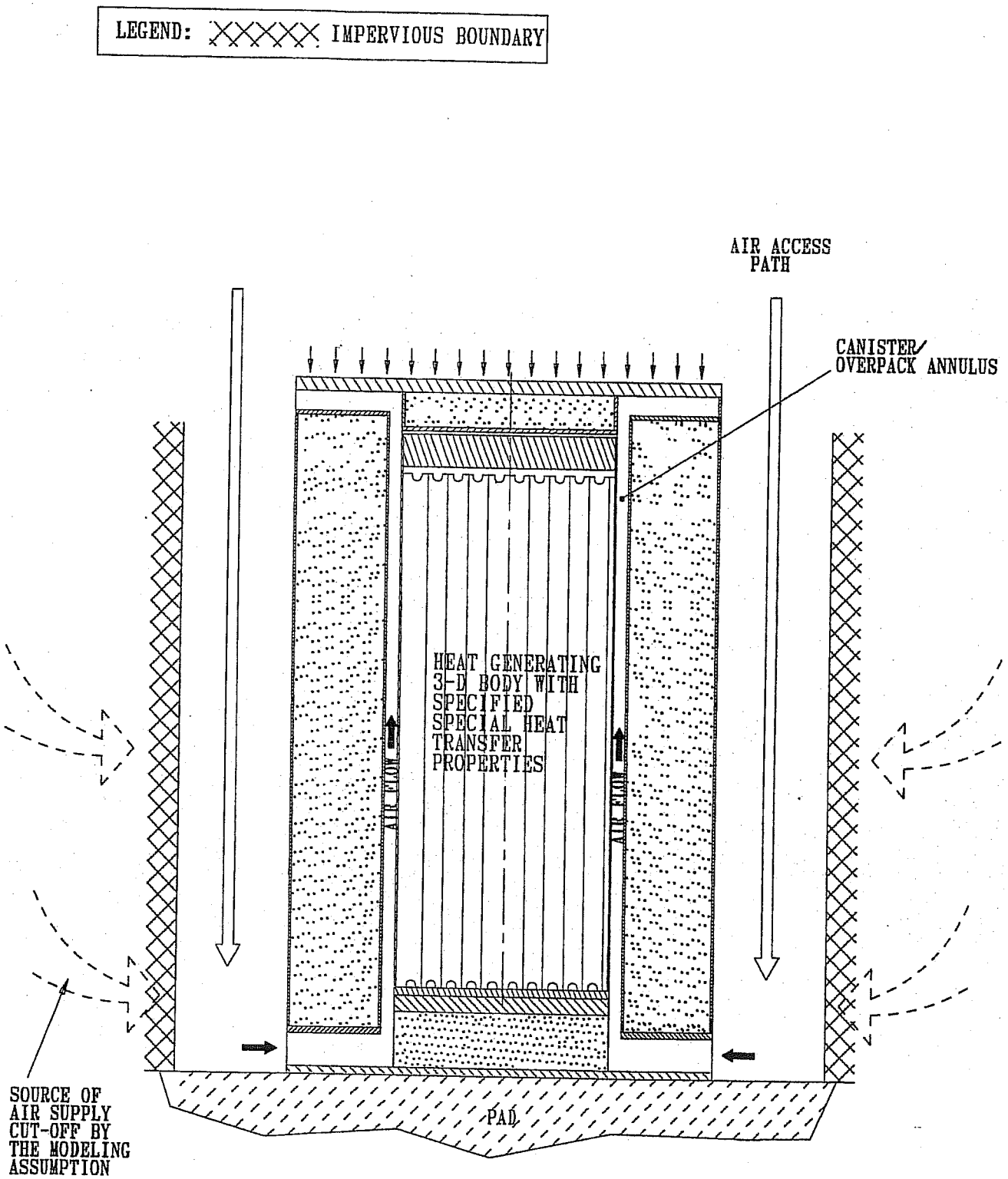

FIGURE 4.B.4: AIR ACCESS RESTRICTIONS IN THE HI-STORM THERMAL MODEL

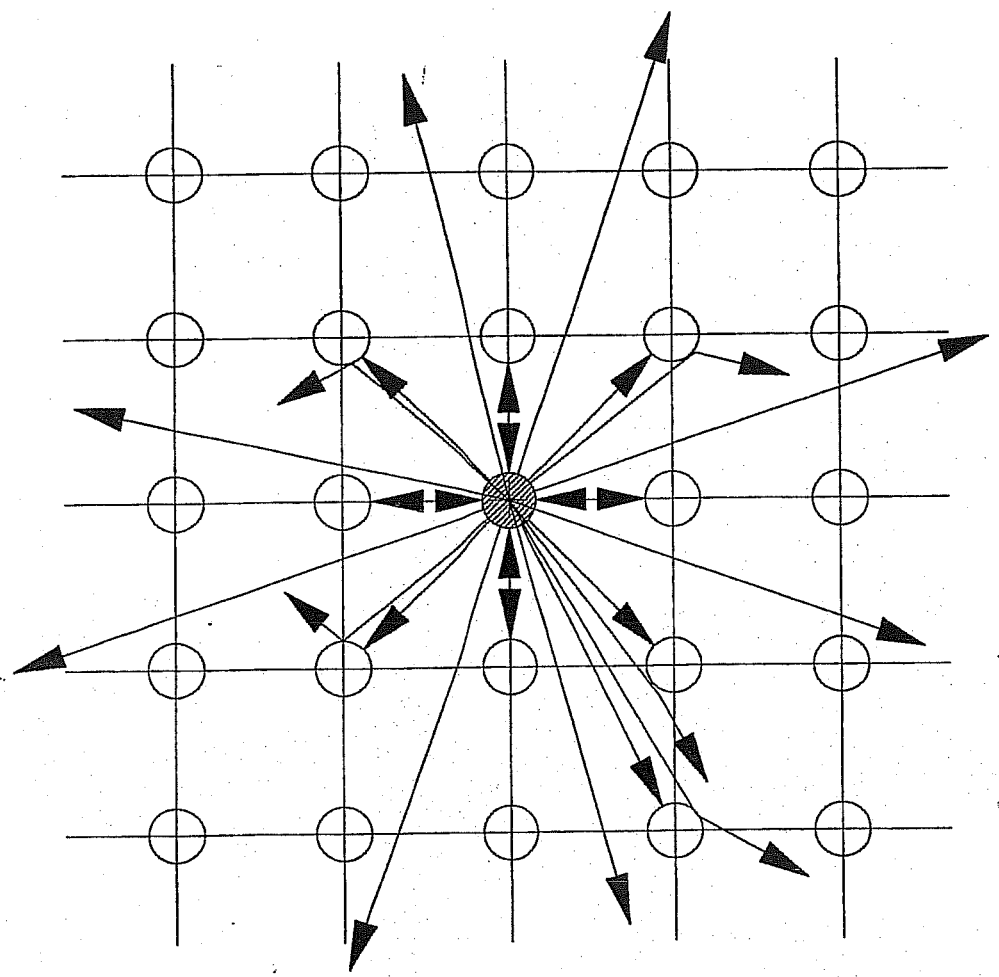

FIGURE 4.B.5: IN-PLANE RADIATIVE COOLING OF A HI-STORM CASK IN AN ARRAY

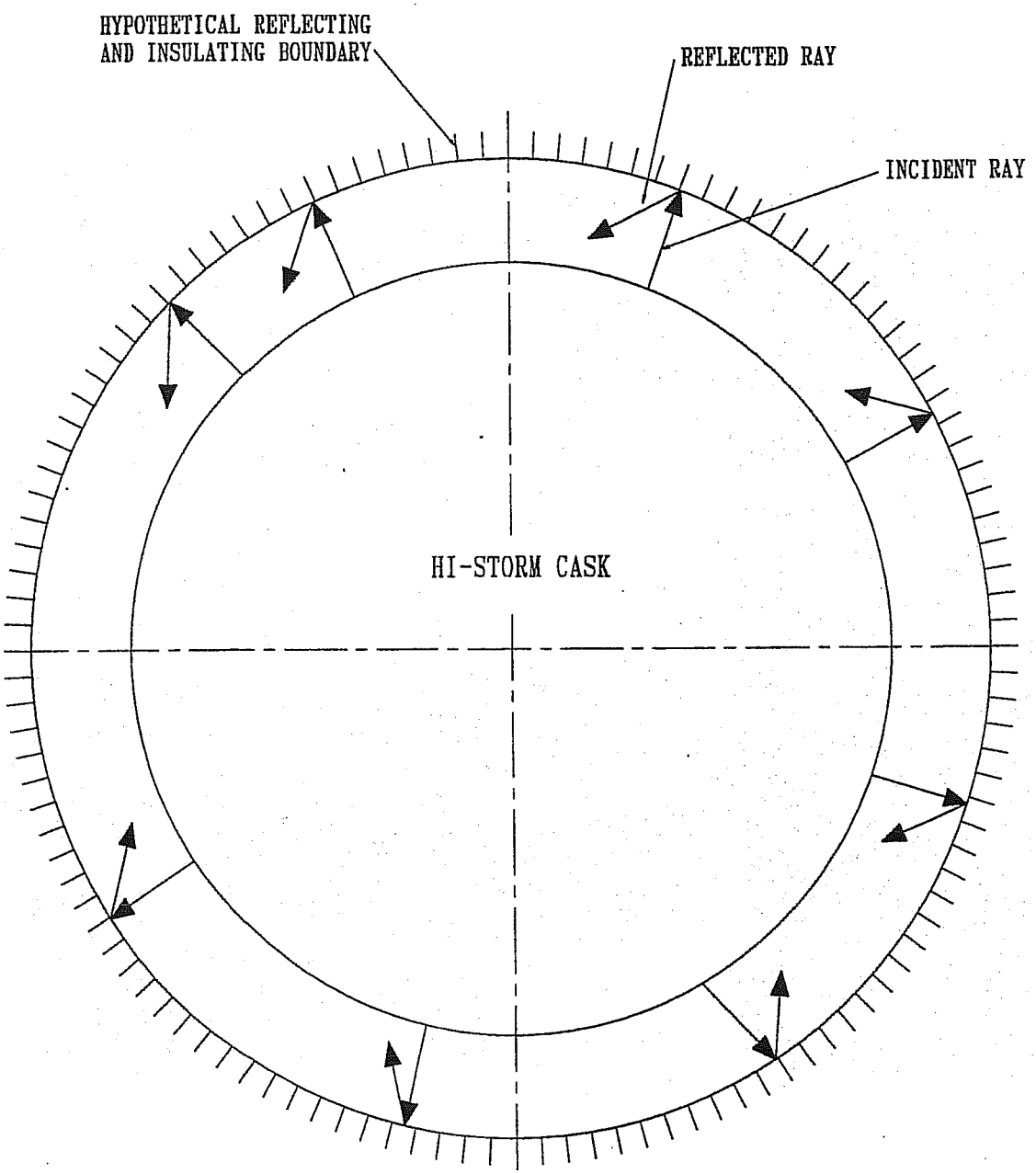

FIGURE 4.B.6: IN-PLANE RADIATIVE BLOCKING OF A HI-STORM CASK BY HYPOTHETICAL REFLECTING BOUNDARY

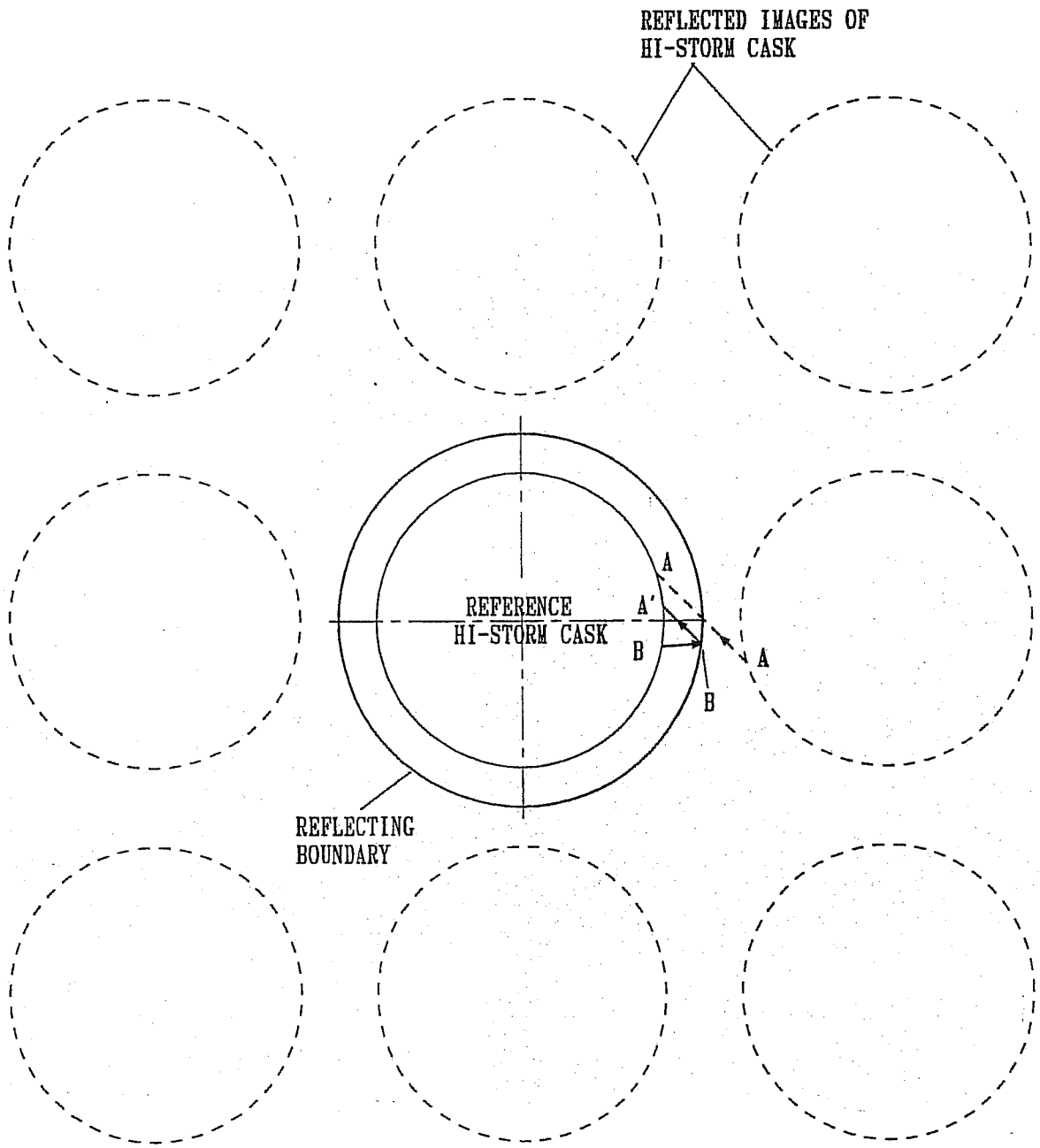

FIGURE 4.B.7: RADIATIVE HEATING OF REFERENCE HI-STORM CASK BY SURROUNDING CASKS

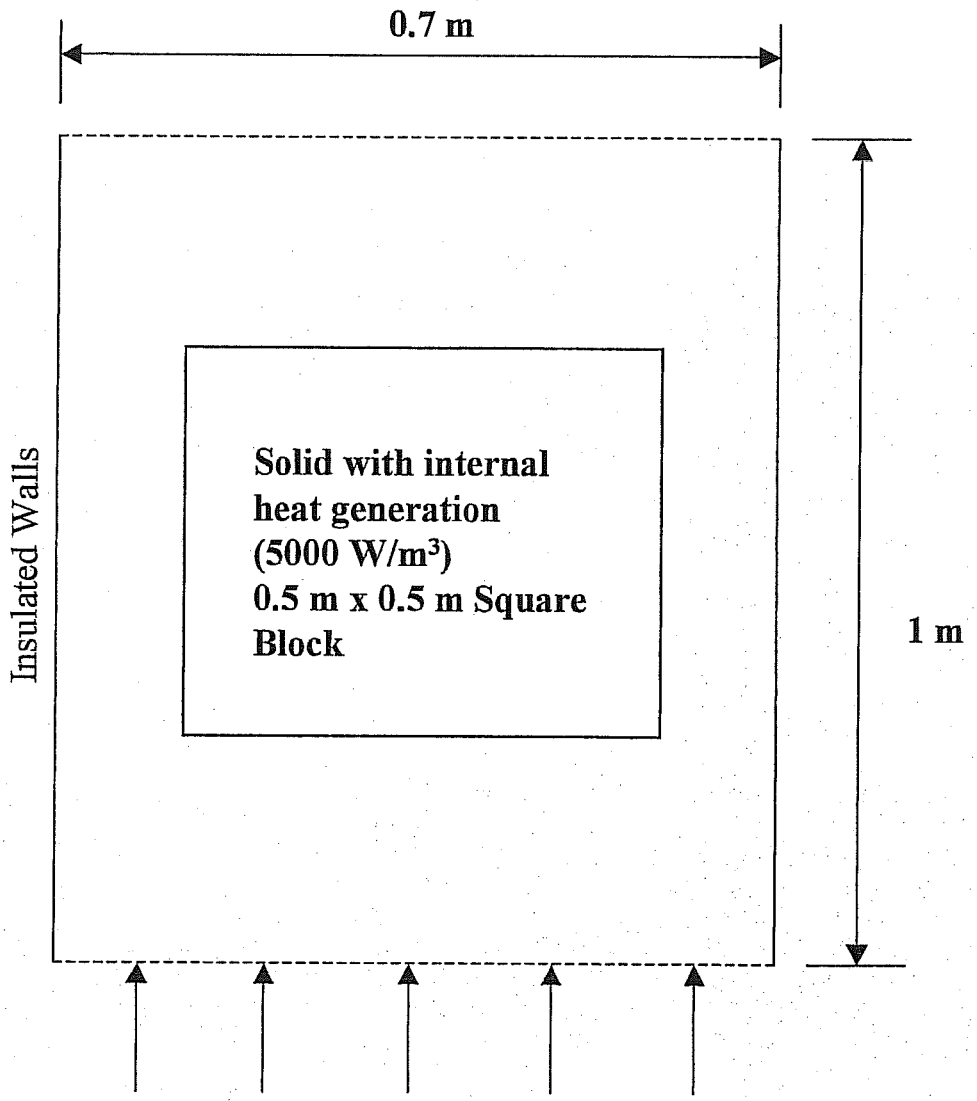

FIGURE 4.B.8: A CLASSICAL THERMAL SCENARIO: AIR COOLING OF A HEATED SQUARE BLOCK

SUPPLEMENT 4.I

(This Section Reserved for Future Use)

HOLTEC INTERNATIONAL COPYRIGHTED MATERIAL

SUPPLEMENT 4.II

THERMAL EVALUATION OF HI-STORM 100 SYSTEM FOR IP1

4.II.1 INTRODUCTION

The HI-STORM 100S-185 is a shorter version of the generic HI-STORM 100S Version B overpack specifically designed to store Indian Point 1 (IP1) spent nuclear fuel assemblies. A shorter version of MPC-32 (MPC-32-IP1) is designed for the shorter IP1 fuel assemblies and a shorter version of HI-TRAC 100D (HI-TRAC 100D Version IP1) is designed for short-term transfer operations. All the fuel assemblies will be stored in Damaged Fuel Containers in the MPC-32-IP1. The MPC-32-IP1 may also be stored in the generic HI-STORM 100S Version B overpack. In this supplement, compliance of the HI-STORM 100S-185, MPC-32-IP1 and HI-TRAC 100D Version IP1 systems to 10CFR72 and ISG-11, Rev. 3 thermal requirements are evaluated for storage. The analysis considers passive rejection of decay heat from the spent nuclear fuel. The IP1 fuel storage system is evaluated for normal storage, short-term transfer and accident scenarios defined in the principal design criteria in Chapter 2. The regulatory requirements and acceptance criteria for these evaluations are listed in Section 2.2 and 4.0.

4.II.2 THERMAL PROPERTIES OF MATERIALS

The materials of construction of the HI-STORM 100S-185 system, HI-TRAC 100D Version IP1 and MPC-32-IP1 are the same as those for the generic HI-STORM 100 System, HI-TRAC 100D and MPC-32. The thermophysical data compiled in Section 4.2 of the FSAR provides the required materials information for all components of the system.

4.II.3 TECHNICAL SPECIFICATIONS OF COMPONENTS

The HI-STORM 100S-185 system materials and components to be maintained within safe operating limits are listed in Section 4.3. The temperature limits specified in Section 2.2 of the FSAR are adopted for this evaluation.

4.II.4 NORMAL STORAGE THERMAL EVALUATION

The HI-STORM 100S-185 cask features an all-welded multi-purpose canister (MPC-32-IP1) containing spent nuclear fuel emplaced in a steel-concrete overpack. From a thermal standpoint the IP1 specific cask components are identical to their generic counterparts except that the height of the HI-STORM 100S-185, MPC-32-IP1 and HI-TRAC 100D Version IP1 are shorter to be compatible with the short-length IP1 fuel. The thermal payload of the MPC-32-IP1 is given in Table 4.II.1.

HOLTEC INTERNATIONAL COPYRIGHTED MATERIAL

4.II.4.1 Thermal Model

Thermal modeling of the HI-STORM 100S-185 and the HI-TRAC 100D Version IP1 adopts the same methodologies used for the evaluation of the generic HI-STORM 100 System presented in Section 4.4 of the FSAR and the HI-TRAC 100D thermal evaluation presented in Section 4.5 of the FSAR. Two-dimensional axisymmetric Computational Fluid Dynamics (CFD) models of the IP1 fuel storage system are used in these evaluations. For a conservative portrayal of cask system temperatures, the thermal evaluation incorporates the following assumptions:

1. *No credit is taken for motion of helium in the MPC fuel storage cells.*

2. *The decay heat load used in this thermal evaluation is 8 kW. The IP1 cask heat load will be less than 5 kW.*

3. *The most severe levels of environmental factors for long-term normal storage, which are an ambient temperature of 80°F and 10CFR71 insolation levels, were coincidentally imposed on the system.*

4. *No credit was considered for contact between fuel assemblies and the MPC basket wall or between the MPC basket and the basket supports. The fuel assemblies and MPC basket were conservatively considered to be in concentric alignment.*

5. *Axial heat transfer through fuel pellets is ignored.*

6. *Heat dissipation by fuel assembly grid spacers and top & bottom fittings is ignored.*

7. *Insolation heating assumed with a bounding absorbtivity (=1.0).*

8. *A margin between the computed peak cladding temperature and 400°C limit is provided.*

9. *Conservative values of the inlet and outlet debris screen flow resistances were used in the analyses.*

10. *Conservatively, the IP1 fuel rod fill gas amount is assumed to be the same as the B&W 15x15 PWR fuel assembly. This assumption is very conservative since the IP1 fuel assemblies are much shorter and lighter than this fuel assembly.*

Thermal analysis results are provided in the next sections.

4.II.4.2 Maximum Temperatures

Steady-state thermal analysis of HI-STORM 100S-185 containing an MPC-32-IP1 is performed

HOLTEC INTERNATIONAL COPYRIGHTED MATERIAL

for normal conditions of long-term storage (normal ambient temperature of 80°F, maximum insolation and quiescent air). Table 4.II.2 presents the results of the analysis. All MPC and HI-STORM component temperatures are lower than the allowable limits presented in Section 2.2. Based on the results in Table 4.II.2 and those presented in Section 4.4, the following conclusions can be made:

a) Fuel temperatures are bounded by generic HI-STORM.
b) Confinement boundary temperatures are bounded by generic HI-STORM.
c) Surface temperatures are bounded by generic HI-STORM.
d) MPC internal pressure is bounded by generic HI-STORM.

As the HI-STORM 100S-185 temperatures and pressure are bounded by the generic HI-STORM 100 System evaluation and the generic HI-STORM 100 System complies with 10CFR Part 72 and ISG 11, Rev. 3 requirements (see Section 4.4), it can be concluded that the HI-STORM 100S-185 system is in compliance with the 10CFR Part 72 and ISG 11, Rev. 3 requirements for normal storage.

Placement of the MPC-32-IP1 in a generic HI-STORM 100 overpack is bounded by the evaluation presented above, since the generic overpack has a larger height. This will allow for more efficient heat transfer from the top of the MPC-32-IP1 due to the larger airflow area between the MPC lid and the overpack lid, increased air flow due to an increase in the chimney height and a larger heat transfer area on the overpack surface.

4.II.4.3 Minimum Temperatures

As specified in 10CFR72, the minimum ambient temperature conditions for the HI-STORM 100 and HI-TRAC 100D System are -40°F and 0°F, respectively. The HI-STORM 100 System and HI-TRAC 100D System design does not have any minimum decay heat load restrictions for transport. Therefore, under bounding cold conditions (zero decay heat and no insolation), the cask components temperatures will approach ambient conditions. All HI-STORM 100 System and HI-TRAC 100D System materials of construction satisfactorily perform their intended function at these cold temperatures. Evaluations in Chapter 3 demonstrate the acceptable structural performance of the overpack and MPC steel materials at low temperature. Shielding and criticality functions of the cask materials are unaffected by cold.

4.II.4.4 Maximum Internal Pressures

The IP1 multi-purpose canister is pressurized with helium prior to sealing the lid ports. In Table 4.II.3 the initial backfill pressures are listed. In response to higher than ambient storage temperatures the helium pressure rises above the initial backfill pressures. For conservatism the maximum normal operating pressure (MNOP) is computed assuming 100% fuel rods rupture and the MPC-32-IP1 is assumed to be backfilled at the maximum backfill pressure (See Table

HOLTEC INTERNATIONAL COPYRIGHTED MATERIAL

4.II.3). The MNOP for normal storage condition is provided in Table 4.II.2 and is less than the allowable limit.

4.II.4.5 Maximum Thermal Stresses

Thermal expansion induced mechanical stresses are evaluated, using bounding temperature distributions, in Chapter 4.

4.II.5 THERMAL EVALUATION OF SHORT TERM OPERATIONS

The heat load in the MPC-32-IP1 to be transported in the HI-TRAC 100D Version IP1 is much lower (8kW) as compared to that allowed for the generic HI-TRAC 100D. The short-term evaluations presented in Section 4.5 bound short-term operations in a HI-TRAC 100D Version IP1 overpack.

4.II.6 THERMAL EVALUATION OF OFF-NORMAL AND ACCIDENT CONDITIONS

4.II.6.1 Off-Normal Conditions

(a) Elevated Ambient Air Temperature

The off-normal ambient condition is defined in Chapter 2 as an ambient temperature of 100°F. This is 20°F higher than the normal condition ambient temperature of 80°F. This condition is conservatively evaluated by adding 20°F to the calculated normal condition fuel cladding and component temperatures. Results for this off-normal condition are presented in Table 4.II.4. The results are confirmed to be less than short-term temperature limits for fuel cladding, concrete, and ASME Code materials.

(b) Partial Blockage of Air Inlets

Since the MPC-32-IP1 and HI-STORM 100S-185 component temperatures are all lower than those for the generic HI-STORM system, the effect of 50% inlet ducts blockage discussed in Chapter 11 for the generic HI-STORM remain bounding.

HOLTEC INTERNATIONAL COPYRIGHTED MATERIAL

4.II.6.2 Accident Conditions

(a) Fire

The fire accident is defined in Table 2.0.2 as a 1475 °F fire lasting 217 seconds. This is the same intensity and duration as the fire accident discussed in Chapter 11 of this FSAR for the generic HI-STORM 100 System. The existing fire evaluation therein bounds the HI-STORM 100S-185 fire event, for the following reasons:

Observation	***Basis***
Fire heat input to HI-STORM 100S-185 overpack is bounded by the generic HI-STORM 100 System	*Exposed area of overpack is bounded by larger generic design*
Start of fire conditions are bounded by generic HI-STORM 100 System.	*See Section 4.II.4.2*
Rate of MPC heatup is bounded by generic HI-STORM 100 System.	*Heat load in the MPC-IP1 is much lower than that permitted in the generic HI-STORM 100 System. Moreover, the reduction in the permitted heat load in the MPC-IP1 is much greater than the reduction in the thermal inertia of the HI-STORM 100S-185 cask as compared to the generic HI-STORM 100 system (about 30%).*

(b) Burial Under Debris

The burial under debris accident is defined in Table 2.0.2. The generic burial under debris described in Chapter 11 bounds the HI-STORM 100S-185 burial under debris event because the permissible heat load in the MPC-32-IP1 is much lower than the generic MPC-32 placed in a HI-STORM 100 System. Moreover, the reduction in the permitted heat load in the MPC-IP1 is much greater than the reduction in the thermal inertia of the HI-STORM 100S-185 cask as compared to the generic HI-STORM 100 system (about 30%).

(c) 100% Blockage of Air Ducts

The 100% air ducts blockage accident is defined in Table 2.0.2 as the blockage of 100% of the air inlet duct flow area. The initial condition for this transient thermal evaluation is the long-tem normal storage condition results. As the normal storage results for HI-STORM 100S-185

HOLTEC INTERNATIONAL COPYRIGHTED MATERIAL

temperatures and pressure are bounded by the generic HI-STORM 100 System results and the heat load in the generic HI-STORM 100 System is higher, the transient evaluation discussed in Chapter 11 for the generic HI-STORM 100 system remain bounding.

(d) Extreme Environmental Temperature

The extreme environmental temperature accident condition is defined in Table 2.0.2 as an ambient temperature of 125°F. This is 45°F higher than the normal condition ambient temperature of 80°F. This condition is conservatively evaluated by adding 45°F to the calculated normal condition fuel cladding and component temperatures. Results for this off-normal condition are presented in Table 4.II.5. The results are confirmed to be less than accident temperature limits for fuel cladding, concrete, and ASME Code materials.

4.II.7 REGULATORY COMPLIANCE

As required by ISG-11, the fuel cladding temperature at the beginning of dry cask storage is maintained below the anticipated damage-threshold temperatures for normal conditions for the licensed life of the HI-STORM System.

As required by NUREG-1536 (4.0,IV,3), the maximum internal pressure of the cask remains within its design pressure for normal, off-normal, and accident conditions. Design pressures are summarized in Table 2.2.1.

As required by NUREG-1536 (4.0,IV,4), all cask materials and fuel cladding are maintained within their temperature limits for normal, off-normal and accident conditions. Material temperature limits are summarized in Tables 2.2.3.

As required by NUREG-1536 (4.0,IV,5), the cask system ensures a very low probability of cladding breach during long-term storage. For long-term normal conditions, the maximum CSF cladding temperature is below the ISG-11 limit of 400 °C (752°F).

As required by NUREG-1536 (4.0,IV,7), the cask system is passively cooled. All heat rejection mechanisms described in this supplement, including conduction, natural convection, and thermal radiation, are passive.

As required by NUREG-1536 (4.0,IV,8), the thermal performance of the cask is within the allowable design criteria specified in Chapter 2 for normal, off-normal and accident conditions. All thermal results are within the allowable limits for all conditions of storage.

HOLTEC INTERNATIONAL COPYRIGHTED MATERIAL

Table 4.II.1: MPC-32-IP1 Thermal Payload

Total Decay Heat	*8 kW*

Table 4.II.2: Bounding HI-STORM 100S-185 System Long-Term Normal Storage Maximum Temperatures and Pressure

Component	***Temperature (°F)***
Fuel Cladding	*498*
Fuel Basket	*492*
Fuel Basket Periphery	*247*
MPC Shell	*210*
MPC Lid	*213*
Lid Concrete	*182*
Average Air Outlet Temperature	*96*
Pressure (psig)	
MPC	*83*

Table 4.II.3: Helium Backfill Pressures

Minimum Pressure	*22.0 psig @ 70°F*
Maximum Pressure	*33.3 psig @ 70°F*

HOLTEC INTERNATIONAL COPYRIGHTED MATERIAL

Table 4.II.4: Results for Elevated Ambient Air Temperature Off-Normal Event

Component	***Temperature (°F)***
Fuel Cladding	*518*
Fuel Basket	*512*
Fuel Basket Periphery	*267*
MPC Shell	*230*
MPC Lid	*233*
Lid Concrete	*202*
Average Air Outlet Temperature	*116*
Pressure (psig)	
MPC	*86*

Table 4.II.5: Results for Extreme Environmental Temperature Accident

Component	***Temperature (°F)***
Fuel Cladding	*543*
Fuel Basket	*537*
Fuel Basket Periphery	*292*
MPC Shell	*255*
MPC Lid	*258*
Lid Concrete	*227*
Average Air Outlet Temperature	*141*
Pressure (psig)	
MPC	*89*

HOLTEC INTERNATIONAL COPYRIGHTED MATERIAL